Universidad de Concepción
Dirección de Postgrado
Facultad de Ciencias Físicas y Matemáticas
Programa de Doctorado en Ciencias Aplicadas
con Mención en Ingeniería Matemática

ELEMENTOS FINITOS CON DIVERGENCIA NULA EN DOMINIOS CON TOPOLOGÍA GENERAL Y APLICACIONES

(DIVERGENCE-FREE FINITE ELEMENTS IN GENERAL TOPOLOGICAL DOMAINS AND APPLICATIONS)

Tesis para optar al grado de Doctor en Ciencias
Aplicadas con mención en Ingeniería Matemática

Eduardo Antonio De Los Santos Núñez
CONCEPCIÓN-CHILE
2019

Profesor Guía: Jessika P. Camaño V.
Departamento de Matemática y Física Aplicadas, Facultad de Ingeniería
Universidad Católica de la Santísima Concepción, Chile
CI^{2}MA, Universidad de Concepción, Chile

Cotutor: Ana Alonso Rodríguez
Dipartimento di Matematica
Università degli Studi di Trento, Italia

Cotutor: Rodolfo Rodríguez
CI^{2}MA y Departamento de Ingeniería Matemática
Universidad de Concepción, Chile

Divergence-Free Finite Elements in General Topological Domains and Applications

Eduardo A. De Los Santos Núñez

Directores de Tesis: Ana Alonso Rodríguez, Università degli Studi di Trento, Italia.
Jessika P. Camaño V., Universidad Católica de la Santísima Concepción, Chile.
Rodolfo Rodríguez, Universidad de Concepción, Chile.

Director de Programa: Rodolfo Rodríguez, Universidad de Concepción, Chile.

Comisión evaluadora

Prof.

Prof.

Prof.

Prof.

Comisión examinadora

Firma: _____
Prof.

Firma: _____
Prof.

Firma: _____
Prof.

Firma: _____
Prof.

Firma: _____
Prof.

Calificación: _____

Concepción, 22 de marzo del 2019

Abstract

The main goal of this thesis is to extend to the high order case some techniques for the construction of bases of the space of divergence-free Raviart–Thomas finite elements, which are well-known in the case of order one. The knowledge of a basis of the constrained subspace is a convenient alternative to impose the divergence-free condition, avoiding in this way the standard technique that uses Lagrange multipliers. The disadvantage with Lagrange multipliers is that they introduce a new unknown that has to be discretized and leads to a bigger linear system with a matrix that is not symmetric positive definite even though the bilinear form associated to the variational formulation of the problem in the constrained space is symmetric and coercive.

Firstly we propose and analyze an efficient algorithm for the construction of a basis of the space of divergence-free Raviart–Thomas finite elements based on graph techniques. The key point is to realize that, with very natural degrees of freedom for fields in the space of Raviart–Thomas finite elements of degree $r+1$ and also for elements of the space of discontinuous piecewise polynomial functions of degree $r \geq 0$, the matrix associated with the divergence operator is the incidence matrix of a particular directed, connected and without self-loop graph. By choosing a spanning tree of this graph, it is possible to identify an invertible square submatrix of the divergence matrix and with this invertible matrix it is easy to compute the moments of a field in the space of Raviart–Thomas finite elements with assigned divergence. This approach extends to finite elements of high degree the method introduced by Alotto and Perugia in [10] for finite elements of degree one, in other hand, the tree-cotree method can be traced back to Kirchhoff. The analyzed approach is used to construct a basis of the space of divergence-free Raviart–Thomas finite elements. The numerical tests show that the performance of the algorithm depends neither on the topology of the domain nor of the polynomial degree r.

Next we extend to the high order case a second approach based on the construction of a basis of the range of the curl operator. If the boundary of the domain is connected, the moments of the elements of a high order Raviart–Thomas divergence-free (RT^0_{r+1}) basis, are

computed by selecting first (in an appropriate way) some elements of a high order Nédélec (N_{r+1}) cardinal (dual) basis, and then computing their curls. The method use the graph associated to the gradient operator and a spanning tree of this graph to select the elements of the basis.

Finally we apply a divergence-free finite element method to solve a fluid-structure interaction spectral problem in the three-dimensional case. The main unknowns of the resulting formulation are given by displacements for the fluid and the solid, and the pressure of the fluid on the interface separating the fluid and the solid. The resulting mixed eigenvalue problem is approximated by using appropriate basis of the divergence-free lowest order Raviart–Thomas elements for the fluid, piecewise linear elements for the solid and piecewise constant elements for the pressure. It is proved that eigenvalues and eigenfunctions are efficiently approximated and some numerical results are presented in order to assess the performance of the method, and also showing that this method avoid spurious modes.

Resumen

El objetivo principal de esta tesis es extender al alto orden algunas técnicas de construcción de bases de los espacios de elementos finitos de Raviart–Thomas con divergencia nula, las cuales son conocidas en el caso de grado uno. Conocer una base del subespacio de funciones con divergencia nula es una alternativa conveniente a la técnica usual que usa multiplicadores de Lagrange. La desventaja de usar multiplicadores de Lagrange es que se introduce una nueva incógnita que hay que discretizar dando lugar a un sistema linear más grande con una matriz que no es simétrica definida positiva incluso cuando que la forma bilineal asociada a la formulación variacional del problema en el espacio con restricciones es simétrica y coerciva.

En primer lugar proponemos y analizamos un algoritmo eficiente para la construcción de una base del espacio de elementos finitos de Raviart–Thomas con divergencia nula basado en técnicas de grafo. El punto clave es notar que con grados de libertad usuales para los campos en el espacio de los elementos finitos de Raviart–Thomas de grado $r+1$ y también para los elementos del espacio de las funciones polinomiales a trozo de grado $r \geq 0$, la matriz asociada al operador divergencia es la matriz de incidencia de un grafo particular orientado, conexo y sin auto-bucles. Por medio de la elección de un árbol generador de este grafo, es posible identificar una submatriz cuadrada invertible de la matriz de divergencia y con esta matriz invertible es fácil calcular los momentos de un campo en el espacio de los elementos finitos de Raviart–Thomas con divergencia asignada. Este enfoque extiende a los elementos finitos de alto orden el método introducido por Alotto y Perugia en [10] para los elementos finitos de grado uno, por otra parte, los métodos que involucran al árbol generador de un grafo conexo se remontan a Kirchhoff. El enfoque analizado es utilizado para construir una base del espacio de los elementos finitos de Raviart–Thomas a divergencia nula. Los experimentos numéricos muestran que la eficiencia del algoritmo no depende de la topología del dominio ni tampoco del grado polinomial r.

A continuación extendemos al caso del alto orden un segundo enfoque basado en la construcción de una base de la imagen del operador rotacional. Si la frontera del dominio es

conexa, los momentos de los elementos de una base de los Raviart–Thomas con divergencia nula de alto orden (RT^0_{r+1}), son calculados seleccionando primero, en un modo apropiado, algunos elementos de una base cardinal (dual) de los Nédélec de alto orden (N_{r+1}), y luego son calculados sus rotacionales. El método utiliza el grafo asociado al operador gradiente y un árbol generador de este grafo para seleccionar los elementos de la base.

Finalmente aplicamos un método de elementos finitos con divergencia nula para resolver un problema espectral de interacción fluido-estructura en el caso tridimensional. Las incógnitas principales de la formulación resultante son el desplazamiento del fluido y del sólido, y la presión del fluido en la interfaz que separa el fluido y el sólido. El problema mixto de valores propios resultante es aproximado por medio de la utilización de bases apropiadas de los elementos de Raviart–Thomas con divergencia nula de orden más bajo para el fluido, elementos lineales a trozo para el sólido y constantes a trozo para la presión. Se demuestra que los valores propios y las funciones propias son aproximados de manera eficiente y son presentados algunos resultados numéricos con el objetivo de evaluar la eficiencia del método, y también mostrar que este método elimina los modos espurios.

Agradecimientos

En estas líneas quiero destacar a algunas personas que fueron muy importantes en mi transitar por la vida académica, desde antes y durante el desarrollo de este trabajo de tesis.

A mi mamá, quien siempre se ha preocupado de buscar para mi lo mejor y a Delo quien ha impulsado esta tarea para poder conseguirlo, sin escatimar esfuerzos ambos. A Rafaela Núñez, por brindarme tanto cariño y tiempo para discutir mis diferentes dudas, que me ayudaron a mantener durante mi niñez el espíritu crítico y curioso, ingredientes fundamentales para llegar a estas instancias. A Lourdes Sosa y Marcial Sánchez, por brindarme horas (incluso aquellas destinadas para descansar) de discusión ya sea sobre física, matemática o tecnologías, por las estimulantes conversaciones de la vida en general, por acompañarme de cerca en lo académico durante la adolescencia, y hasta el día de hoy con buenos consejos. A aquellos profesores que me han impulsado a dar lo mejor de mi. Mi gratitud por siempre.

A Miguel Volpe, por brindarme la oportunidad de prepararme para ingresar a la universidad junto a profesores excelentes como Hugo Checo y Verónica Rojas. Este periodo de formación lo recuerdo con mucha alegría, a mis compañeros de incontables horas de estudios, sin ellos el trabajo habría sido mucho más pesado. También ha sido un honor que luego me hayan dado la oportunidad de colaborar con ustedes. Mi gratitud por siempre.

Alrededor del año 2006, gracias al profesor Benjamín Barán me enteraba que doctor no era solamente aquella persona que ejercía la profesión de médico o la de abogado, inmediatamente después de su primera clase sobre física de ondas, me acerqué para preguntarle más sobre esto que para mi era nuevo y café de por medio fue el primero que me hablaba de ciencia como profesión y de los desafíos de plantearse la misma en Paraguay. Al finalizar este curso me brindó la oportunidad de colaborar con él en la misma asignatura, y aquí pude compartir con amigos geniales, quienes en su mayoría también han tomado el desafío de desarrollar ciencia para el Paraguay, ya sea desde afuera o desde adentro. Pasó poco tiempo, para que se hicieran frecuentes los diversos cursos internacionales de matemática, donde la

UNA recibía a profesores especialistas de diversos países y mediante estos podíamos experimentar un poco de lo que siempre exigimos (como regla) para nuestra casa de estudios, verdaderas clases magistrales. En este contexto pude conocer a Christian Schaerer, quien en medio de mucho esfuerzo era el que impulsaba estos cursos "extraordinarios" dentro de nuestro ámbito, a quien agradezco por habernos ofrecido esta oportunidad, incluso la de viajar para congresos y cursos fuera de la UNA, y por haberme orientado junto con la profesora Miki Saito el trabajo final de ingeniería. Mi gratitud hacia ellos por impulsarme siempre a crecer y también hacia aquellos profesores que nos proponían el desafío de impulsar a un Paraguay mejor, quienes de uno u otro modo nos transmitían el mensaje que la universidad no debe ser tan solo una institución que emite títulos, sino que forja a hombres y mujeres libres de bien. A aquellos ayudantes de cátedra que no se limitaban solamente con lo que les exigía el programa, sino que daban mucho más. A Inocencio Ortiz, por dedicar muchas horas conmigo en diversas discusiones de una matemática un poco más rigurosa de la que estábamos acostumbrados, fueron los pasos iniciales para poder leer correctamente varias ideas matemáticas. A OMAPA, por tanto esfuerzo en detectar y estimular a jóvenes brillantes de todo el país, y por sobre todo, por darme la oportunidad de compartir con ellos. Mi gratitud por siempre.

A Silvia Ramírez, a mis amigos y familiares, por alentarme y brindarme su confianza de diversas maneras para salir de Paraguay y enfrentar el desafío del doctorado, gestos sumamente importantes que influyeron en la decisión de viajar. Mi gratitud por siempre.

A Katherine Pintos, Teresa Pintos, Marcelo Montiel, Carlos Cañete, José Riveros (tata), Guillermo Argüello, Gladys Alegre, Julián Cárdenas, David Morínigo, Lilian Ovelar, Nicole Chilavert, Ana Delvalle, Líder González, Deolinda Olmedo, Silvio Núñez, Rosa Tosato, Sonia Villalba, Francisco Núñez, Ana Núñez, Nicha Salinas, Valeria De Los Santos, Agustín Villalba, Flora De Los Santos, Julia Salinas, Julián Salinas, José Núñez, Priscila Núñez, Ninfa Pereira, Celsa Segovia, Marcelo Sánchez, Diego Núñez, Lissa Bogado, Nelly Riveros, Sandra Aguilar, Nully Riveros, Ángel Núñez, Cami Montiel y tantos otros que al igual que los anteriores han estado cerca de mamá y papá, posiblemente en los momentos donde más me han necesitado y no he podido acompañarlos todo el tiempo que hubiese querido, con toda seguridad afirmo que si no fuese por todos ustedes, este proceso no hubiese llegado a culminar. Mi gratitud por siempre.

A mis compañeros, aquellos que ingresaron antes que yo al doctorado, aquellos quienes incluso antes de llegar a Chile ya me han demostrado su ayuda, con sugerencias y buenos consejos para llegar a Chile sin demasiados contratiempos, me han recibido como a un amigo de siempre e incluso me han abierto las puertas de sus hogares. Estos, que además de consejeros han desempeñado un rol (aún no institucionalizado) de "tutores iniciales"

para mi, compartiendo conmigo su experiencia en las diversas áreas que llamaban a mi curiosidad, además de indicarme los mejores materiales que estaban a su conocimiento, esto definitivamente ayudó a que las horas de estudio sean bastante más amenas. Mi gratitud por siempre.

A Raimund Büger, quien ejercía el rol de director del programa de doctorado cuando ingresaba al mismo, gracias a sus gestiones puedo dar testimonio que pude disponer de todas las herramientas que me fueron necesarias durante el doctorado e incluso muchas otras que se fueron presentando, como anécdota de sus diligencias puedo comentar que si no fuera por sus gestiones (fuera del periodo laboral normal: febrero), no hubiese podido organizarme en tiempo para poder ingresar al programa. Mi gratitud por siempre.

A Gabriel Gatica, director del CI^{2}MA, por tantas horas dedicadas a gestión y promoción del centro, que finalmente se transforma en recursos para conseguir las mejores herramientas para un buen trabajo. Por tanto esmero en la elaboración de materiales de formación, estos en verdad se transforman en profesores de 24 horas, por aceptarme "clandestinamente" como estudiante en los diferentes cursos que dictaba, y por sobre todo, por los buenos consejos de siempre y la confianza expresada en diferentes acciones concretas a lo largo del doctorado, espero poder retornar tan solo un poco a tal gesto. Pude aprender de usted mucho de lo que tenía intención de transmitirnos e incluso más que esto. Mi gratitud por siempre.

A los colaboradores del Departamento de Ingeniería Matemática, por sus atenciones durante el periodo que nos alojamos en el cuarto piso, y por sus diligencias durante todo este periodo, María Eugenia, Cecilia, muchas gracias. A José Parra, por salvarme más de una vez con las metidas de pata en el computador, por compartir con nosotros tu enorme experiencia en el ámbito computacional. Mi gratitud por siempre.

A los colaboradores del CI^{2}MA, por ayudarnos en los diversos detalles del día a día, Jorge, muchas gracias. A Lorena, por ayudarnos a mantener en orden (en más de un aspecto) toda la casa, y por sobre todo, por recibirnos todas las mañanas con una enorme sonrisa, de seguro esto no está estipulado en ninguna de sus varias funciones, pero puedo asegurar que para más de uno esta es una de las más importantes en algunos días que se presentan muy grises. A quienes fueron parte, Jacqueline, Angelina y Eduardo, que en su momento me han brindado de una manera muy gentil su ayuda en diferentes aspectos. Mi gratitud por siempre.

A mis profesores en los diferentes cursos del doctorado, en especial a aquellos que me tuvieron como único estudiante, Rodolfo Rodríguez, Manuel Solano, Mauricio Sepúlveda, aprecio y disfruto mucho dialogar sobre temas de matemática, gracias por ayudarme a ganar intuición en diferentes temas, es un gesto que valoro en gran medida. A Dhanya Rajendran,

por ayudarnos a leer un tema tan técnico como lo es el de regularidad de EDPs elípticas, y por sobre todo por brindarnos su amistad y compartir con nosotros un poco de su cultura. Mi gratitud por siempre.

A Jessika Camaño, primero por brindarme la oportunidad de trabajar con ella en un momento donde yo estaba necesitando iniciar la búsqueda de un problema a encarar para la tesis, por ponerme en contacto en el contexto de la tesis con personas maravillosas y por brindarme la contención necesaria en aquellos momentos de crisis que siempre se presentan en un emprendimiento como lo es el desarrollo de una tesis doctoral, gracias por brindarme apoyo incluso fuera del aspecto académico. Mi gratitud por siempre.

A Ana Alonso, por plantearme un problema tan bonito que me permitió leer sobre temas matemáticos de diferentes áreas, si bien al inicio me cuestionaba seriamente el por qué metí las patas en un tema como este, después de interactuar más tiempo directamente con ella durante la pasantía, primero pude entender verdaderamente lo que me pedían y en ese proceso apreciar y disfrutar muchísimo del tema, las últimas conversaciones en Concepción en verdad fueron sumamente estimulantes. Además, muchas gracias por presentarme a Francesca Rapetti, en las ocasiones que pude coincidir con ella, siempre fue muy gentil conmigo, compartiendo conmigo su experiencia, y por sobre todo por sus buenos consejos para el futuro en medio de conversaciones muy motivadoras. Mi gratitud por siempre.

A Rodolfo Rodríguez, por ayudarme a forjar el rigor en el pensamiento matemático, por enseñarme el concepto de "pensar con economía mental", por brindarme mediante su experiencia la mirada intuitiva de varios aspectos, por sus sugerencias y muchísimas correcciones en el ámbito computacional, pero por sobre todo, por aquellas enseñanzas que me ha dejado fuera del aspecto académico, si bien él piensa que su modo gentil y humilde de ser es "usual", definitivamente no lo es, y en particular me siento afortunado de haber podido conocerlo en sus diferentes roles. Mi gratitud por siempre.

A los diferentes proyectos, Red Doctoral REDOC.CTA, proyecto del MINEDUC UCO1202, por permitirme llegar a Concepción con la seguridad de contar con un año de financiamiento y poder así postular con tranquilidad a las becas de doctorado nacional de CONACYT, a esta última por financiarme 4 años de estudios, además de la pasantía y gastos relacionados a asistencia a eventos y compra de insumos relacionados al desarrollo de la tesis. Al proyecto BASAL del CMM, por apoyarme en el último tramo de redacción de este trabajo. Mi gratitud por siempre.

Eduardo A. De Los Santos Núñez

Contents

List of Tables

List of Figures

Introduction

In different physical problems the main unknown is the field $\mathbf{v} = A\nabla p$, being p the solution of an elliptic partial differential equation of the form $\operatorname{div}(A\nabla p) = f$, assuming that A is symmetric and uniformly positive definite, and that its entries are smooth enough.

A possibility is to compute an approximation $\mathbf{v}_h$ of $\mathbf{v}$ from p_h, approximation of p. However, the relation $\operatorname{div}(\mathbf{v}_h) = f_h$ holds only in a weak sense, where f_h is the $L^2(\Omega)$ projection of f over a suitable discrete subspace of $L^2(\Omega)$. In fact, the gradient of a Lagrange finite element approximating the solution of $\operatorname{div}(A\nabla p) = f$ has a distributional divergence which is not a function, and therefore this divergence cannot be equal to an assigned finite element, as was pointed out in [57, 9].

In order to avoid this difficulty, in 1977, P.A. Raviart and J.M. Thomas consider the saddle point formulation of the elliptic and second order problem $\operatorname{div}(A\nabla p) = f$,

$$\begin{cases} \mathbf{v} - A\nabla p = \mathbf{0} \\ \operatorname{div} \mathbf{v} = f\,. \end{cases} \tag{1}$$

To approximate numerically the field $\mathbf{v}$, they introduced the nowadays well-known Raviart–Thomas finite elements (see [62]).

It is worth noting that problem (1) can be expressed in the form

$$\begin{cases} \mathbf{u} - A\nabla p = \mathbf{g} \\ \operatorname{div} \mathbf{u} = 0\,, \end{cases} \tag{2}$$

by computing an auxiliary unknown $\mathbf{u}^f$ such that $\operatorname{div} \mathbf{u}^f = f$, denoting then $\mathbf{u} = \mathbf{v} - \mathbf{u}^f$ and $\mathbf{g} = -\mathbf{u}^f$. This is the reason why we focus on problem (2). From the physical point of view divergence-free constraint appears naturally in the incompressibility condition of fluids and also in the Gauss's law for magnetic induction fields.

Let us consider the problem with the homogeneous Dirichlet boundary condition for $p = 0$. By integration by parts one obtains the standard formulation: find $\mathbf{u} \in H(\operatorname{div}; \Omega) :=$

$\{\mathbf{w} \in (L^2(\Omega))^3 \mid \operatorname{div} \mathbf{w} \in L^2(\Omega)\}$ and $p \in L^2(\Omega)$ such that

$$\begin{cases} \displaystyle\int_\Omega A^{-1}\mathbf{u} \cdot \mathbf{w} - \int_\Omega p \operatorname{div} \mathbf{w} = \int_\Omega A^{-1}\mathbf{g} \cdot \mathbf{w} \\ \displaystyle\int_\Omega q \operatorname{div} \mathbf{u} = 0\,, \end{cases} \tag{3}$$

for all $\mathbf{w} \in H(\operatorname{div};\Omega)$ and $q \in L^2(\Omega)$. However, a simpler variational formulation of problem (2) is given as follows: find $\mathbf{u} \in H^0(\operatorname{div};\Omega) := \{\mathbf{w} \in H(\operatorname{div};\Omega) \mid \operatorname{div} \mathbf{w} = 0 \text{ in } \Omega\}$, such that

$$\int_\Omega A^{-1}\mathbf{u} \cdot \mathbf{w} = \int_\Omega A^{-1}\mathbf{g} \cdot \mathbf{w}\,, \tag{4}$$

for all $\mathbf{w} \in H^0(\operatorname{div};\Omega)$. To approximate the vector field in this formulation, we have to solve a symmetric positive definite linear system.

The solution of problems like (3), using Lagrange multiplier, and by applying finite element methods is well-known (see, e.g., Boffi, Brezzi and Fortin [24]). However, the numerical approximation of problems like (4) has not been frequently considered, since a conforming approximation of $H^0(\operatorname{div};\Omega)$ presents some technical difficulties, in particular in finding a basis for its discrete counterpart.

The key point is the construction of a basis for high order ($r \geq 0$) divergence-free Raviart–Thomas (RT^0_{r+1}) finite elements, for $\Omega \subset \mathbb{R}^3$. To our knowledge this has been done, for the lowest order case $r = 0$, by Hecht [45], Dubois [35] and Scheichl [66] for Ω simply-connected with $\partial\Omega$ non-connected (see also [38], [42], [30], [51] and [29]), and also has been done by Rapetti, Dubois and Bossavit [61] for a κ-fold torus; Gustafson and Hartman [41], [40] had also related results concerned with hydrodynamics problems. Having a basis for RT^0_{r+1} allows us to efficiently compute a numerical approximation of the solution of (4). To our knowledge, there are not yet results for the case of Raviart–Thomas finite elements of higher polynomial degree. In [69] the authors construct a basis of divergence-free finite elements of degree $r \geq 1$ by taking the curl of corresponding potential spaces in two-dimensional domains, $\Omega \subset \mathbb{R}^2$. However in the three-dimensional case this approach is not so direct due to the large kernel of the curl operator.

The methods proposed in this thesis use not only the space of Raviart–Thomas (RT_{r+1}) finite elements of degree $r+1$ with $r \geq 0$, but also Lagrange (L_{r+1}) and Nédélec (N_{r+1}) finite elements of degree $r+1$, and discontinuous piecewise polynomials (P_r) of degree r, considering domains of general topology.

We recall here the relation between the classical Sobolev spaces and their discrete counterpart, given by the well-known de Rham diagram (see Fig. 1), since it gives us the

guidelines for the construction of the desired basis. Moreover it is worth noting that (i) the constant functions are in the kernel of the gradient operator, (ii) the range of the gradient operator is contained in the kernel of the curl operator, (iii) the range of the curl operator is contained in the kernel of the div operator, (iv) the range of the div operator is the space $L^2(\Omega)$.

Note that all the inclusions between the ranges and the kernels of this differential operators mentioned before are actually equalities when the topology of the domain Ω is trivial. In this context a divergence-free Raviart–Thomas basis can be constructed just taking a basis in the range of the curl operator, this means discard the curl of those Nédélec finite elements that are in the kernel of the curl operator, namely, those Nédélec finite elements which are the gradient of some Lagrange finite element. However, when there exists in the domain Ω loops that are not boundary of any surface contained in the domain Ω, namely, when Ω is not simply connected, then the kernel of the curl operator is larger than the range of the gradient operator. In this case, the procedure for the construction of a basis of the range of the curl operator in RT_{r+1} is more complex. On other hand, when the boundary of Ω is not connected, the kernel of the div operator is larger than the range of the curl operator. In this case a basis of RT^0_{r+1} includes also linearly independent elements that are not curl of any Nédélec finite element. The relevance of the homology at the discrete level has been studied by Gross & Kotiuga [39] and Bossavit [26].

$$\begin{array}{ccccccccccc}
\mathbb{R} & \xrightarrow{\imath} & H^1(\Omega) & \xrightarrow{\text{grad}} & H(\text{curl},\Omega) & \xrightarrow{\text{curl}} & H(\text{div},\Omega) & \xrightarrow{\text{div}} & L^2(\Omega) & \xrightarrow{\theta} & 0 \\
 & & \uparrow{\scriptstyle \imath} & & \uparrow{\scriptstyle \imath} & & \uparrow{\scriptstyle \imath} & & \uparrow{\scriptstyle \imath} & & \\
\mathbb{R} & \xrightarrow{\imath} & L_{r+1} & \xrightarrow{\text{grad}} & N_{r+1} & \xrightarrow{\text{curl}} & RT_{r+1} & \xrightarrow{\text{div}} & P_r & \xrightarrow{\theta} & 0
\end{array}$$

Figure 1: de Rham chain, for $\Omega \subset \mathbb{R}^3$ (figure produced by the author).

In the lowest order case ($r = 0$) Alonso Rodríguez et al [8] computed a basis for RT^0_1, where each element of this basis is an appropriate linear combination of the elements of the basis of RT_1. The coefficients for those appropriate linear combinations were obtained by a method based on graph techniques, named in section 3.2 of [8] as the algebraic approach.

Another possibility to construct a basis for RT^0_1 is to use the curl of some Nédélec finite elements, as was done in section 3.1 of [8] and in [66]. In this context, they computed a basis of the range of the curl operator, eliminating those Nédélec finite elements that are the gradient of some Lagrange finite element and also those that are curl-free but that are not gradient of any Lagrange finite element. If the boundary of Ω is not connected they have to add RT_1 finite elements that are not curl of any Nédélec finite element but with

the divergence-free property.

This thesis focus on the challenge of extending to an arbitrary polynomial degree both approaches presented in [8]. In this context, in Chapter 1 we propose and analyze an efficient algorithm for the construction of a basis of the space of divergence-free Raviart–Thomas finite elements based on graph techniques. The key point is to realize that, with very natural degrees of freedom for fields in the space of Raviart–Thomas finite elements of degree $r+1$ and also for elements of the space of discontinuous piecewise polynomial functions of degree $r \geq 0$, the matrix associated with the divergence operator is the incidence matrix of a particular directed, connected and without self-loop graph. By choosing a spanning tree of this graph, it is possible to identify an invertible square submatrix of the divergence matrix and with this invertible matrix it is easy to compute the moments of a field in the space of Raviart–Thomas finite elements with assigned divergence. This approach extends to finite elements of high degree the method introduced by Alotto and Perugia in [10] for finite elements of degree one, in other hand, the tree-cotree method can be traced back to Kirchhoff. The analyzed approach is used to construct a basis of the space of divergence-free Raviart–Thomas finite elements. The numerical tests show that the performance of the algorithm depends neither on the topology of the domain nor of the polynomial degree r. The contents of this chapter gave rise to the following paper:

> [7] A. Alonso Rodríguez, J. Camaño, E. De Los Santos, and F. Rapetti, *A graph approach for the construction of high order divergence-free Raviart-Thomas finite elements*. **Calcolo**, vol. 55, 4, Art. 42, 28, (2018).

Next, in Chapter 2 we extend to the high order case the approach based on the construction of a basis of the range of the curl operator. If the boundary of the domain is connected, the moments of the elements of a basis of RT^0_{r+1}, are computed by selecting first, in an appropriate way, some elements of a cardinal (dual) basis of N_{r+1} and then computing their curls. The method use the graph associated to the gradient operator and a spanning tree of this graph to select the elements of the basis. The contents of this chapter gave rise to the following document:

> A. Alonso Rodríguez, J. Camaño, E. De Los Santos, and F. Rapetti, *A tree-cotree splitting for the construction of high order divergence-free finite elements*. **In preparation**.

In Chapter 3 we consider a problem in which we apply the divergence-free finite element basis proposed in the previous chapters. In particular we study the fluid-structure

interaction that involves the motion of a deformable structure in contact with an internal or surrounding incompressible fluid. These kind of interactions are a crucial consideration in the design of many engineering systems, e.g., aircraft, engines and bridges. As a result, much effort has gone into the development of general finite element methods for fluid-structure systems.

In this chapter we are concerned with the interaction between a fluid and an elastic structure. We consider the problem that consists of a bounded domain completely filled by the fluid and limited by the solid. Different formulations have been proposed to solve this problem (see, for instance, [20] and references therein).

Pure displacement formulations are very much used in applications. Indeed, they lead to simple well-posed generalized eigenvalue problems and are convenient to handle more complex interactions between fluids and structures (for instance, in presence of wall dissipation [18]). However, it is well-known that standard discretizations with Lagrange elements lead to spurious vibration frequencies interspersed among the physical ones [43]. In [17] (see also [15]) a finite element method for a 2D (two-dimensional) domain that does not present spurious modes has been introduced. It is based on using displacement variables for both the fluid and the solid. The pressure of the fluid is also used for the theoretical analysis. The displacements are approximated by piecewise linear elements for the solid and Raviart–Thomas elements of lowest order for the fluid. The interface coupling of both discretization is achieved in a non-conforming way. In the case of an incompressible fluid, the fluid displacement variables can be eliminated by using the so-called *added mass* formulation (see, for instance, [55]). This consists of taking into account the effect of the fluid by means of a Neumann-to-Dirichlet operator (also called Steklov-Poincaré operator) on the fluid-solid interface. The finite element discretization of this problem has been treated, for instance, in [14], [22].

Another strategy was presented in [16, 17]. It consists of using divergence-free fields for describing the incompressible fluid displacements. This was theoretically analyzed and conveniently implemented in the 2D case by means of curls of piecewise linear elements. However, its extension to 3D (three-dimensional case) is not straightforward. In particular, in order to use a similar approach in 3D, we use the basis proposed in [8], which was commented previously. The contents of this chapter gave rise to the following document:

> A. Alonso Rodríguez, J. Camaño, E. De Los Santos, and R. Rodríguez, *Divergence-Free Finite Elements for the numerical solution of a Hydroelastic Vibration Problem.* Preprint 2019-02, Centro de Investigación en Ingeniería Matemática (CI^{2}MA), Universidad de Concepción, Chile, (2019).

Introducción

En diferentes problemas físicos la incógnita principal es el campo vectorial $\mathbf{v} = A\nabla p$, siendo p la solución de una ecuación diferencial parcial elíptica de la forma $\operatorname{div}(A\nabla p) = f$, asumiendo que A es simétrica y uniformemente definida positiva, y que sus entradas son suficientemente regulares.

Una posibilidad es calcular una aproximación $\mathbf{v}_h$ de $\mathbf{v}$ a partir de p_h, aproximación de p. Sin embargo, la relación $\operatorname{div}(\mathbf{v}_h) = f_h$ se verifica solamente en el sentido débil, donde f_h es la proyección $L^2(\Omega)$ de f sobre un subespacio discreto de $L^2(\Omega)$ adecuado. De hecho, el gradiente de un elemento finito de Lagrange que aproxima la solución de $\operatorname{div}(A\nabla p) = f$ posee divergencia distribucional, la cual no es una función, y por lo tanto esta divergencia no puede ser igual a un elemento finito asignado, como ya fue indicado en [57, 9].

Con el objetivo de evitar esta dificultad, en 1977, P.A. Raviart y J.M. Thomas consideraron la formulación de punto silla del problema elíptico de segundo orden $\operatorname{div}(A\nabla p) = f$,

$$\begin{cases} \mathbf{v} - A\nabla p = \mathbf{0} \\ \operatorname{div} \mathbf{v} = f\,. \end{cases} \tag{5}$$

Para aproximar numéricamente el campo $\mathbf{v}$, ellos introdujeron los ahora bien conocidos elementos finitos de Raviart–Thomas (see [62]).

Vale la pena notar que el problema (5) puede ser expresado en la forma

$$\begin{cases} \mathbf{u} - A\nabla p = \mathbf{g} \\ \operatorname{div} \mathbf{u} = 0\,, \end{cases} \tag{6}$$

mediante el cálculo de una variable auxiliar $\mathbf{u}^f$ tal que $\operatorname{div} \mathbf{u}^f = f$, denotando de este modo $\mathbf{u} = \mathbf{v} - \mathbf{u}^f$ y $\mathbf{g} = -\mathbf{u}^f$. Este es el motivo por el cual nos enfocamos en el problema (6). Desde el punto de vista físico, la restricción de divergencia nula aparece naturalmente en la condición de incompresibilidad de los fluidos y también en la ley de Gauss par el campo de inducción magnética.

Consideremos el problema con condiciones de frontera Dirichlet homogénea para $p = 0$. Mediante integración por partes se obtiene la formulación usual: buscar $\mathbf{u} \in H(\mathrm{div};\Omega) := \{\mathbf{w} \in (L^2(\Omega))^3 \mid \mathrm{div}\,\mathbf{w} \in L^2(\Omega)\}$ y $p \in L^2(\Omega)$ tal que

$$\left\{ \begin{array}{l} \displaystyle\int_\Omega A^{-1}\mathbf{u}\cdot\mathbf{w} - \int_\Omega p\ \mathrm{div}\,\mathbf{w} = \int_\Omega A^{-1}\mathbf{g}\cdot\mathbf{w} \\ \displaystyle\int_\Omega q\ \mathrm{div}\,\mathbf{u} = 0\,, \end{array} \right. \tag{7}$$

para todo $\mathbf{w} \in H(\mathrm{div};\Omega)$ y $q \in L^2(\Omega)$.

Sin embargo, una formulación variacional más simple del problema (6) está dada como sigue: buscar $\mathbf{u} \in H^0(\mathrm{div};\Omega) := \{\mathbf{w} \in H(\mathrm{div};\Omega) \mid \mathrm{div}\,\mathbf{w} = 0 \text{ in } \Omega\}$, tal que

$$\int_\Omega A^{-1}\mathbf{u}\cdot\mathbf{w} = \int_\Omega A^{-1}\mathbf{g}\cdot\mathbf{w}\,, \tag{8}$$

para todo $\mathbf{w} \in H^0(\mathrm{div};\Omega)$. Para aproximar el campo vectorial en esta formulación, debemos resolver un sistema lineal simétrico definido positivo.

Resolver problemas como (7), con multiplicador de Lagrange, aplicando el método de elementos finitos es bien conocido (ver, e.g., Boffi, Brezzi and Fortin [24]). Sin embargo, la aproximación numérica de problemas como (8) no ha sido considerada frecuentemente, dado que una aproximación conforme de $H^0(\mathrm{div};\Omega)$ presenta algunas dificultades técnicas, en particular en encontrar una base para su contraparte discreta.

El punto clave es la construcción de una base para los elementos finitos de Raviart–Thomas con divergencia nula (RT^0_{r+1}) de alto orden ($r \geq 0$), para $\Omega \subset \mathbb{R}^3$. Hasta donde sabemos esto ha sido realizado, para el orden más bajo $r = 0$, por Hecht [45], Dubois [35] y Scheichl [66] para Ω simplemente conexo con $\partial\Omega$ no conexa (ver también [38], [42], [30], [51] y [29]), y también fue hecho por Rapetti, Dubois y Bossavit [61] para el toro tridimensional de género κ; Gustafson y Hartman [41], [40] poseen también resultados similares relacionados con problemas de la hidrodinámica. Poseer una base para RT^0_{r+1} permite calcular eficientemente una aproximación numérica de la solución de (8). Hasta donde sabemos, no existen aún resultados para los elementos finitos de Raviart–Thomas de alto grado polinomial. En [69] los autores construyeron una base de los elementos finitos con divergencia nula de grado $r \geq 1$ considerando el rotacional del espacio de los potenciales correspondiente al caso de un dominio bidimensional, $\Omega \subset \mathbb{R}^2$. Sin embargo, en el caso tridimensional este enfoque no es tan inmediato debido al gran núcleo del operador rotacional.

Los métodos propuestos en esta tesis no utilizan exclusivamente el espacio de los elementos finitos de Raviart–Thomas (RT_{r+1}) de grado $r + 1$, sino también los elementos finitos

de Lagrange (L_{r+1}) y de Nédélec (N_{r+1}) de grado $r+1$, y polinomiales a trozo discontinuos (P_r) de grado r, considerando dominios con topología general.

Recordamos aquí la relación entre los espacios de Sobolev clásicos y de su contraparte discreta, dado por el bien conocido diagrama de de Rham (ver Fig. 2), dado que este nos proporciona los delineamientos para la construcción de la base deseada. Además vale la pena notar que (i) las funciones constantes están en el núcleo del operador gradiente, (ii) la imagen del operador gradiente está contenida en el núcleo del operador rotacional, (iii) la imagen del operador rotacional está contenida en el núcleo del operador divergencia, (iv) la imagen del operador divergencia es el espacio $L^2(\Omega)$.

Note que todas las inclusiones entre las imágenes y los núcleos de estos operadores diferenciales mencionados anteriormente son en realidad igualdades cuando la topología del dominio Ω es trivial. En este contexto una base de Raviart–Thomas con divergencia nula puede ser construida simplemente considerando una base en la imagen del operador rotacional, esto significa descartar el rotacional de aquellos elementos finitos de Nédélec que están en el núcleo del operador rotacional, es decir, aquellos elementos finitos de Nédélec que son el gradiente de algún elemento finito de Lagrange. Sin embargo, cuando existen en el dominio Ω lazos que no son frontera de ninguna superficie contenida en el dominio Ω, por ejemplo, cuando Ω no es simplemente conexo, entonces el núcleo del operador rotacional es más grande que la imagen del operador gradiente. En este caso, el procedimiento para la construcción de una base de la imagen del operador rotacional en RT_{r+1} es más complicado. Por otro lado, cuando la frontera de Ω no es conexa, el núcleo del operador divergencia es más grande que la imagen del operador rotacional. En este caso una base de RT^0_{r+1} incluye también elementos linealmente independientes que nos son rotacional de ningún elemento finito de Nédélec. La relevancia de la homología a nivel discreto ha sido estudiado por Gross & Kotiuga [39] y Bossavit [26].

$$\begin{array}{ccccccccccc}
\mathbb{R} & \xrightarrow{\imath} & H^1(\Omega) & \xrightarrow{\text{grad}} & H(\text{curl},\Omega) & \xrightarrow{\text{curl}} & H(\text{div},\Omega) & \xrightarrow{\text{div}} & L^2(\Omega) & \xrightarrow{\theta} & 0 \\
 & & \uparrow{\scriptstyle \imath} & & \uparrow{\scriptstyle \imath} & & \uparrow{\scriptstyle \imath} & & \uparrow{\scriptstyle \imath} & & \\
\mathbb{R} & \xrightarrow{\imath} & L_{r+1} & \xrightarrow{\text{grad}} & N_{r+1} & \xrightarrow{\text{curl}} & RT_{r+1} & \xrightarrow{\text{div}} & P_r & \xrightarrow{\theta} & 0
\end{array}$$

Figure 2: Cadena de de Rham, para $\Omega \subset \mathbb{R}^3$ (figura hecha por el autor).

En el grado más bajo ($r = 0$) Alonso Rodríguez et al [8] calcularon una base para RT^0_1, donde cada elemento de esta base es una combinación lineal adecuada de los elementos de la base de RT_1. Los coeficientes para esta combinación lineal adecuada fueron obtenidos mediante un método basado en técnicas de grafo, nombrado en la sección 3.2 de [8] como

el enfoque algebraico.

Otra posibilidad para construir una base para RT_1^0 es usar el rotacional de algunos elementos finitos de Nédélec, como fue hecho en la sección 3.1 de [8] y en [66]. En este contexto, ellos calcularon una base de la imagen del operador rotacional, eliminando aquellos elementos finitos de Nédélec que son el gradiente de algún elemento finito de Lagrange y también aquellos que son de rotacional nulo pero que no son gradiente de ningún elemento finito de Lagrange. Si la frontera de Ω no es conexa, se deben agregar elementos finitos de RT_1 que no son rotacional de ningún elemento finito de Nédélec pero que posean la propiedad de divergencia nula.

Esta tesis se enfoca en el desafío de extender a un orden polinomial arbitrario ambos enfoques presentados en [8]. En este contexto, en el Capítulo 1 proponemos y analizamos un algoritmo eficiente para la construcción de una base del espacio de los elementos finitos de Raviart–Thomas con divergencia nula basado en técnicas de grafo. El punto clave es notar que, con grados de libertad usuales para los campos en el espacio de los elementos finitos de Raviart–Thomas de grado $r+1$ y también para los elementos del espacio de las funciones polinomiales a trozo discontinuas de grado $r \geq 0$, la matriz asociada con el operador divergencia es la matriz de incidencia de un grafo orientado, conexo y sin autobucles particular. Mediante la elección de un árbol generador de este grafo, es posible identificar una submatriz cuadrada invertible de la matriz de divergencia y con esta matriz invertible es fácil calcular los momentos de un campo en el espacio de los elementos finitos de Raviart–Thomas con divergencia asignada. Este enfoque extiende a los elementos finitos de alto orden el método introducido por Alotto y Perugia en [10] para los elementos finitos de grado uno, por otra parte, los métodos que involucran al árbol generador de un grafo conexo se remontan a Kirchhoff.. El enfoque analizado es utilizado para construir una base del espacio de los elementos finitos de Raviart–Thomas con divergencia nula. Los experimentos numéricos muestran que el desempeño del algoritmo no depende de la topología del dominio ni tampoco del grado polinomial r. Los contenidos de este capítulo dieron origen al siguiente artículo:

> [7] A. Alonso Rodríguez, J. Camaño, E. De Los Santos, and F. Rapetti, *A graph approach for the construction of high order divergence-free Raviart-Thomas finite elements.* **Calcolo**, vol. 55, 4, Art. 42, 28, (2018).

A continuación, en el Capítulo 2 extendemos al caso de alto orden el enfoque basado en la construcción de una base de la imagen del operador rotacional. Si la frontera del dominio es conexa, los momentos de los elementos de una base de RT_{r+1}^0, son calculados seleccionando

primero, en un modo apropiado, algunos elementos de una base cardinal (dual) de N_{r+1} y luego se calcula sus rotacionales. El método utiliza el grafo asociado al operador gradiente y un árbol generador de este grafo para seleccionar los elementos de esta base. Los contenidos de este capítulo dieron origen al siguiente documento:

> A. Alonso Rodríguez, J. Camaño, E. De Los Santos, and F. Rapetti, *A tree-cotree splitting for the construction of high order divergence-free finite elements*. **En preparación**.

En el Capítulo 3 consideramos un problema en el cual aplicamos la base de los elementos finitos con divergencia nula propuesta en los capítulos precedentes. En particular estudiamos la interacción fluido-estructura que involucra el movimiento de una estructura deformable en contacto con un fluido incompresible interno o envolvente a la estructura. Este tipo de interacciones son importantes en el diseño de varios sistemas de la ingeniería, e.g., diseño de: aeronaves, motores y puentes. En consecuencia, se ha puesto mucho esfuerzo en el desarrollo de métodos de elementos finitos para los sistemas fluido-estructura.

En este capítulo nos centramos en la interacción entre un fluido y una estructura elástica. Consideramos el problema que consiste en un dominio acotado completamente lleno por un fluido, el cual está limitado por el sólido. Diferentes formulaciones han sido propuestas para resolver este problema (ver, por ejemplo, [20] y sus referencias).

Formulaciones basadas en desplazamientos son muy utilizadas en aplicaciones. De hecho, inducen problemas de valores propios generalizados simples y bien puestos y son convenientes para manejar interacciones más complejas entre fluidos y estructuras (por ejemplo, en presencia de un muro de disipación [18]). Sin embargo, es bien sabido que discretizaciones usuales con los elementos finitos de Lagrange introducen frecuencias de vibración espurias dispersas entre las frecuencias con relevancia física del problema [43]. En [17] (ver también [15]) se ha introducido un método de elementos finitos para un dominio bidimensional (2D) que no presenta modos espurios. Se basa en el uso de variables de desplazamiento tanto para el sólido como para el fluido. La presión del fluido es también utilizada para los análisis teóricos. Los desplazamientos son aproximados mediante elementos lineales a trozos y continuos para el sólido y elementos de Raviart–Thomas de bajo orden para el fluido. La interfaz que acopla ambas discretizaciones es considerada en un modo no conforme. En el caso de un fluido incompresible la variable de desplazamiento del fluido puede ser eliminada usando la denominada formulación de *masa añadida* (ver, por ejemplo, [55]). Esta consiste en tener en cuenta el efecto del fluido por medio de un operador Neumann-a-Dirichlet (también denominado operador Steklov-Poincaré) en la interfaz sólido fluido. La discretización por elementos finitos de este problema ha sido tratado, por ejemplo, en [14], [22].

Otra estrategia fue presentada en [16, 17]. La misma consiste en usar campos con divergencia nula para describir el desplazamiento del fluido incompresible. Esta fue analizada teóricamente e implementada convenientemente en el caso 2D por medio de rotacionales de elementos lineales a trozo y continuos. Sin embargo, su extensión a 3D (caso tridimensional) no es directo. En particular, con el objetivo de utilizar un enfoque similar en 3D, usamos las bases propuestas en [8], las cuales fueron comentadas previamente. Los contenidos de este capítulo dieron origen al siguiente documento:

> A. Alonso Rodríguez, J. Camaño, E. De Los Santos, and R. Rodríguez, *Divergence-Free Finite Elements for the numerical solution of a Hydroelastic Vibration Problem.* Preprint 2019-02, Centro de Investigación en Ingeniería Matemática (CI^{2}MA), Universidad de Concepción, Chile, (2019).

CHAPTER 1

A graph approach for the construction of high order divergence-free Raviart–Thomas finite elements

1.1 Introduction

Given a function $\rho \in L^2(\Omega)$, the classical way to compute $\mathbf{u} \in H(\mathrm{div};\Omega)$ such that $\mathrm{div}\,\mathbf{u} = \rho$ is to solve the Dirichlet boundary value problem

$$\begin{cases} \Delta\phi = \rho & \text{in } \Omega\,, \\ \phi = 0 & \text{on } \partial\Omega\,, \end{cases}$$

and take $\mathbf{u} = \mathrm{grad}\,\phi$. The situation is not so easy if ρ is a discontinuous finite element piecewise polynomial ρ_h and one looks for an approximation $\mathbf{u}_h$ of $\mathbf{u}$ in an appropriate finite element space such that $\mathrm{div}\,\mathbf{u}_h = \rho_h$. If ρ_h is piecewise constant, then $\mathbf{u}_h$ belongs to the space of Raviart–Thomas finite elements of degree one. For this case an efficient algorithm has been proposed in [9]. We now consider a discrete function ρ_h, that is a polynomial of degree $r \geq 0$ in each tetrahedron of the mesh of Ω, and we look for $\mathbf{u}_h$ in the space of Raviart–Thomas finite elements of degree $r+1$. The algorithm we present is based on graph techniques and extends to higher polynomial degree the ideas introduced in [10] for the case of Raviart–Thomas finite elements of degree one.

The proposed algorithm can be also used to construct a basis of the space of divergence-free Raviart–Thomas finite elements of degree $r+1$. This space appears naturally in different applications. Let us consider the well-known Darcy problem

$$\begin{cases} \mathbf{u} + \mathcal{K}\,\mathrm{grad}\,p = \mathbf{g} & \text{in } \Omega, \\ \mathrm{div}\,\mathbf{u} = 0 & \text{in } \Omega, \\ \mathbf{u}\cdot\mathbf{n} = 0 & \text{on } \partial\Omega, \end{cases}$$

that models the velocity $\mathbf{u}$ of an incompressible fluid flowing in a porous medium occupying the domain Ω, with coefficient of porosity equal to $\mathcal{K}$. Its simpler variational formulation is: find $\mathbf{u} \in H^0(\mathrm{div};\Omega) := \{\mathbf{v} \in H(\mathrm{div};\Omega) \,:\, \mathrm{div}\,\mathbf{v} = 0\}$ such that

$$\int_\Omega \mathcal{K}^{-1}\mathbf{u}\cdot\mathbf{v} = \int_\Omega \mathcal{K}^{-1}\mathbf{g}\cdot\mathbf{v} \quad \forall\,\mathbf{v} \in H^0(\mathrm{div};\Omega)\,.$$

Let us also mention the electromagnetic problem in its curl-div formulation

$$\begin{cases} \mathrm{curl}\,\mathbf{u} = \mathbf{J} \ \text{ in } \Omega, \\ \mathrm{div}\,\mathbf{u} = \rho \ \text{ in } \Omega, \\ \mathbf{u}\times\mathbf{n} = \mathbf{a} \ \text{ or } \ \mathbf{u}\cdot\mathbf{n} = b \ \text{ on } \partial\Omega, \end{cases}$$

as proposed in [6]. For a magnetostatic situation, $\mathbf{u}$ is the magnetic field in Ω generated by an electric current density $\mathbf{J}$ (in this case, $\rho = 0$ and $\mathbf{u}\cdot\mathbf{n} = b$ on $\partial\Omega$). For an electrostatic situation, $\mathbf{u}$ is the electric field in Ω generated by the charge density ρ (in this case, $\mathbf{J} = \mathbf{0}$ and $\mathbf{u}\times\mathbf{n} = \mathbf{a}$ on $\partial\Omega$).

There are different techniques for constructing basis of a divergence free (or approximately divergence free) finite elements spaces in $\mathbb{R}^2$ and $\mathbb{R}^3$; see, for instance, [45], [38], [41], [42], [30], [51], [29]. Concerning the construction of a basis of the space of Raviart–Thomas finite elements that are divergence-free, it has been done, for elements of degree one, in [66] for a simply-connected domain with a non-connected boundary (see also [35] where curvilinear elements are considered), in [61] for a g-fold torus, and in [8] for a domain with arbitrary topology. To our knowledge, there are not yet results for the case of Raviart–Thomas finite elements of higher degree. (In [69] the authors construct a basis of divergence-free finite elements of degree $r \geq 1$ by taking the curl of corresponding potential spaces in two-dimensional domains, $\Omega \subset \mathbb{R}^2$. However, in the three-dimensional case, this approach is not so direct due to the large kernel of the curl operator.) We treat the three-dimensional case, $\Omega \subset \mathbb{R}^3$, and the same approach is valid in the two-dimensional case too.

This chapter is organized as follows. In Section 1.2 we introduce the necessary notation and briefly present some results of graph theory that will be used in the sequel. Then in Section 1.3 we write the matrix associated to the divergence operator when using the standard degrees of freedom (moments) for fields in the space of Raviart–Thomas finite elements of degree $r+1$ and for elements of the space of discontinuous piecewise polynomial functions of degree $r \geq 0$. Moreover we prove that it is an incidence matrix of a particular connected graph with no self-loop. Using this last property we compute in Section 1.4 the moments of a discrete field in the space of Raviart–Thomas finite elements of degree $r+1$ with assigned divergence. Notice that when using high order approximations, the cardinal basis $\{\boldsymbol{\phi}_{h,j}\}_{j=1}^{d_{RT}}$ of the finite elements space with respect to a chosen set of degrees of freedom

$\{m_\ell\}_{\ell=1}^{d_{RT}}$, (in this case the moments), has generally to be constructed from a given (favorite) basis $\{\boldsymbol{\psi}_{h,k}\}_{k=1}^{d_{RT}}$ of the finite elements space. This construction involves the inversion of a generalized Vandermonde matrix V, with $[V]_{\ell,k} = m_\ell(\boldsymbol{\psi}_{h,k})$. The inverse matrix V^{-1} provides, column by column, the coefficients to express the cardinal functions as a linear combination of elements of $\{\boldsymbol{\psi}_{h,k}\}_{k=1}^{d_{RT}}$ (see [25]), namely $\boldsymbol{\phi}_{h,j}(\mathbf{x}) = \sum_{k=1}^{d_{RT}}[V^{-1}]_{k,j}\boldsymbol{\psi}_{h,k}(\mathbf{x})$. Once one has the vector $\mathbf{U}$ gathering the moments of a discrete function $\mathbf{u}_h$, and a cardinal basis, we obtain

$$\begin{aligned}\mathbf{u}_h(\mathbf{x}) &= \sum_{j=1}^{d_{RT}} U_j\boldsymbol{\phi}_{h,j}(\mathbf{x}) = \sum_{j=1}^{d_{RT}} U_j \sum_{k=1}^{d_{RT}}[V^{-1}]_{k,j}\boldsymbol{\psi}_{h,k}(\mathbf{x})\\ &= \sum_{k=1}^{d_{RT}}\sum_{j=1}^{d_{RT}}[V^{-1}]_{k,j}U_j\boldsymbol{\psi}_{h,k}(\mathbf{x}) = \sum_{k=1}^{d_{RT}}\mathbf{U}^\top[V^{-1}]_{k,\cdot}\boldsymbol{\psi}_{h,k}(\mathbf{x})\,.\end{aligned}$$

In Section 1.5 we use the algorithm presented in Section 1.4 to compute the moments of a basis of the divergence-free Raviart–Thomas finite elements space for any degree, and Section 1.6 contains some numerical experiments illustrating the performance of the method for the construction of a basis of the space of divergence-free Raviart–Thomas finite elements of degree two and degree three.

1.2 Notation and preliminary results

Let Ω be a bounded polyhedral domain of $\mathbb{R}^3$ with Lipschitz boundary. Let us consider a tetrahedral mesh $\mathcal{T}_h = (\mathcal{V}, \mathcal{E}, \mathcal{F}, \mathcal{T})$ over $\overline{\Omega}$. Here $\mathcal{V}$ is the set of vertices, $\mathcal{E}$ that of edges, $\mathcal{F}$ that of faces and $\mathcal{T}$ the set of tetrahedra of $\mathcal{T}_h$. By $n_\mathcal{V}$, $n_\mathcal{E}$, $n_\mathcal{F}$, and $n_\mathcal{T}$ we denote their cardinalities, namely the number of vertices, edges, faces and tetrahedra of the mesh, respectively.

Fixing a total ordering $\mathbf{v}_1, \mathbf{v}_2, \ldots, \mathbf{v}_{n_\mathcal{V}}$ of the elements of $\mathcal{V}$ we induce an orientation of the edges, faces, and tetrahedra of $\mathcal{T}_h$.

- To any edge $e \in \mathcal{E}$ we can associate an increasing function $m_e : \{0,1\} \to \{1,2,\ldots,n_\mathcal{V}\}$ indicating the vertices of e. In this way we assign an (inner) orientation to e and by abuse of notation, the oriented edge $[\mathbf{v}_{m_e(0)}, \mathbf{v}_{m_e(1)}]$ is still denoted by e. The unit tangential vector to e is $\boldsymbol{\tau}_e = \frac{\mathbf{v}_{m_e(1)}-\mathbf{v}_{m_e(0)}}{|\mathbf{v}_{m_e(1)}-\mathbf{v}_{m_e(0)}|}$.
- We can associate an increasing function $m_f : \{0,1,2\} \to \{1,2,\ldots,n_\mathcal{V}\}$ indicating the vertices of f, to any face $f \in \mathcal{F}$. The oriented face $[\mathbf{v}_{m_f(0)}, \mathbf{v}_{m_f(1)}, \mathbf{v}_{m_f(2)}]$, by abuse of notation, is still denoted by f. Where $\mathbf{n}_f = \frac{(\mathbf{v}_{m_f(1)}-\mathbf{v}_{m_f(0)})\times(\mathbf{v}_{m_f(2)}-\mathbf{v}_{m_f(0)})}{|(\mathbf{v}_{m_f(1)}-\mathbf{v}_{m_f(0)})\times(\mathbf{v}_{m_f(2)}-\mathbf{v}_{m_f(0)})|}$. is the unit vector normal to f.

- To any tetrahedron $t \in \mathcal{T}$ we can associate an increasing function $m_t : \{0,1,2,3\} \to \{1,2,\ldots,n_{\mathcal{V}}\}$ indicating the vertices of t. By abuse of notation, the oriented tetrahedron $[\mathbf{v}_{m_t(0)}, \mathbf{v}_{m_t(1)}, \mathbf{v}_{m_t(2)}, \mathbf{v}_{m_t(3)}]$ is still denoted by t. The outward unit vector normal to the boundary ∂t of t is $\mathbf{n}_t$.

We will denote $\Delta_d(\mathcal{T}_h)$ the set of oriented subsimplex of $\mathcal{T}_h$ of dimension $d \leq 3$.

In the following λ_k will be the barycentric coordinate function of the vertex $\mathbf{v}_k$, namely, the continuous piecewise linear function ($\lambda_k|_t \in \mathbb{P}_1$ for all $t \in \mathcal{T}$) such that $\lambda_k(\mathbf{v}_j) = \delta_{k,j}$.

We will use multi-indices of the form

$$\boldsymbol{\eta} \in \mathcal{I}(n, d+1) = \left\{ \boldsymbol{\eta}^\top = (\eta_0, \ldots, \eta_d) \in \mathbb{N}^{d+1} \, : \sum_{i=0}^{d} \eta_i = n \right\}, \ \#\mathcal{I}(n, d+1) = \begin{pmatrix} n+d \\ d \end{pmatrix}.$$

For any $\boldsymbol{\eta} \in \mathcal{I}(n, d+1)$ we denote

$$a_{\boldsymbol{\eta}} = \frac{n!}{\eta_0! \eta_1! \cdots \eta_d!}.$$

Given $s \in \Delta_d(\mathcal{T}_h)$ and $\boldsymbol{\eta} \in \mathcal{I}(n, d+1)$ we denote

$$\lambda^{\boldsymbol{\eta}} = \prod_{i=0}^{d} \lambda_{m_s(i)}^{\eta_i}.$$

Note that

$$1 = \left(\sum_{i=0}^{d} \lambda_{m_s(i)}|_s \right)^n = \sum_{\boldsymbol{\eta} \in \mathcal{I}(n,d+1)} a_{\boldsymbol{\eta}} \, \lambda^{\boldsymbol{\eta}}. \tag{1.1}$$

Let $\mathcal{D}_{r+1}$ be the following space of vector polynomials of degree $r+1$ in $\mathbb{R}^3$:

$$\mathcal{D}_{r+1} := (\mathbb{P}_r)^3 \oplus \widetilde{\mathbb{P}}_r \, \boldsymbol{x},$$

being $\widetilde{\mathbb{P}}_r$ the space of homogeneous polynomials of degree r. The space of Raviart–Thomas finite elements of degree $r+1$ is

$$RT_{h,r+1} = \{ \mathbf{z}_h \in H(\mathrm{div}; \Omega) \, : \, \mathbf{z}_h|_t \in \mathcal{D}_{r+1} \, \forall \, t \in \mathcal{T} \}.$$

It is known that $\dim RT_{h,r+1} = d_{RT} = n_{\mathcal{F}} \begin{pmatrix} r+2 \\ 2 \end{pmatrix} + 3 n_{\mathcal{T}} \begin{pmatrix} r-1+3 \\ 3 \end{pmatrix}$. This space have been introduced in [56], but originally it had been introduced in [62] for $\Omega \subset \mathbb{R}^2$.

We denote $P_{h,r}$ the space of discontinuous finite elements that are piecewise polynomial of degree r, namely,

$$P_{h,r} = \{p \in L^2(\Omega) \,:\, p|_t \in \mathbb{P}_r \,\forall\, t \in \mathcal{T}\}\,.$$

It is known that $\dim P_{h,r} = d_P = n_{\mathcal{T}} \binom{r+3}{3}$.

For a brief overview of these spaces and of the Nédélec finite elements of degree $r+1$ that will be mentioned in Section 1.5, see, e.g., [54]. The classical set of degrees of freedom used to identify the elements of $RT_{h,r+1}$ are moments supported in faces

$$\int_f \mathbf{z}_h \cdot \mathbf{n}_f \, q\,, \quad q \in \mathbb{P}_r(f)\,,\ f \in \mathcal{F}\,,$$

and moments supported in tetrahedra

$$\int_t \mathbf{z}_h \cdot \mathbf{q}\,, \quad \mathbf{q} \in [\mathbb{P}_{r-1}(t)]^3\,,\ t \in \mathcal{T}\,.$$

Similarly, the classical set of degrees of freedom used to identify the elements of $P_{h,r}$ are moments supported in tetrahedra

$$\int_t p_h \, q\,, \quad q \in \mathbb{P}_r(t)\,,\ t \in \mathcal{T}\,.$$

Since we are free to choose any basis of the spaces $\mathbb{P}_r(f)$, $[\mathbb{P}_{r-1}(t)]^3$ and $\mathbb{P}_r(t)$, a possibility is to consider the following set of moments for $RT_{h,r+1}$:

$$C_{\boldsymbol{\alpha}'} \int_f \mathbf{z}_h \cdot \mathbf{n}_f \, \lambda^{\boldsymbol{\alpha}'} \text{ with } \boldsymbol{\alpha}' \in \mathcal{I}(r,3)\,,\ f \in \mathcal{F}\,,$$

and

$$\widehat{C}_{\boldsymbol{\beta}} \int_t \mathbf{z}_h \cdot \lambda^{\boldsymbol{\beta}} \operatorname{grad} \lambda_{m_t(j)}\,,\ \text{with } \boldsymbol{\beta} \in \mathcal{I}(r-1,4)\,,\ 1 \le j \le 3\,,\ t \in \mathcal{T}\,.$$

For $P_{h,r}$ one can consider moments of the form

$$C_{\boldsymbol{\alpha}} \int_t p_h \, \lambda^{\boldsymbol{\alpha}} \text{ with } \boldsymbol{\alpha} \in \mathcal{I}(r,4)\,,\ t \in \mathcal{T}\,.$$

Here, $C_{\boldsymbol{\alpha}}$, $C_{\boldsymbol{\alpha}'}$ and $\widehat{C}_{\boldsymbol{\beta}}$ are real numbers. We anticipate that we have introduced some parameters in the definition of moments to have the divergence operator represented by an incidence matrix in the high order case, as it occurs naturally in the low order case. We will thus set, for any $\boldsymbol{\eta} \in \mathcal{I}(n, d+1)$,

$$C_{\boldsymbol{\eta}} = a_{\boldsymbol{\eta}} \text{ and } \widehat{C}_{\boldsymbol{\eta}} = (n+1) a_{\boldsymbol{\eta}}\,.$$

We recall some basic definitions and results of graph theory that will be used later (they can be found, for instance, in [68]).

Definition 1.1. *The all-nodes incidence matrix $M^e \in \mathbb{Z}^{n\times m}$ of a directed graph $\mathcal{M} = (\mathcal{N}, \mathcal{A})$, with n nodes $\mathcal{N} = \{\mathfrak{n}_i\}_{i=1}^n$, m arcs $\mathcal{A} = \{\mathfrak{a}_j\}_{j=1}^m$ and with no self-loop, is the matrix with entries*

$$[M^e]_{i,j} = \begin{cases} 1 & \text{if } \mathfrak{a}_j \text{ is incident on } \mathfrak{n}_i \text{ and oriented away from it,} \\ -1 & \text{if } \mathfrak{a}_j \text{ is incident on } \mathfrak{n}_i \text{ and oriented toward it,} \\ 0 & \text{if } \mathfrak{a}_j \text{ is not incident on } \mathfrak{n}_i\,. \end{cases}$$

An incidence matrix M of $\mathcal{M}$ is any submatrix of M^e with $n-1$ rows and m columns. The node that corresponds to the row of M^e that is not in M will be called the reference node of M.

Note that

$$\operatorname{rank} M^e = \operatorname{rank} M \leq n-1\,,$$

and if $\mathcal{M}$ is connected, then $\operatorname{rank} M^e = \operatorname{rank} M = n-1$, see, e.g., [68, Thm. 6.2].

We recall the definition of spanning tree of a graph $\mathcal{M} = (\mathcal{N}, \mathcal{A})$.

Definition 1.2. *A tree of a graph $\mathcal{M} = (\mathcal{N}, \mathcal{A})$ is a connected acyclic subgraph of $\mathcal{M}$. A spanning tree $\mathcal{S}$ is a tree of $\mathcal{M}$ containing all its nodes.*

If $\mathcal{S}$ is a spanning tree of $\mathcal{M} = (\mathcal{N}, \mathcal{A})$, then $\mathcal{S} = (\mathcal{N}, \mathcal{B})$ with $\mathcal{B} \subset \mathcal{A}$. Moreover $\mathcal{B}$ has exactly $n-1$ arcs.

In the next sections we will use the following result that joins Theorem 6.9 and Theorem 6.12 in [68].

Theorem 1.1. *Let $\mathcal{M} = (\mathcal{N}, \mathcal{A})$ be a directed connected graph with no self-loop and $M \in \mathbb{Z}^{(n-1)\times m}$ an incidence matrix of $\mathcal{M}$. Let $\mathcal{S} = (\mathcal{N}, \mathcal{B})$ be a spanning tree of $\mathcal{M}$ and M_{st} the submatrix of order $n-1$ of M given by the columns of M that correspond to the arcs in $\mathcal{B}$. Then M_{st} is invertible and the nonzero elements in each row of M_{st}^{-1} are either all 1 or all -1.*

Proof. The proof can be found, for instance, in [68]. However, for the sake of completeness, we recall in the sequel the main ideas. Each column of M_{st} corresponds to an arc of the spanning tree $\mathcal{S} = (\mathcal{N}, \mathcal{B})$ with $\mathcal{B} = \{\mathfrak{a}_{j(k)}\}_{k=1}^{n-1}$, for a certain function $j : \{1, \ldots, n-1\} \to \{1, \ldots, m\}$.

Each arc $\mathfrak{a}_{j(k)} \in \mathcal{B}$ divides the graph $\mathcal{S}$ in two connected components $\mathcal{S}_r^{(k)}$ and $\mathcal{S}_{nr}^{(k)}$; (the subindex r refers to reference node). We will denote $\mathcal{S}_r^{(k)} = (\mathcal{N}_r^{(k)}, \mathcal{B}_r^{(k)})$ the connected component containing the reference node and $\mathcal{S}_{nr}^{(k)} = (\mathcal{N}_{nr}^{(k)}, \mathcal{B}_{nr}^{(k)})$ the other one. We associate

to $\mathfrak{a}_{j(k)}$ the vector $\mathbf{w}^{(k)} \in \mathbb{Z}^{n-1}$ with components:

$$[\mathbf{w}^{(k)}]_i = \begin{cases} -1 & \text{if } \mathfrak{n}_i \notin \mathcal{N}_r^{(k)} \text{ and } \mathfrak{a}_{j(k)} \text{ points from } \mathcal{S}_r^{(k)} \text{ to } \mathcal{S}_{nr}^{(k)}\,, \\ 1 & \text{if } \mathfrak{n}_i \notin \mathcal{N}_r^{(k)} \text{ and } \mathfrak{a}_{j(k)} \text{ points from } \mathcal{S}_{nr}^{(k)} \text{ to } \mathcal{S}_r^{(k)}\,, \\ 0 & \text{if } \mathfrak{n}_i \in \mathcal{N}_r^{(k)}\,. \end{cases}$$

Now we will check that

$$[(\mathbf{w}^{(k)})^\top M_{st}]_l = \delta_{k,l}\,.$$

In fact, $[(\mathbf{w}^{(k)})^\top M_{st}]_l$ is the scalar product of the vector $\mathbf{w}^{(k)}$ and the column of M_{st} corresponding to the arc $\mathfrak{a}_{j(l)}$.

If the reference node is an extreme node of $\mathfrak{a}_{j(l)}$, then

- for $k \neq l$, the extreme node of $\mathfrak{a}_{j(l)}$ that is not the reference node, is in $\mathcal{N}_r^{(k)}$, hence $[(\mathbf{w}^{(k)})^\top M_{st}]_l = (0)\,(1) = 0$ (if the extreme node, that is not the reference node, is the initial one), or $[(\mathbf{w}^{(k)})^\top M_{st}]_l = (0)\,(-1) = 0$ (if the extreme node, that is not the reference node, is the final one);
- for $k = l$, the extreme node of $\mathfrak{a}_{j(l)}$ that is not the reference node, is not in $\mathcal{N}_r^{(k)}$. If $\mathfrak{a}_{j(k)}$ points from $\mathcal{S}_r^{(k)}$ to $\mathcal{S}_{nr}^{(k)}$, then $[(\mathbf{w}^{(k)})^\top M_{st}]_l = (-1)\,(-1) = 1$ while if $\mathfrak{a}_{j(k)}$ points from $\mathcal{S}_{nr}^{(k)}$ to $\mathcal{S}_r^{(k)}$, then $[(\mathbf{w}^{(k)})^\top M_{st}]_l = (1)\,(1) = 1$.

If the reference node is not an extreme node of $\mathfrak{a}_{j(l)}$, then

- for $k \neq l$, the two extreme nodes of the arc $\mathfrak{a}_{j(l)}$, $\mathfrak{n}_i^l$ and $\mathfrak{n}_{i'}^l$ are in the same connected component $\mathcal{S}_r^{(k)}$ or $\mathcal{S}_{nr}^{(k)}$; we have

$$[(\mathbf{w}^{(k)})^\top M_{st}]_l = \begin{cases} (-1)\,(-1) + (1)\,(-1) & \text{if } \mathfrak{n}_i^l\,,\ \mathfrak{n}_{i'}^l \notin \mathcal{N}_r^{(k)} \text{ and } \mathfrak{a}_{j(k)} \\ & \quad \text{points from } \mathcal{S}_r^{(k)} \text{ to } \mathcal{S}_{nr}^{(k)} \\ (-1)\,(1) + (1)\,(1) & \text{if } \mathfrak{n}_i^l\,,\ \mathfrak{n}_{i'}^l \notin \mathcal{N}_r^{(k)} \text{ and } \mathfrak{a}_{j(k)} \\ & \quad \text{points from } \mathcal{S}_{nr}^{(k)} \text{ to } \mathcal{S}_r^{(k)} \\ (-1)\,(0) + (1)\,(0) & \text{if } \mathfrak{n}_i^l\,,\ \mathfrak{n}_{i'}^l \in \mathcal{N}_r^{(k)} \end{cases}$$

  so $[(\mathbf{w}^{(k)})^\top M_{st}]_l = 0$;
- for $k = l$, one of the extreme nodes of $\mathfrak{a}_{j(l)}$ is in $\mathcal{N}_r^{(k)}$ and the other is not. If $\mathfrak{a}_{j(k)}$ points from $\mathcal{S}_r^{(k)}$ to $\mathcal{S}_{nr}^{(k)}$, then the final node of $\mathfrak{a}_{j(k)}$ (with entry equal -1 in the k-th column of M_{st}) is not in $\mathcal{N}_r^{(k)}$ and the scalar product is $(-1)\,(-1)+(0)\,(1) = 1$. If $\mathfrak{a}_{j(k)}$ points from $\mathcal{S}_{nr}^{(k)}$ to $\mathcal{S}_r^{(k)}$, then the initial node of $\mathfrak{a}_{j(k)}$ (with entry equal 1 in the k-th column of M_{st}) is not in $\mathcal{N}_r^{(k)}$ and the scalar product now is $(1)\,(1) + (0)\,(-1) = 1$.

So, it follows that M_{st}^{-1} is the matrix with entries

$$[M_{st}^{-1}]_{k,j} = [\mathbf{w}^{(k)}]_j \,,$$

since we have showed that

$$\sum_j [M_{st}^{-1}]_{k,j}[M_{st}]_{j,l} = \sum_j [\mathbf{w}^{(k)}]_j [M_{st}]_{j,l} = \delta_{k,l} \,.$$

□

1.3 The divergence matrix

Our aim now is to identify the matrix that relates the moments of $\mathbf{z}_h \in RT_{h,r+1}$ with the moments of $p_h = \operatorname{div} \mathbf{z}_h \in P_{h,r}$. From the divergence theorem in a tetrahedron, for any $\boldsymbol{\alpha} \in \mathcal{I}(r,4)$ we have

$$\int_t p_h a_{\boldsymbol{\alpha}} \lambda^{\boldsymbol{\alpha}} = \int_t \operatorname{div} \mathbf{z}_h a_{\boldsymbol{\alpha}} \lambda^{\boldsymbol{\alpha}} = \int_{\partial t} \mathbf{z}_h \cdot \mathbf{n}_t \, a_{\boldsymbol{\alpha}} \lambda^{\boldsymbol{\alpha}} - \int_t \mathbf{z}_h \cdot a_{\boldsymbol{\alpha}} \operatorname{grad} \lambda^{\boldsymbol{\alpha}} \,. \tag{1.2}$$

Note that

$$\operatorname{grad} \lambda^{\boldsymbol{\alpha}} = \sum_{i=0}^{d} \alpha_i \lambda^{\boldsymbol{\alpha}-\mathbf{e}_i} \operatorname{grad} \lambda_{m_t(i)} \,,$$

being $\mathbf{e}_i \in \mathbb{N}^4$ the vector with components $(\mathbf{e}_i)_j = \delta_{i,j}$, $0 \le i,j \le 3$. Clearly $\alpha_i \lambda^{\boldsymbol{\alpha}-\mathbf{e}_i}$ is zero if $\alpha_i = 0$, otherwise it is a polynomial of degree $r-1$ of the form $\alpha_i \lambda^{\boldsymbol{\beta}}$ with $\boldsymbol{\beta} \in \mathcal{I}(r-1,4)$. We recall also that, since $1 = \sum_{i=0}^{d} \lambda_{m_t(i)}$, then $\operatorname{grad} \lambda_{m_t(0)} = -\sum_{i=1}^{d} \operatorname{grad} \lambda_{m_t(i)}$ on the tetrahedron t. So we have

$$\operatorname{grad} \lambda^{\boldsymbol{\alpha}} = \sum_{i=1}^{d} \left(\alpha_i \lambda^{\boldsymbol{\alpha}-\mathbf{e}_i} - \alpha_0 \lambda^{\boldsymbol{\alpha}-\mathbf{e}_0} \right) \operatorname{grad} \lambda_{m_t(i)} \,.$$

Finally we note that $a_{\boldsymbol{\alpha}} \alpha_i = \frac{r!}{\alpha_0! \cdots \alpha_3!} \alpha_i = r a_{\boldsymbol{\alpha}-\mathbf{e}_i}$, hence

$$\int_t \mathbf{z}_h \cdot a_{\boldsymbol{\alpha}} \operatorname{grad} \lambda^{\boldsymbol{\alpha}} = \sum_{i=1}^{d} \int_t \mathbf{z}_h \cdot \left(r a_{\boldsymbol{\alpha}-\mathbf{e}_i} \lambda^{\boldsymbol{\alpha}-\mathbf{e}_i} - r a_{\boldsymbol{\alpha}-\mathbf{e}_0} \lambda^{\boldsymbol{\alpha}-\mathbf{e}_0} \right) \operatorname{grad} \lambda_{m_t(i)} \,.$$

Here $\boldsymbol{\alpha} \in \mathcal{I}(r,4)$. However, if $f \in \partial t$ and $\mathbf{v}_{m_t(i)} \notin f$, then

$$(a_{\boldsymbol{\alpha}} \lambda^{\boldsymbol{\alpha}})|_f = \begin{cases} 0 & \text{if } \alpha_i \neq 0 \,, \\ a_{\boldsymbol{\alpha}'} \lambda^{\boldsymbol{\alpha}'} \text{ for a certain } \boldsymbol{\alpha}' \in \mathcal{I}(r,3) & \text{if } \alpha_i = 0 \,. \end{cases}$$

The multi-index $\boldsymbol{\alpha}' \in \mathcal{I}(r,3)$ is $R_{t,f}\boldsymbol{\alpha}$, being $R_{t,f} \in \mathbb{Z}^{3\times 4}$ the matrix obtained from the 4×4 identity matrix by omitting the i-th row. For instance, if $f = [\mathbf{v}_{m_t(0)}, \mathbf{v}_{m_t(2)}, \mathbf{v}_{m_t(3)}]$, then

$$\boldsymbol{\alpha}' = R_{t,f}\boldsymbol{\alpha} = \begin{bmatrix} 1 & 0 & 0 & 0 \\ 0 & 0 & 1 & 0 \\ 0 & 0 & 0 & 1 \end{bmatrix} \boldsymbol{\alpha} = \begin{pmatrix} \alpha_0 \\ \alpha_2 \\ \alpha_3 \end{pmatrix}.$$

Notice that, since $\alpha_i = 0$, then $a_{\boldsymbol{\alpha}'} = a_{\boldsymbol{\alpha}}$. Hence

$$\int_{\partial t} \mathbf{z}_h \cdot \mathbf{n}_t \, a_{\boldsymbol{\alpha}} \lambda^{\boldsymbol{\alpha}} = \sum_{f\in\partial t} \mathbf{n}_f \cdot \mathbf{n}_t \int_f \mathbf{z}_h \cdot \mathbf{n}_f \, a_{(R_{t,f}\boldsymbol{\alpha})} \lambda^{(R_{t,f}\boldsymbol{\alpha})},$$

and for each $f \in \partial t$, the multi-index $\boldsymbol{\alpha}' = R_{t,f}\boldsymbol{\alpha}$ is in $\mathcal{I}(r,3)$, as it is the case in moments supported in faces.

So, equation (1.2) reads

$$\begin{aligned} \int_t \operatorname{div} \mathbf{z}_h a_{\boldsymbol{\alpha}} \lambda^{\boldsymbol{\alpha}} \;=\; & \sum_{f\in\partial t} \mathbf{n}_f \cdot \mathbf{n}_t \int_f \mathbf{z}_h \cdot \mathbf{n}_f \, a_{(R_{t,f}\boldsymbol{\alpha})} \lambda^{(R_{t,f}\boldsymbol{\alpha})} \\ & - \sum_{i=1}^{d} \int_t \mathbf{z}_h \cdot \left(r a_{\boldsymbol{\alpha}-\mathbf{e}_i} \lambda^{\boldsymbol{\alpha}-\mathbf{e}_i} - r a_{\boldsymbol{\alpha}-\mathbf{e}_0} \lambda^{\boldsymbol{\alpha}-\mathbf{e}_0} \right) \operatorname{grad} \lambda_{m_t(i)} \,. \end{aligned} \tag{1.3}$$

Let $\mathbf{p} \in \mathbb{R}^{d_P}$ be the vector with entries the moments of $p_h = \operatorname{div} \mathbf{z}_h \in P_{h,r}$ and $\mathbf{Z} \in \mathbb{R}^{d_{RT}}$ the vector with entries the moments of $\mathbf{z}_h \in RT_{h,r+1}$, then we can write (1.3) as:

$$\mathbf{p} = D_{\mathcal{T}_h} \mathbf{Z} \,,$$

where the matrix $D_{\mathcal{T}_h}$ is the matrix associated to the divergence operator that is, in fact, a linear operator from $RT_{h,r+1}$ to $P_{h,r}$.

From the divergence theorem in the whole domain Ω we have also

$$\int_\Omega p_h = \int_\Omega \operatorname{div} \mathbf{z}_h = \int_{\partial\Omega} \mathbf{z}_h \cdot \mathbf{n}_{\partial\Omega} = \sum_{f\in\partial\Omega} \left(\mathbf{n}_f \cdot \mathbf{n}_{\partial\Omega}|_f \int_f \mathbf{z}_h \cdot \mathbf{n}_f \right),$$

where $\mathbf{n}_{\partial\Omega}$ denotes the outward unit vector normal to the boundary $\partial\Omega$. From (1.1) we have

$$1 = \sum_{\boldsymbol{\alpha}'\in\mathcal{I}(r,3)} a_{\boldsymbol{\alpha}'} \, \lambda^{\boldsymbol{\alpha}'}\Big|_f$$

for any $f \in \mathcal{F}$. Hence

$$-\int_\Omega \operatorname{div} \mathbf{z}_h = -\sum_{f\in\partial\Omega} \left(\mathbf{n}_f \cdot \mathbf{n}_{\partial\Omega}|_f \sum_{\boldsymbol{\alpha}'\in\mathcal{I}(r,3)} \int_f \mathbf{z}_h \cdot \mathbf{n}_f a_{\boldsymbol{\alpha}'} \lambda^{\boldsymbol{\alpha}'} \right). \tag{1.4}$$

Denoting $\mathbf{p}^e \in \mathbb{R}^{d_P+1}$ the vector $\mathbf{p}^e = [\mathbf{p}^\top, -\int_\Omega p_h]^\top$, we can write (1.3) and (1.4) as

$$\mathbf{p}^e = D^e_{\mathcal{T}_h}\mathbf{Z}\,.$$

Proposition 1.1. *The matrix $D^e_{\mathcal{T}_h}$ is the all-nodes incidence matrix of an oriented graph $\mathcal{M} = (\mathcal{N}, \mathcal{A})$ with d_P+1 nodes: $\binom{r+3}{3}$ for each tetrahedron plus one corresponding to $\partial\Omega$, and d_{RT} arcs. The divergence matrix $D_{\mathcal{T}_h}$ is the incidence matrix with reference node the one corresponding to $\partial\Omega$.*

Proof. To see that each column of $D^e_{\mathcal{T}_h}$ has exactly two elements different from zero, one equal 1 and the other equal -1, we note that each column corresponds to a face moment

$$\int_f \mathbf{z}_h \cdot \mathbf{n}_f\, a_{\boldsymbol{\alpha}'}\lambda^{\boldsymbol{\alpha}'},\ f \in \mathcal{F},\ \boldsymbol{\alpha}' \in \mathcal{I}(r,3)\,,$$

or to a tetrahedron moment

$$\int_t \mathbf{z}_h r a_{\boldsymbol{\beta}}\lambda^{\boldsymbol{\beta}}\,\mathrm{grad}\,\lambda_{m_t(i)},\ t \in \mathcal{T},\ \boldsymbol{\beta} \in \mathcal{I}(r-1,4),\ i = 1,2,3\,.$$

The faces can be internal, if their interior is in Ω, or they can be on the boundary of Ω.

- If f is an internal face, then it belongs to two different tetrahedra, t^- and t^+. Hence, in the column that corresponds to the moment $\int_f \mathbf{z}_h\cdot\mathbf{n}_f a_{\boldsymbol{\alpha}'}\lambda^{\boldsymbol{\alpha}'}$, there are two entries different from zero, one in the row corresponding to the moment $\int_{t^-} p_h a_{(R^\top_{t^-,f}\boldsymbol{\alpha}')}\lambda^{(R^\top_{t^-,f}\boldsymbol{\alpha}')}$ and another one in the row corresponding to the moment $\int_{t^+} p_h a_{(R^\top_{t^+,f}\boldsymbol{\alpha}')}\lambda^{(R^\top_{t^+,f}\boldsymbol{\alpha}')}$. They have opposite sign, because the non zero coefficients are $\mathbf{n}_f\cdot\mathbf{n}_{t^-}$ and $\mathbf{n}_f\cdot\mathbf{n}_{t^+}$, with $\mathbf{n}_{t^-} = -\mathbf{n}_{t^+}$.
- If f is on the boundary of Ω, then it belongs to just one tetrahedron, say $\hat{t}$, and, on f, $\mathbf{n}_{\hat{t}} = \mathbf{n}_{\partial\Omega}$. In the column that corresponds to the moment $\int_f \mathbf{z}_h\cdot\mathbf{n}_f a_{\boldsymbol{\alpha}'}\lambda^{\boldsymbol{\alpha}'}$ there is one entry different from zero in the row corresponding to the moment $\int_{\hat{t}} p_h a_{(R^\top_{\hat{t},f}\boldsymbol{\alpha}')}\lambda^{(R^\top_{\hat{t},f}\boldsymbol{\alpha}')}$. This entry is equal to $\mathbf{n}_f\cdot\mathbf{n}_{\hat{t}}$. There is another entry different from zero in the row corresponding to $\partial\Omega$ with opposite signs, because it is equal to $-(\mathbf{n}_f\cdot\mathbf{n}_{\partial\Omega}) = -(\mathbf{n}_f\cdot\mathbf{n}_{\hat{t}})$.
- The column corresponding to $\int_t \mathbf{z}_h r a_{\boldsymbol{\beta}}\lambda^{\boldsymbol{\beta}}\,\mathrm{grad}\,\lambda_{m_t(i)}$ has two entries different from zero: one in the row corresponding to $\int_t p_h a_{\boldsymbol{\beta}+\mathbf{e}_0}\lambda^{\boldsymbol{\beta}+\mathbf{e}_0}$, and the other in the row corresponding to $\int_t p_h a_{\boldsymbol{\beta}+\mathbf{e}_i}\lambda^{\boldsymbol{\beta}+\mathbf{e}_i}$ with opposite sign as can be seen in (1.3). □

Proposition 1.2. *The graph $\mathcal{M} = (\mathcal{N}, \mathcal{A})$ corresponding to the all-nodes incidence matrix $D^e_{\mathcal{T}_h}$ is connected.*

Proof. Let us recall that the set of nodes $\mathcal{N}$ is composed by elements of the form

$$\int_t \operatorname{div} \mathbf{z}_h \, a_{\boldsymbol{\alpha}} \lambda^{\boldsymbol{\alpha}} \,, \ t \in \mathcal{T} \,, \ \boldsymbol{\alpha} \in \mathcal{I}(r,4) \qquad \text{and} \qquad \int_{\partial\Omega} \mathbf{z}_h \cdot \mathbf{n}_{\partial\Omega} \,,$$

(that we will denote by $[\boldsymbol{\alpha}, t]$ and $[\partial\Omega]$, respectively) and the set of arcs $\mathcal{A}$, by elements of the form

$$\int_f \mathbf{z}_h \cdot \mathbf{n}_f a_{\boldsymbol{\alpha}'} \lambda^{\boldsymbol{\alpha}'} \,, \ f \in \mathcal{F} \,, \ \boldsymbol{\alpha}' \in \mathcal{I}(r,3)$$

and

$$\int_t \mathbf{z}_h \cdot r a_{\boldsymbol{\beta}} \lambda^{\boldsymbol{\beta}} \operatorname{grad} \lambda_{m_t(i)}, \ t \in \mathcal{T}, \ \boldsymbol{\beta} \in \mathcal{I}(r-1,4), \ i = 1,2,3,$$

(that we will denote by $[\boldsymbol{\alpha}', f]$, and $[\boldsymbol{\beta}, t, i]$, respectively). As consequence of the divergence theorem, we observe that

(i) for a fixed $t \in \mathcal{T}$ and any $\boldsymbol{\beta} \in \mathcal{I}(r-1,4)$ the arc $[\boldsymbol{\beta}, t, i]$ link the nodes $[\boldsymbol{\beta} + \mathbf{e}_0, t]$ and $[\boldsymbol{\beta} + \mathbf{e}_i, t]$, $i = 1,2,3$.

(ii) for any $\boldsymbol{\alpha}' \in \mathcal{I}(r,3)$, the arc $[\boldsymbol{\alpha}', f]$ link the nodes

$[R^\top_{t^-,f}\boldsymbol{\alpha}', t^-]$ and $[R^\top_{t^+,f}\boldsymbol{\alpha}', t^+]$, if f is an internal face such that $f = \partial t^+ \cap \partial t^-$ with $t^+, t^- \in \mathcal{T}$.

$[R^\top_{t,f}\boldsymbol{\alpha}', t]$ and $[\partial\Omega]$, if f is a face on the boundary of Ω, namely, $f \subseteq \partial t \cap \partial\Omega$ for some $t \in \mathcal{T}$.

Now we will show that, for a fixed $t \in \mathcal{T}$, any two nodes of the set $S(t) = \{[\boldsymbol{\alpha}, t] : \boldsymbol{\alpha} \in \mathcal{I}(r,4)\}$ are connected. More precisely we will show that any node $[\boldsymbol{\alpha}, t] \in S(t)$ is connected with the node $[\overline{\boldsymbol{\alpha}}, t] = [(r,0,0,0), t] \in S(t)$. In fact, by using (i), it is possible to construct a path of length α_1 between the node $[\overline{\boldsymbol{\alpha}}, t]$ and the node $[(r-\alpha_1, \alpha_1, 0, 0), t]$. In the same way, there exists a path of length α_2 between the nodes $[(r-\alpha_1, \alpha_1, 0, 0), t]$ and $[(r-\alpha_1-\alpha_2, \alpha_1, \alpha_2, 0), t]$ and finally, a path of length α_3 between the nodes $[(r-\alpha_1-\alpha_2, \alpha_1, \alpha_2, 0), t]$ and $[(r-\alpha_1-\alpha_2-\alpha_3, \alpha_1, \alpha_2, \alpha_3), t] = [\boldsymbol{\alpha}, t]$. Thus, the nodes $[\overline{\boldsymbol{\alpha}}, t]$ and $[\boldsymbol{\alpha}, t]$ are connected.

Moreover if f is an internal face, then there exists t_1 and t_2 in $\mathcal{T}$ such that $f = \partial t_1 \cap \partial t_2$. From (ii), we know that any arc $[\boldsymbol{\alpha}', f]$ connects the nodes $[R^\top_{t_1,f}\boldsymbol{\alpha}', t_1]$ and $[R^\top_{t_2,f}\boldsymbol{\alpha}', t_2]$. On the other hand, if f is a face on the boundary of Ω, then $f \subseteq \partial t \cap \partial\Omega$ for some $t \in \mathcal{T}$. In this case, the arc $[\boldsymbol{\alpha}', f]$ connects the nodes $[R^\top_{t,f}\boldsymbol{\alpha}', t]$ and $[\partial\Omega]$.

Since Ω is connected we can arrive from any tetrahedron in the mesh to any other following a path constructed by its common faces and this fact guarantees that all nodes are connected. □

Example 1: the case $r = 1$.
The moments of $p_h \in P_{h,1}$ are $\int_t p_h \lambda_{m_t(i)}$ for all $t \in \mathcal{T}$. So, for $0 \le i \le 3$ we have

$$\int_t \operatorname{div} \mathbf{z}_h \ \lambda_{m_t(i)} = \int_{\partial t} \mathbf{z}_h \cdot \mathbf{n}_t \ \lambda_{m_t(i)} - \int_t \mathbf{z}_h \cdot \operatorname{grad} \lambda_{m_t(i)} \,. \tag{1.5}$$

Moreover

$$\begin{aligned} \partial[\mathbf{v}_{m_t(0)}, \mathbf{v}_{m_t(1)}, \mathbf{v}_{m_t(2)}, \mathbf{v}_{m_t(3)}] \ &= \ -[\mathbf{v}_{m_t(0)}, \mathbf{v}_{m_t(1)}, \mathbf{v}_{m_t(2)}] + [\mathbf{v}_{m_t(0)}, \mathbf{v}_{m_t(1)}, \mathbf{v}_{m_t(3)}] \\ &\quad -[\mathbf{v}_{m_t(0)}, \mathbf{v}_{m_t(2)}, \mathbf{v}_{m_t(3)}] + [\mathbf{v}_{m_t(1)}, \mathbf{v}_{m_t(2)}, \mathbf{v}_{m_t(3)}] \,. \end{aligned}$$

This means that

$$\begin{aligned} \mathbf{n}_t\big|_{[\mathbf{v}_{m_t(0)}, \mathbf{v}_{m_t(1)}, \mathbf{v}_{m_t(2)}]} &= -\mathbf{n}_{[\mathbf{v}_{m_t(0)}, \mathbf{v}_{m_t(1)}, \mathbf{v}_{m_t(2)}]} \,, \\ \mathbf{n}_t\big|_{[\mathbf{v}_{m_t(0)}, \mathbf{v}_{m_t(1)}, \mathbf{v}_{m_t(3)}]} &= \mathbf{n}_{[\mathbf{v}_{m_t(0)}, \mathbf{v}_{m_t(1)}, \mathbf{v}_{m_t(3)}]} \,, \\ \mathbf{n}_t\big|_{[\mathbf{v}_{m_t(0)}, \mathbf{v}_{m_t(2)}, \mathbf{v}_{m_t(3)}]} &= -\mathbf{n}_{[\mathbf{v}_{m_t(0)}, \mathbf{v}_{m_t(2)}, \mathbf{v}_{m_t(3)}]} \,, \\ \mathbf{n}_t\big|_{[\mathbf{v}_{m_t(1)}, \mathbf{v}_{m_t(2)}, \mathbf{v}_{m_t(3)}]} &= \mathbf{n}_{[\mathbf{v}_{m_t(1)}, \mathbf{v}_{m_t(2)}, \mathbf{v}_{m_t(3)}]} \,. \end{aligned}$$

Finally, taking into account that $\operatorname{grad} \lambda_{m_t(0)} = -\sum_{i=1}^{d} \operatorname{grad} \lambda_{m_t(i)}$, we see that the matrix D_t relating the moments of $p_h = \operatorname{div} \mathbf{z}_h \in P_{h,1}$ and $\mathbf{z}_h \in RT_{h,2}$ in a tetrahedron t is

$$D_t = \begin{array}{c} \\ [0\,1\,2] \\ [0\,1\,3] \\ [0\,2\,3] \\ [1\,2\,3] \end{array} \begin{array}{c} \begin{array}{ccc} [0\,1\,2] & [0\,1\,3] & [0\,2\,3] \end{array} \\ \left[\begin{array}{ccc|ccc|ccc|ccc|ccc} -1 & 0 & 0 & 1 & 0 & 0 & -1 & 0 & 0 & 0 & 0 & 0 & 1 & 1 & 1 \\ 0 & -1 & 0 & 0 & 1 & 0 & 0 & 0 & 0 & 1 & 0 & 0 & -1 & 0 & 0 \\ 0 & 0 & -1 & 0 & 0 & 0 & 0 & -1 & 0 & 0 & 1 & 0 & 0 & -1 & 0 \\ 0 & 0 & 0 & 0 & 0 & 1 & 0 & 0 & -1 & 0 & 0 & 1 & 0 & 0 & -1 \end{array}\right] \\ \begin{array}{ccc} [0\,1\,2] & [0\,1\,3] & [1\,2\,3] \end{array} \end{array} \begin{array}{c} \\ [0\,1\,2\,3] \,. \end{array}$$

When assembling the whole matrix, $D_{\mathcal{T}_h}$, relating the moments of p_h and $\mathbf{z}_h$, we will have four lines for each tetrahedron, three columns for each face and another three columns for each tetrahedron. In the three columns corresponding to an internal face, there are exactly two non null blocks of four lines corresponding to the two tetrahedra sharing this face. The non zero elements on each block have opposite signs, due to the different orientation of the face on the boundary of the two tetrahedra. On the other hand, each boundary face has exactly one non zero block on its columns, because such a face belongs to the boundary of just one tetrahedron.

Let us consider now the matrix D_t^e that incorporates to D_t a row corresponding to the

equation (1.4)

$$D_t^e = \left[\begin{array}{ccc|ccc|ccc|ccc|ccc} -1 & 0 & 0 & 1 & 0 & 0 & -1 & 0 & 0 & 0 & 0 & 0 & 1 & 1 & 1 \\ 0 & -1 & 0 & 0 & 1 & 0 & 0 & 0 & 0 & 1 & 0 & 0 & -1 & 0 & 0 \\ 0 & 0 & -1 & 0 & 0 & 0 & 0 & -1 & 0 & 0 & 1 & 0 & 0 & -1 & 0 \\ 0 & 0 & 0 & 0 & 0 & 1 & 0 & 0 & -1 & 0 & 0 & 1 & 0 & 0 & -1 \\ \hline 1 & 1 & 1 & -1 & -1 & -1 & 1 & 1 & 1 & -1 & -1 & -1 & 0 & 0 & 0 \end{array}\right].$$

The last (blue) row is the one corresponding to equation (1.4).

Example 2: the case $r = 2$.
The moments of $p_h \in P_{h,2}$ are $\int_t p_h \left(a_{i,j}\lambda_{m_t(i)}\lambda_{m_t(j)}\right)$, for all $t \in \mathcal{T}$, with $0 \le i \le j \le 3$ and

$$a_{i,j} = \begin{cases} 1 & \text{if } i = j\,, \\ 2 & \text{if } i \neq j\,. \end{cases}$$

The face moments in $RT_{h,3}$ are

$$\int_f \mathbf{z}_h \cdot \mathbf{n}_f (a_{i,j}\lambda_{m_f(i)}\lambda_{m_f(j)})\,, \quad 0 \le i \le j \le 2\,,$$

and the tetrahedron moments are

$$\int_t \mathbf{z}_h \cdot (2\,\lambda_{m_t(i)}\,\mathrm{grad}\,\lambda_{m_t(j)})\,, \quad 0 \le i \le 3\,, \quad 1 \le j \le 3\,.$$

So

$$\int_t \mathrm{div}\,\mathbf{z}_h\,(a_{i,j}\lambda_{m_t(i)}\lambda_{m_t(j)}) = \int_{\partial t} \mathbf{z}_h \cdot \mathbf{n}_t\,(a_{i,j}\lambda_{m_t(i)}\lambda_{m_t(j)}) - \int_t \mathbf{z}_h\ \mathrm{grad}(a_{i,j}\lambda_{m_t(i)}\lambda_{m_t(j)})\,,$$

where $\mathrm{grad}\,\lambda_{m_t(0)} = -\sum_{i=1}^{d} \mathrm{grad}\,\lambda_{m_t(i)}$ and

$$\mathrm{grad}(a_{i,j}\lambda_{m_t(i)}\lambda_{m_t(j)}) = a_{i,j}(\lambda_{m_t(i)}\,\mathrm{grad}\,\lambda_{m_t(j)} + \lambda_{m_t(j)}\,\mathrm{grad}\,\lambda_{m_t(i)}) =$$

$$= \begin{cases} 2\lambda_{m_t(i)}\,\mathrm{grad}\,\lambda_{m_t(i)} & \text{if } i = j\,, \\ 2(\lambda_{m_t(i)}\,\mathrm{grad}\,\lambda_{m_t(j)} + \lambda_{m_t(j)}\,\mathrm{grad}\,\lambda_{m_t(i)}) & \text{if } i \neq j\,. \end{cases}$$

So in the case of just one tetrahedron we can write the divergence matrix. We divide it in two blocks: the block D^{tf}, that relates the tetrahedron moments of $P_{h,2}$ with the face moments of $RT_{h,3}$, and the block D^{tt}, that relates the tetrahedron moments of $P_{h,2}$ with the tetrahedron moments of $RT_{h,3}$.

$$
\begin{array}{c}
\\ 00 \\ 01 \\ 02 \\ 03 \\ 11 \\ 12 \\ 13 \\ 22 \\ 23 \\ 33 \\
\\ \scriptstyle 00\ 01\ 02\ 11\ 12\ 22 \\ \scriptstyle [0\,1\,2]
\end{array}
\begin{bmatrix}
-1 & 0 & 0 & 0 & 0 & 0 \\
0 & -1 & 0 & 0 & 0 & 0 \\
0 & 0 & -1 & 0 & 0 & 0 \\
0 & 0 & 0 & 0 & 0 & 0 \\
0 & 0 & 0 & -1 & 0 & 0 \\
0 & 0 & 0 & 0 & -1 & 0 \\
0 & 0 & 0 & 0 & 0 & 0 \\
0 & 0 & 0 & 0 & 0 & -1 \\
0 & 0 & 0 & 0 & 0 & 0 \\
0 & 0 & 0 & 0 & 0 & 0
\end{bmatrix}
\begin{array}{c}
\\ \scriptstyle 00\ 01\ 03\ 11\ 13\ 33 \\ \scriptstyle [0\,1\,3]
\end{array}
\begin{bmatrix}
1 & 0 & 0 & 0 & 0 & 0 \\
0 & 1 & 0 & 0 & 0 & 0 \\
0 & 0 & 0 & 0 & 0 & 0 \\
0 & 0 & 1 & 0 & 0 & 0 \\
0 & 0 & 0 & 1 & 0 & 0 \\
0 & 0 & 0 & 0 & 0 & 0 \\
0 & 0 & 0 & 0 & 1 & 0 \\
0 & 0 & 0 & 0 & 0 & 0 \\
0 & 0 & 0 & 0 & 0 & 0 \\
0 & 0 & 0 & 0 & 0 & 1
\end{bmatrix}
\begin{array}{c}
\\ \scriptstyle 00\ 02\ 03\ 22\ 23\ 33 \\ \scriptstyle [0\,2\,3]
\end{array}
\begin{bmatrix}
-1 & 0 & 0 & 0 & 0 & 0 \\
0 & 0 & 0 & 0 & 0 & 0 \\
0 & -1 & 0 & 0 & 0 & 0 \\
0 & 0 & -1 & 0 & 0 & 0 \\
0 & 0 & 0 & 0 & 0 & 0 \\
0 & 0 & 0 & 0 & 0 & 0 \\
0 & 0 & 0 & -1 & 0 & 0 \\
0 & 0 & 0 & 0 & -1 & 0 \\
0 & 0 & 0 & 0 & 0 & -1
\end{bmatrix}
\begin{array}{c}
\\ \scriptstyle 11\ 12\ 13\ 22\ 23\ 33 \\ \scriptstyle [1\,2\,3]
\end{array}
\begin{bmatrix}
0 & 0 & 0 & 0 & 0 & 0 \\
0 & 0 & 0 & 0 & 0 & 0 \\
0 & 0 & 0 & 0 & 0 & 0 \\
0 & 0 & 0 & 0 & 0 & 0 \\
1 & 0 & 0 & 0 & 0 & 0 \\
0 & 1 & 0 & 0 & 0 & 0 \\
0 & 0 & 1 & 0 & 0 & 0 \\
0 & 0 & 0 & 1 & 0 & 0 \\
0 & 0 & 0 & 0 & 1 & 0 \\
0 & 0 & 0 & 0 & 0 & 1
\end{bmatrix}
= D^{tf},
$$

$$
\begin{array}{c}
\\ 00 \\ 01 \\ 02 \\ 03 \\ 11 \\ 12 \\ 13 \\ 22 \\ 23 \\ 33 \\
\\ \scriptstyle 01\ 02\ 03\ 11\ 12\ 13\ 21\ 22\ 23\ 31\ 32\ 33
\end{array}
\begin{bmatrix}
1 & 1 & 1 & 0 & 0 & 0 & 0 & 0 & 0 & 0 & 0 & 0 \\
-1 & 0 & 0 & 1 & 1 & 1 & 0 & 0 & 0 & 0 & 0 & 0 \\
0 & -1 & 0 & 0 & 0 & 0 & 1 & 1 & 1 & 0 & 0 & 0 \\
0 & 0 & -1 & 0 & 0 & 0 & 0 & 0 & 0 & 1 & 1 & 1 \\
0 & 0 & 0 & -1 & 0 & 0 & 0 & 0 & 0 & 0 & 0 & 0 \\
0 & 0 & 0 & 0 & -1 & 0 & -1 & 0 & 0 & 0 & 0 & 0 \\
0 & 0 & 0 & 0 & 0 & -1 & 0 & 0 & 0 & -1 & 0 & 0 \\
0 & 0 & 0 & 0 & 0 & 0 & 0 & -1 & 0 & 0 & 0 & 0 \\
0 & 0 & 0 & 0 & 0 & 0 & 0 & 0 & -1 & 0 & -1 & 0 \\
0 & 0 & 0 & 0 & 0 & 0 & 0 & 0 & 0 & 0 & 0 & -1
\end{bmatrix}
= D^{tt}.
$$

Then

$$D_t = [D^{tf}, D^{tt}].$$

1.4 An element of $RT_{h,r+1}$ with assigned divergence

We now propose an efficient algorithm for the computation of the moments of a solution of the following problem: given $\rho_h \in P_{h,r}$, find $\mathbf{u}_h \in RT_{h,r+1}$ such that $\operatorname{div} \mathbf{u}_h = \rho_h$. Denoting $\mathbf{U} \in \mathbb{R}^{d_{RT}}$ the vector with entries the moments of $\mathbf{u}_h$ and $\boldsymbol{\rho} \in \mathbb{R}^{d_P}$ the vector with entries the moments of ρ_h, we are looking for a solution of the rectangular linear system

$$D_{\mathcal{T}_h} \mathbf{U} = \boldsymbol{\rho}. \tag{1.6}$$

Let $\mathcal{S} = (\mathcal{N}, \mathcal{B})$ be a spanning tree of $\mathcal{M} = (\mathcal{N}, \mathcal{A})$. By definition $\mathcal{B}$ has exactly d_P of

the d_{RT} arcs of $\mathcal{A}$. For instance, if $r = 1$, the submatrix in red of the matrix D_t^e below

$$D_t^e = \begin{bmatrix} -1 & 0 & 0 & 1 & 0 & 0 & -1 & 0 & 0 & 0 & 0 & 0 & 1 & 1 & 1 \\ 0 & -1 & 0 & 0 & 1 & 0 & 0 & 0 & 0 & 1 & 0 & 0 & -1 & 0 & 0 \\ 0 & 0 & -1 & 0 & 0 & 0 & 0 & -1 & 0 & 0 & 1 & 0 & 0 & -1 & 0 \\ 0 & 0 & 0 & 0 & 0 & 1 & 0 & 0 & -1 & 0 & 0 & 1 & 0 & 0 & -1 \\ 1 & 1 & 1 & -1 & -1 & -1 & 1 & 1 & 1 & -1 & -1 & -1 & 0 & 0 & 0 \end{bmatrix},$$

is the all-nodes incidence matrix of a spanning tree $\mathcal{S}$ of $\mathcal{M}$. In Figure 2.1 we present, on the left, the graph $\mathcal{M}$ (one style of line for each block of three columns in the matrix D_t^e), and on the right, the spanning tree $\mathcal{S}$.

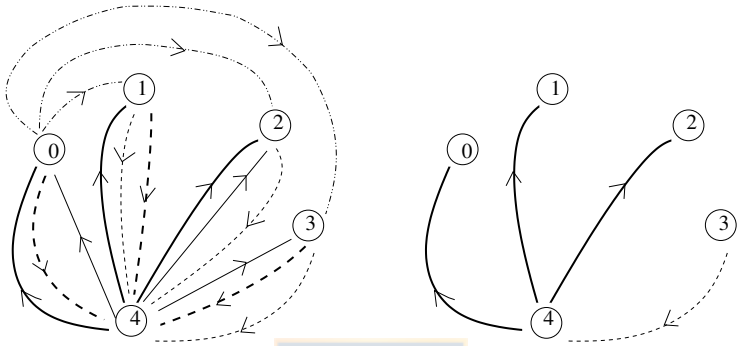

Figure 1.1: The graph $\mathcal{M}$ that corresponds to the matrix D_t^e with a different style of line for each three-column block in D_t^e (left) and the spanning tree $\mathcal{S}$ (right) (figure produced by the author).

In the matrix $D_{\mathcal{T}_h}$ we distinguish the columns corresponding to the arcs in $\mathcal{S}$ (and we denote D_{st} the submatrix of $D_{\mathcal{T}_h}$ composed by these columns; the subindex st refers to spanning tree), and the columns corresponding to arcs not in $\mathcal{S}$ (and we denote D_{ct} the submatrix of $D_{\mathcal{T}_h}$ composed by these columns; the subindex ct refers to co-tree). So, reordering the columns of $D_{\mathcal{T}_h}$ by using a permutation matrix P, we can write

$$D_{\mathcal{T}_h} P = [D_{st}, D_{ct}] .$$

From Theorem 1.1 and Propositions 1.1 and 1.2, we know that D_{st} is non singular. Denoting $\mathfrak{U} = P^\top \mathbf{U}$, we have

$$D_{\mathcal{T}_h} \mathbf{U} = \boldsymbol{\rho} \Leftrightarrow D_{\mathcal{T}_h} P \mathfrak{U} = \boldsymbol{\rho} ,$$

and $D_{\mathcal{T}_h} P = [D_{st},\, D_{ct}]$. So, if we denote $\mathfrak{U}_{st}$ the vector with the first d_P components of $\mathfrak{U}$ and $\mathfrak{U}_{ct}$ the vector with the remaining $d_{RT} - d_P$ components, we can write the rectangular

linear system to be solved as

$$D_{st}\,\mathfrak{U}_{st} + D_{ct}\,\mathfrak{U}_{ct} = \boldsymbol{\rho}\,. \tag{1.7}$$

For any choice of $\mathfrak{U}_{ct} \in \mathbb{R}^{d_{RT}-d_P}$, solving $D_{st}\mathfrak{U}_{st} = \boldsymbol{\rho} - D_{ct}\mathfrak{U}_{ct}$, we obtain a solution of (1.7). If we choose for instance $\mathfrak{U}_{ct} = \mathbf{0}$ we obtain

$$\mathfrak{U} = \begin{bmatrix} D_{st}^{-1}\boldsymbol{\rho} \\ \mathbf{0} \end{bmatrix},$$

and then $\mathbf{U} = P\mathfrak{U}$.

1.5 A basis of the space $RT^0_{h,r+1} = RT_{h,r+1} \cap H^0(\mathrm{div};\Omega)$

Proceeding in a similar way, we can compute the moments of the elements of a basis of the space $RT^0_{h,r+1} = RT_{h,r+1} \cap H^0(\mathrm{div};\Omega)$.

Proposition 1.3. *The columns of the matrix*

$$B = P \begin{bmatrix} -D_{st}^{-1}D_{ct} \\ I \end{bmatrix} \in \mathbb{Z}^{d_{RT}\times(d_{RT}-d_P)},$$

being I the identity matrix in $\mathbb{R}^{(d_{RT}-d_P)\times(d_{RT}-d_P)}$, are the moments of $d_{RT} - d_P$ linear independent functions in $RT_{h,r+1}$, that are divergence-free.

Proof. Taking $\boldsymbol{\rho} = \mathbf{0}$ in (1.7) and replacing $\mathfrak{U}_{ct}$ with the identity matrix of dimension $d_{RT} - d_P$, it is easy to check that

$$D_{\mathcal{T}_h}B = D_{\mathcal{T}_h}P \begin{bmatrix} -D_{st}^{-1}D_{ct} \\ I \end{bmatrix} = [D_{st}\,, D_{ct}] \begin{bmatrix} -D_{st}^{-1}D_{ct} \\ I \end{bmatrix} = -D_{ct} + D_{ct} = 0\,.$$

The fact that the corresponding functions are linearly independent is a consequence of the identity block in the definition of B. □

Let $N_{h,r+1}$ be the space of Nédélec curl conforming finite elements of degree $r+1$. If $\partial\Omega$ has $p+1$ connected components $(\partial\Omega)_0, \ldots, (\partial\Omega)_p$, then it is well known (see e.g. [31]) that given $\mathbf{z}_h \in RT_{h,r+1}$, there exists $\mathbf{w}_h \in N_{h,r+1}$, such that $\mathrm{curl}\,\mathbf{w}_h = \mathbf{z}_h$ if and only if $\mathrm{div}\,\mathbf{z}_h = 0$ and $\int_{(\partial\Omega)_k} \mathbf{z}_h \cdot \mathbf{n}_{\partial\Omega} = 0$, for $k = 1, 2, \ldots, p$. Moreover, the dimension of the space of functions in $H^0(\mathrm{div};\Omega)$ that are not the curl of any vector potential in $H(\mathrm{curl};\Omega)$ (the second de Rham cohomology group) is equal to p.

It is possible to construct a basis of the space $RT^0_{h,r+1}$ with p elements that are representatives of a basis of the second de Rham cohomology group and the remaining $d_{RT}-(p+d_P)$ that are the curl of vector potentials in $N_{h,r+1}$.

Let $(\partial\Omega)_0$ be the external connected component of $\partial\Omega$. We consider the following problem: given $\rho_h \in P_{h,r}$ and $\mathbf{C} \in \mathbb{R}^p$, find $\widetilde{\mathbf{u}}_h \in RT_{h,r+1}$ such that

$$\begin{cases} \mathrm{div}\,\widetilde{\mathbf{u}}_h = \rho_h\,, \\ \int_{(\partial\Omega)_k} \widetilde{\mathbf{u}}_h \cdot \mathbf{n}_{\partial\Omega} = C_k\,, \quad \text{for } k = 1,2,\ldots,p\,. \end{cases}$$

The number of equations is now equal to $d_P + p$, while the number of unknowns remains equal to d_{RT}. From (1.1), we have $1 = \sum_{\boldsymbol{\alpha}'\in\mathcal{I}(r,3)} a_{\boldsymbol{\alpha}'}\ \lambda^{\boldsymbol{\alpha}'}\Big|_f$ for any $f \in \mathcal{F}$, hence

$$\begin{aligned} \int_{(\partial\Omega)_k} \widetilde{\mathbf{u}}_h \cdot \mathbf{n}_{\partial\Omega} &= \sum_{f\in(\partial\Omega)_k} \left(\mathbf{n}_f \cdot \mathbf{n}_{\partial\Omega}|_f \int_f \widetilde{\mathbf{u}}_h \cdot \mathbf{n}_f\right) \\ &= \sum_{f\in(\partial\Omega)_k} \left(\mathbf{n}_f \cdot \mathbf{n}_{\partial\Omega}|_f \sum_{\boldsymbol{\alpha}'\in\mathcal{I}(r,3)} \int_f \widetilde{\mathbf{u}}_h \cdot \mathbf{n}_f a_{\boldsymbol{\alpha}'}\lambda^{\boldsymbol{\alpha}'}\right)\,. \end{aligned}$$

So, the new p equations (multiplied by -1) can be written as

$$-\sum_{f\in(\partial\Omega)_k} \left(\mathbf{n}_f \cdot \mathbf{n}_{\partial\Omega}|_f \sum_{\boldsymbol{\alpha}'\in\mathcal{I}(r,3)} \int_f \widetilde{\mathbf{u}}_h \cdot \mathbf{n}_f a_{\boldsymbol{\alpha}'}\lambda^{\boldsymbol{\alpha}'}\right) = -C_k, \quad k = 1,\ldots,p\,, \tag{1.8}$$

or using matrix notation, $H\widetilde{\mathbf{U}} = -\mathbf{C}$, being $\widetilde{\mathbf{U}} \in \mathbb{R}^{d_{RT}}$ the vector with the moments of $\widetilde{\mathbf{u}}_h$. Note that the entries of matrix $H \in \mathbb{R}^{p\times d_{RT}}$ are 0, if $f \notin (\partial\Omega)_k$, or, $-\mathbf{n}_f \cdot \mathbf{n}_{\partial\Omega}|_f$, that is equal to 1 or -1, if $f \in (\partial\Omega)_k$.

Denoting by $\mathbf{V} \in \mathbb{R}^{d_P+p}$ the vector $\mathbf{V} = \begin{bmatrix} \boldsymbol{\rho} \\ \mathbf{C} \end{bmatrix}$ and by $\widetilde{D}_{\mathcal{T}_h} \in \mathbb{R}^{(d_P+p)\times d_{RT}}$ the matrix $\widetilde{D}_{\mathcal{T}_h} = \begin{bmatrix} D_{\mathcal{T}_h} \\ H \end{bmatrix}$, we want to solve the rectangular linear system $\widetilde{D}_{\mathcal{T}_h}\widetilde{\mathbf{U}} = \mathbf{V}$.

The matrix $\widetilde{D}_{\mathcal{T}_h} \in \mathbb{R}^{(d_P+p)\times d_{RT}}$ is an incidence matrix of a new connected and directed graph $\widetilde{\mathcal{M}} = (\widetilde{\mathcal{N}}, \widetilde{\mathcal{A}})$, with no self loops. This new graph $\widetilde{\mathcal{M}}$ is similar to the graph $\mathcal{M}$: the node of $\mathcal{M}$ that corresponds to $\partial\Omega$ has been replaced in $\widetilde{\mathcal{M}}$ by $p+1$ nodes corresponding to the different connected components of $\partial\Omega$

$$\int_{(\partial\Omega)_k} \mathbf{z}_h \cdot \mathbf{n}_{\partial\Omega}\,,\ k = 0,...,p\,,$$

and the number of arcs in $\widetilde{\mathcal{M}}$ is equal to the number of arcs in $\mathcal{M}$. If f is a face on $\partial\Omega$, then $f \subseteq (\partial\Omega)_k \cap \partial t$ for some $t \in \mathcal{T}$ and some $k \in \{0,...,p\}$. In this case the arc $[\boldsymbol{\alpha}', f]$,

with $\boldsymbol{\alpha}' \in \mathcal{I}(r,3)$, connects the nodes $[R^\top_{t,f}\boldsymbol{\alpha}', t]$ and $[(\partial\Omega)_k]$ of the graph $\widetilde{\mathcal{M}}$ and hence also $\widetilde{\mathcal{M}}$ is connected.

The all-nodes incidence matrix of $\widetilde{\mathcal{M}} = (\widetilde{\mathcal{N}}, \widetilde{\mathcal{A}})$ has a row for each connected component of $\partial\Omega$. The sum of these $p+1$ rows is equal to the row corresponding to $\partial\Omega$ in the all-nodes incidence matrix of $\mathcal{M}$. The reference node for the incidence matrix $\widetilde{D}_{\mathcal{T}_h}$ is the one that corresponds to the external connected component of $\partial\Omega$, $(\partial\Omega)_0$. This means that in the matrix $\widetilde{D}_{\mathcal{T}_h}$ all the columns corresponding to tetrahedron moments or face moments for internal faces have exactly two entries different from zero, one equal to 1 and the other equal to -1. Both of them are in rows of $D_{\mathcal{T}_h}$. But in $\widetilde{D}_{\mathcal{T}_h}$ also the columns that correspond to face moments for a face $f \in (\partial\Omega)_k$ with $k \in \{1,\dots,p\}$ have two entries different from zero, one in $D_{\mathcal{T}_h}$ and the other in the k-th row of H. Only the columns that correspond to face moments for a face $f \in (\partial\Omega)_0$ have just one entry different from zero.

Let $\widetilde{\mathcal{S}}$ be a spanning tree of $\widetilde{\mathcal{M}}$. According to $\widetilde{\mathcal{S}}$ we identify a set of $d_P + p$ columns of $\widetilde{D}_{\mathcal{T}_h}$ that compose an invertible matrix $\widetilde{D}_{st}$. Reordering the columns of $\widetilde{D}_{\mathcal{T}_h}$ we can write $\widetilde{D}_{\mathcal{T}_h}\widetilde{P} = [\widetilde{D}_{st}\,, \widetilde{D}_{ct}]$. Now we have $\widetilde{D}_{st} \in \mathbb{Z}^{(d_P+p)\times(d_P+p)}$ and $\widetilde{D}_{ct} \in \mathbb{Z}^{(d_P+p)\times(d_{RT}-(d_P+p))}$.

Proceeding as before and denoting $\widetilde{\mathfrak{U}} = \widetilde{P}^\top\widetilde{\mathbf{U}}$ we can write

$$\widetilde{D}_{\mathcal{T}_h}\widetilde{\mathbf{U}} = \mathbf{V} \Leftrightarrow \widetilde{D}_{\mathcal{T}_h}\widetilde{P}\widetilde{\mathfrak{U}} = \mathbf{V} \Leftrightarrow [\widetilde{D}_{st}\,, \widetilde{D}_{ct}] \begin{bmatrix} \widetilde{\mathfrak{U}}_{st} \\ \widetilde{\mathfrak{U}}_{ct} \end{bmatrix} = \mathbf{V}\,.$$

Here $\widetilde{\mathfrak{U}}_{st}$ is the vector with the first $d_P + p$ components of $\widetilde{\mathfrak{U}}$ and $\widetilde{\mathfrak{U}}_{ct}$ the vector with the remaining $d_{RT} - (d_P + p)$ components. Hence

$$\widetilde{D}_{st}\widetilde{\mathfrak{U}}_{st} = \mathbf{V} - \widetilde{D}_{ct}\widetilde{\mathfrak{U}}_{ct} = \begin{bmatrix} \boldsymbol{\rho} \\ \mathbf{C} \end{bmatrix} - \widetilde{D}_{ct}\widetilde{\mathfrak{U}}_{ct}\,.$$

Let $\widehat{\mathbf{e}}_k$, $k \in \{1,\dots,p\}$ be the elements of the canonical basis of $\mathbb{R}^p$ and let $\mathbf{e}_j$, $j \in \{1,\dots,d_{RT} - (p + d_P)\}$ be the elements of the canonical basis of $\mathbb{R}^{d_{RT}-(d_P+p)}$. Let us consider $\boldsymbol{\rho} = \mathbf{0}$. For $k \in \{1,\dots,p\}$, we denote $\widetilde{\mathfrak{U}}_{st,k} \in \mathbb{Z}^{d_P+p}$ the solution of the linear system

$$\widetilde{D}_{st}\widetilde{\mathfrak{U}}_{st,k} = \begin{bmatrix} \mathbf{0} \\ \widehat{\mathbf{e}}_k \end{bmatrix},$$

and for $j \in \{1,\dots,d_{RT} - (p + d_P)\}$, we denote $\widetilde{\mathfrak{U}}_{st,p+j} \in \mathbb{Z}^{d_P+p}$ the solution of the linear system

$$\widetilde{D}_{st}\widetilde{\mathfrak{U}}_{st,p+j} = -\widetilde{D}_{ct}\mathbf{e}_j\,.$$

We denote, respectively, $N_1 \in \mathbb{R}^{(d_P+p)\times p}$ the matrix with column k equal to $\widetilde{\mathfrak{U}}_{st,k}$, and $N_2 \in \mathbb{R}^{(d_P+p)\times(d_{RT}-(d_P+p))}$ the matrix with column j equal to $\widetilde{\mathfrak{U}}_{st,p+j}$. It follows that

$$\widetilde{D}_{st}N_1 = \begin{bmatrix} 0 \\ I_p \end{bmatrix} =: \widetilde{I} \quad \text{and} \quad \widetilde{D}_{st}N_2 = -\widetilde{D}_{ct}\,,$$

being I_p the identity matrix in $\mathbb{R}^{p\times p}$. In a more compact way we have

$$\widetilde{D}_{st}N = [\widetilde{I}, -\widetilde{D}_{ct}]\,, \tag{1.9}$$

with $\widetilde{D}_{st} \in \mathbb{Z}^{(d_P+p)\times(d_P+p)}$, $N = [N_1, N_2] \in \mathbb{R}^{(d_P+p)\times(d_{RT}-d_P)}$, $\widetilde{I} \in \mathbb{R}^{(d_P+p)\times p}$ and $-\widetilde{D}_{ct} \in \mathbb{Z}^{(d_P+p)\times(d_{RT}-(d_P+p))}$.

Proposition 1.4. *The columns of the matrix*

$$\widetilde{B}_1 = \widetilde{P}\begin{bmatrix} N_1 \\ 0 \end{bmatrix} \in \mathbb{Z}^{d_{RT}\times p}$$

are the moments of functions $\widetilde{\mathbf{u}}_{h,k} \in RT_{h,r+1}$ such that

$$\begin{cases} \mathrm{div}\,\widetilde{\mathbf{u}}_{h,k} = 0\,, \\ \int_{(\partial\Omega)_l} \widetilde{\mathbf{u}}_{h,k}\cdot\mathbf{n}_{\partial\Omega} = \delta_{k,l} \quad \textit{for } l = 1,2,\ldots,p\,. \end{cases}$$

The columns of the matrix

$$\widetilde{B}_2 = \widetilde{P}\begin{bmatrix} N_2 \\ I_{d_{RT}-(d_P+p)} \end{bmatrix} \in \mathbb{Z}^{d_{RT}\times(d_{RT}-(d_P+p))}\,,$$

being $I_{d_{RT}-(d_P+p)}$ the identity matrix in $\mathbb{R}^{(d_{RT}-(d_P+p))\times(d_{RT}-(d_P+p))}$, are the moments of $d_{RT}-(d_P+p)$ linearly independent functions, $\widetilde{\mathbf{u}}_{h,p+j} \in RT_{h,r+1}$, such that

$$\begin{cases} \mathrm{div}\,\widetilde{\mathbf{u}}_{h,p+j} = 0\,, \\ \int_{(\partial\Omega)_l} \widetilde{\mathbf{u}}_{h,p+j}\cdot\mathbf{n}_{\partial\Omega} = 0 \quad \textit{for } l = 1,2,\ldots,p\,. \end{cases}$$

Proof. It is enough to check that $\widetilde{D}_{\mathcal{T}_h}\widetilde{B}_1 = \begin{bmatrix} 0 \\ I_p \end{bmatrix}$ and $\widetilde{D}_{\mathcal{T}_h}\widetilde{B}_2 = 0$. In fact,

$$\widetilde{D}_{\mathcal{T}_h}\widetilde{B}_1 = \widetilde{D}_{\mathcal{T}_h}\widetilde{P}\begin{bmatrix} N_1 \\ 0 \end{bmatrix} = [\widetilde{D}_{st}\,, \widetilde{D}_{ct}]\begin{bmatrix} N_1 \\ 0 \end{bmatrix} = \widetilde{D}_{st}N_1 = \begin{bmatrix} 0 \\ I_p \end{bmatrix}.$$

On the other hand

$$\widetilde{D}_{\mathcal{T}_h}\widetilde{B}_2 = \widetilde{D}_{\mathcal{T}_h}\widetilde{P}\begin{bmatrix} N_2 \\ I_{d_{RT}-(d_P+p)} \end{bmatrix} = [\widetilde{D}_{st}\,, \widetilde{D}_{ct}]\begin{bmatrix} N_2 \\ I_{d_{RT}-(d_P+p)} \end{bmatrix} = -\widetilde{D}_{ct} + \widetilde{D}_{ct} = 0\,.$$

□

Remark 1.1. *The functions $\widetilde{\mathbf{u}}_{h,k}$, $k \in \{1,\dots,d_{RT}-d_P\}$ form a basis of the space $RT^0_{h,r+1} = RT_{h,r+1}\cap H^0(\mathrm{div};\Omega)$. The first p elements $\widetilde{\mathbf{u}}_{h,k}$, $k \in \{1,\dots,p\}$ are divergence-free functions that are not the curl of any vector potential. They are representatives of a basis of the second de Rham cohomology group. The remaining $d_{RT}-(d_P+p)$ elements $\widetilde{\mathbf{u}}_{h,p+j}$, $j \in \{1,\dots,d_{RT}-(d_P+p)\}$, are the curl of vector potentials in the space $N_{h,r+1}$ of Nédélec finite elements of degree $r+1$, because they satisfy*

$$\begin{cases} \mathrm{div}\,\widetilde{\mathbf{u}}_{h,p+j} = 0\,, \\ \int_{(\partial\Omega)_l} \widetilde{\mathbf{u}}_{h,p+j}\cdot\mathbf{n}_{\partial\Omega} = 0 \quad \textit{for } l = 1,2,\dots,p\,. \end{cases}$$

1.6 Numerical results

In this section we illustrate the performance of the method for the construction of a basis of $RT^0_{h,r+1} := RT_{h,r+1}\cap H^0(\mathrm{div};\Omega)$ analyzed in Section 5.

The algorithm has been implemented in MATLAB (R2016a). All the numerical computations have been performed by an Intel Core i7-6700HQ, with a processor at 2.60 GHz on a laptop with 12 GB of RAM. The input is a mesh created by TetGen (see [13]), the output is the matrix with the degrees of freedom (moments) of a basis of $RT^0_{h,r+1}$, with a column for each element of the basis, as indicated in Proposition 1.4.

The algorithm has been tested by computing this matrix for $r = 1$ and $r = 2$, in successive uniformly refined meshes of the domains Ω presented in Figure 1.2. We consider four different test cases. In the first one the domain Ω is a sphere, its boundary is connected, so $p = 0$. In the second test case Ω is a cube with a concentric cubic cavity, the boundary has two connected components, so $p = 1$. In the third test case Ω is a torus with a concentric toroidal cavity, its boundary has two connected components, so $p = 1$. In the last one the domain Ω is a cube with two cubic cavities; the boundary has three connected components, so $p = 2$.

In the tables we report, for each test case, the number of elements of the mesh $n_{\mathcal{T}}$, the dimension d_{RT} of the space $RT_{h,r+1}$, the dimension d_P of the space $P_{h,r}$. In the fourth

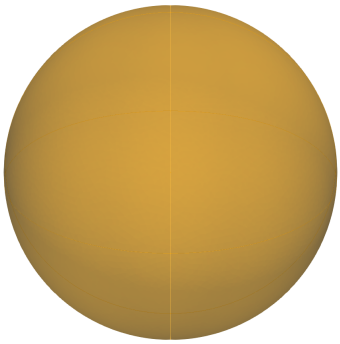

(a) Sphere. $p = 0$.

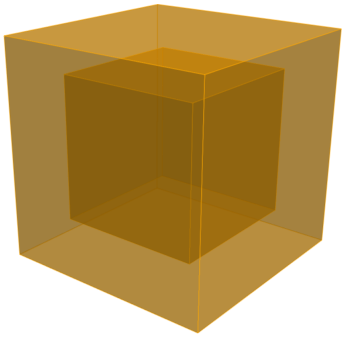

(b) Cube with a cube cavity. $p = 1$.

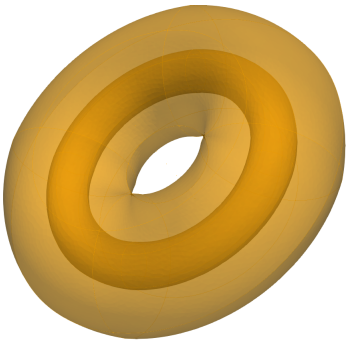

(c) Torus with toroidal cavity. $p = 1$.

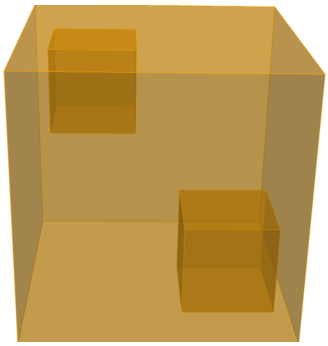

(d) Cube with two cubic cavities. $p = 2$.

Figure 1.2: The geometry of the considered test cases (figure produced by the author).

column, $d_{RT} - d_P$ is the dimension of the space $RT^0_{h,r+1}$. In the fifth column, Prepro. [ms], indicates in milliseconds the time spent to read the mesh, assemble the matrix $\widetilde{D}_{\mathcal{T}_h}$ and build the spanning tree. In the last column, SL [ms], indicates the time in milliseconds spent to solve the $d_{RT} - d_P$ linear systems in equation (1.9) using the command *backslash* of MATLAB and finally construct the matrix of moments $\widetilde{B} = [\widetilde{B}_1, \widetilde{B}_2] \in \mathbb{R}^{d_{RT} \times (d_{RT} - d_P)}$.

1.6.1 The case $r = 1$

For the first test case, the sphere, we consider two different spanning trees. In Table 1.1 (that has in fact seven columns), we report the computational times for eight successive uniformly refined meshes. In the sixth column, SL b.f [ms], we indicate the time in milliseconds for solving the $d_{RT} - d_P$ linear systems in (1.9) and finally construct the matrix of moments $\widetilde{B} = [\widetilde{B}_1, \widetilde{B}_2] \in \mathbb{R}^{d_{RT} \times (d_{RT} - d_P)}$ when using a spanning tree built by using a breadth-first search. In the last column, SL d.f [ms], we indicate again the time for solv-

ing the $d_{RT} - d_P$ linear systems in (1.9) but now using a spanning tree built by using a depth-first search.

$n_{\mathcal{T}}$	d_{RT}	d_P	$d_{RT} - d_P$	Prepro. [ms]	SL b.f [ms]	SL d.f [ms]
104	1 092	416	676	302.7	0.9	7.8
1 035	10 095	4 140	5 955	384.7	4.1	921.8
2 625	25 488	10 500	14 988	407.0	11.8	6 320.5
7 829	75 078	31 316	43 762	404.8	34.3	103 916.7
15 690	150 516	62 760	87 756	520.4	82.0	-
31 748	299 880	126 992	172 888	791.1	256.7	-
64 239	604 086	256 956	347 130	1 325.0	620.6	-
128 609	1 201 494	514 436	687 058	2 451.5	1 665.7	-

Table 1.1: Results for the sphere, ($r = 1$) (table produced by the author).

The results show that the time for solving the $d_{RT} - d_P$ linear systems in (1.9) is much longer when the spanning tree is built by using a depth-first search. Indeed, the number of elements different from zero in the matrix $\widetilde{B} = [\widetilde{B}_1, \widetilde{B}_2] \in \mathbb{R}^{d_{RT} \times (d_{RT} - d_P)}$, that contains the moments of a basis of $RT^0_{h,r+1}$, is larger with a depth-first search than that with a breadth-first search spanning tree.

$n_{\mathcal{T}}$	d_{RT}	$d_{RT} - d_P$	Breadth-first [%]	Depth-first [%]
104	1 092	676	0.322	9.06
1 035	10 095	5 955	0.055	7.86
2 625	25 488	14 988	0.024	7.38
7 829	75 078	43 762	0.010	7.51
15 690	50 516	87 756	0.005	-
31 748	299 880	172 888	0.004	-
64 239	604 086	347 130	0.002	-
128 609	1 201 494	687 058	0.001	-

Table 1.2: Sparsity of the matrix $\widetilde{B}$ containing the moments of a basis of $RT^0_{h,r+1}$, ($r = 1$) (table produced by the author).

In Table 1.2 we report the sparsity of the matrix $\widetilde{B}$ associated to these two kinds of spanning trees.

In Figure 1.3 we illustrate the behavior, with respect to the dimension of the problem, of the total computational time (on the left), and of the time to solve the $d_{RT} - d_P$ linear systems in (1.9) (on the right). In the plot on the left, the slope of the curves changes when the considered mesh attains a critical size. Before this critical size, the preprocessing time is more significative than the resolution time, and after, the other way around. This behavior does not depend on the adopted method to construct the spanning tree. In the

plot on the right, only the resolution time is considered, which has a rather linear (resp. quadratic) behavior when adopting the breadth-first (resp. depth-first) spanning tree.

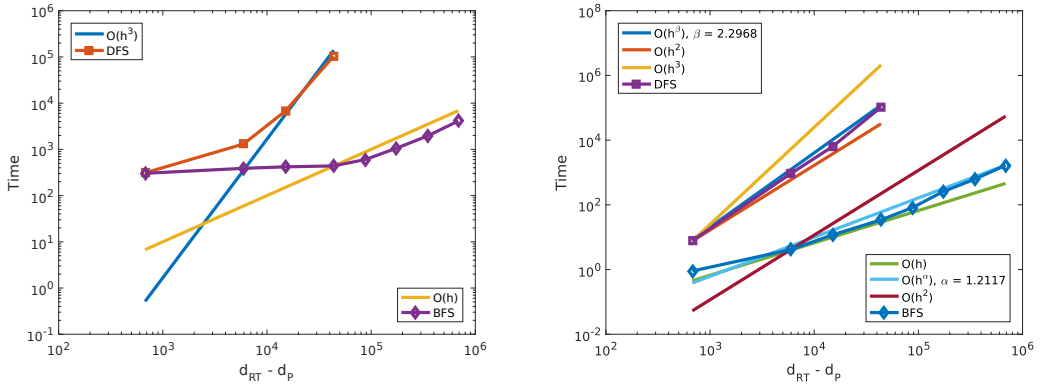

Figure 1.3: Total computational time (left), and time for solving the linear systems using breadth-first or a depth-first spanning tree (right) in the sphere test case, ($r = 1$) (figure produced by the author).

For the second, third and fourth test cases, we present numerical results only for a breadth-first spanning tree. These three examples show that the method is successful in domains with a non connected boundary. In the case of the torus with a toroidal cavity the domain is not simply connected; however this aspect does not influence the performance of the algorithm. The fourth example shows that the algorithm is robust with respect to the number of connected components of the boundary. These considerations are summarized in Figure 1.4 where we can clearly see that the time for solving the linear systems is independent of the topology of the test case domain and depends only on the dimension of the matrix $\widetilde{D}_{st}$.

In Tables 1.3, 1.4 and 1.5, we report the detailed computational times of the second, third and fourth test cases with successive uniformly refined meshes, respectively.

Finally, in Figure 1.5 we plot, on the left, the total computational time, and on the right, the time to solve the $d_{RT} - d_P$ linear systems in (1.9), both as a function of the problem dimension. We notice again the existence of a critical dimension of the mesh size starting from which the preprocessing time is not longer dominant. In the plot on the right, only the resolution time is considered, which has a rather linear behavior with respect to the problem dimension.

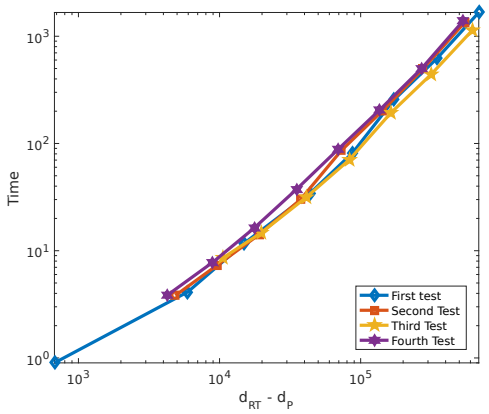

Figure 1.4: Time for solving the linear systems using breadth-first spanning tree in the four test cases, ($r = 1$) (figure produced by the author).

$n_{\mathcal{T}}$	d_{RT}	d_P	$d_{RT} - d_P$	Prepro. [ms]	SL b.f [ms]
807	8 091	3 228	4 863	386.5	3.8
1 606	16 020	6 424	9 596	442.2	7.3
3 221	32 010	12 884	19 126	493.5	14.2
6 468	63 444	25 872	37 572	555.6	30.1
12 964	124 935	51 856	73 079	719.7	86.2
25 940	246 282	103 760	142 522	825.1	201.4
50 995	480 507	203 980	276 527	1 905.4	496.2
102 169	954 693	408 676	546 017	3 896.7	1 346.0

Table 1.3: Results for the cube with a concentric cubic cavity, ($r = 1$) (table produced by the author).

$n_{\mathcal{T}}$	d_{RT}	d_P	$d_{RT} - d_P$	Prepro. [ms]	SL b.f [ms]
1 784	17 664	7 136	10 528	424.5	8.5
3 366	33 327	13 464	19 863	487.8	14.8
6 939	68 781	27 756	41 025	648.5	31.4
13 891	138 555	55 564	82 991	655.9	70.4
27 849	274 611	111 396	163 215	998.0	192.2
55 705	540 477	222 820	317 657	1 414.4	444.4
111 345	1 062 786	445 380	617 406	2 576.3	1 133.8

Table 1.4: Results for the torus with a concentric toroidal cavity, ($r = 1$) (table produced by the author).

$n_{\mathcal{T}}$	d_{RT}	d_P	$d_{RT} - d_P$	Prepro. [ms]	SL b.f [ms]
719	7 149	2 876	4 273	401.2	3.9
1 530	15 072	6 120	8 952	422.7	7.8
3 098	29 991	12 392	17 599	475.6	16.3
6 280	60 150	25 120	35 030	561.3	37.3
12 577	119 199	50 308	68 891	754.7	87.7
25 293	237 951	101 172	136 779	1 168.0	206.4
50 621	472 260	202 484	269 776	2 556.6	498.8
101 288	937 815	405 152	532 663	3 696.9	1 390.7

Table 1.5: Results for the cube with two cubic cavities, ($r = 1$) (table produced by the author).

1.6.2 The case $r = 2$

We use the same meshes as the ones used for the case $r = 1$, and we present tables and figures similar to those of the previous case to show that the algorithm is also robust with respect the polynomial degree r.

$n_{\mathcal{T}}$	d_{RT}	d_P	$d_{RT} - d_P$	Prepro. [ms]	SL b.f [ms]	SL d.f [ms]
104	2 808	1 040	1 768	263.9	0.8	53.6
1 035	26 400	10 350	16 050	359.7	8.7	6 906.5
2 625	66 726	26 250	40 476	398.2	25.9	73 048.1
7 829	197 130	78 290	118 840	550.8	111.6	-
15 690	395 172	156 900	238 272	869.4	285.2	-
31 748	790 248	317 480	472 768	1 518.1	785.2	-
64 239	1 593 606	642 390	951 216	2 990.6	1 819.9	-

Table 1.6: Results for the sphere, ($r = 2$) (table produced by the author).

Again, the time for solving the $d_{RT} - d_P$ linear systems in (1.9) is much longer when using a spanning tree constructed with a depth-first search (see Table 1.6), since the number of elements different from zero in $\widetilde{B} = [\widetilde{B}_1, \widetilde{B}_2] \in \mathbb{R}^{d_{RT} \times (d_{RT} - d_P)}$ is larger using a depth-first search than that using a breadth-first search spanning tree (see Table 1.7).

In Figure 1.6 we represent the total computational time (on the left), and the time to solve the $d_{RT} - d_P$ linear systems in (1.9) (on the right), with respect to the dimension of the problem. The behavior of the case $r = 2$ is similar to the behavior of the case $r = 1$, as we can see in Figure 1.6 and Figure 1.7.

In Tables 1.8, 1.9 and 1.10, we report the detailed computational times of the second, third and fourth test cases with successive uniformly refined meshes, respectively.

$n_{\mathcal{T}}$	d_{RT}	$d_{RT} - d_P$	Breadth-first [%]	Depth-first [%]
104	2 808	1 768	0.143	8.45
1 035	26 400	16 050	0.024	5.95
2 625	66 726	40 476	0.010	5.51
7 829	197 130	118 840	0.004	-
15 690	395 172	238 272	0.002	-
31 748	790 248	472 768	0.001	-
64 239	1 593 606	951 216	< 0.001	-

Table 1.7: Sparsity of the matrix $\widetilde{B}$ containing the moments of a basis of $RT^0_{h,r+1}$, $(r = 2)$ (table produced by the author).

$n_{\mathcal{T}}$	d_{RT}	d_P	$d_{RT} - d_P$	Prepro. [ms]	SL b.f [ms]
807	9 936	3 840	6 096	300.3	4.1
1 606	21 024	8 070	12 954	417.5	9.7
3 221	41 676	16 060	25 616	429.1	19.7
6 468	83 346	32 210	51 136	511.6	43.0
12 964	165 696	64 680	101 016	658.4	96.2
25 940	327 654	129 640	198 014	965.9	306.5
50 995	648 204	259 400	388 804	1 646.2	655.4
102 169	1 266 984	509 950	757 034	3 071.5	1 582.1

Table 1.8: Results for the cube with a concentric cubic cavity, $(r = 2)$ (table produced by the author).

Finally, in Figure 1.8 we plot, on the left, the total computational time, and on the right, the time to solve the $d_{RT} - d_P$ linear systems in (1.9), both as a function of the problem dimension. We remark again the existence of a critical dimension of the mesh size starting from which the preprocessing time is not longer dominant. In the plot on the right, only the resolution time is considered, which has a rather linear behavior with respect to the problem dimension.

$n_{\mathcal{T}}$	d_{RT}	d_P	$d_{RT} - d_P$	Prepro. [ms]	SL b.f [ms]
1 784	46 032	17 840	28 192	427.1	20.4
3 366	86 850	33 660	53 190	484.1	46.6
6 939	179 196	69 390	109 806	765.2	107.2
13 891	360 456	138 910	221 546	889.5	242.2
27 849	716 316	278 490	437 826	1 581.9	640.2
55 705	1 415 184	557 050	858 134	2 792.3	1 482.4

Table 1.9: Results for the torus with a concentric toroidal cavity, ($r = 2$) (table produced by the author).

$n_{\mathcal{T}}$	d_{RT}	d_P	$d_{RT} - d_P$	Prepro. [ms]	SL b.f [ms]
719	18 612	7 190	11 422	372.9	7.3
1 530	39 324	15 300	24 024	411.6	19.9
3 098	78 570	30 980	47 590	476.3	39.9
6 280	157 980	62 800	95 180	635.0	100.1
12 577	313 860	125 770	188 090	998.5	253.4
25 293	627 660	252 930	374 730	1 702.7	581.8
50 621	1 248 246	506 210	742 036	3 069.8	1 401.8

Table 1.10: Results for the cube with two cubic cavities, ($r = 2$) (table produced by the author).

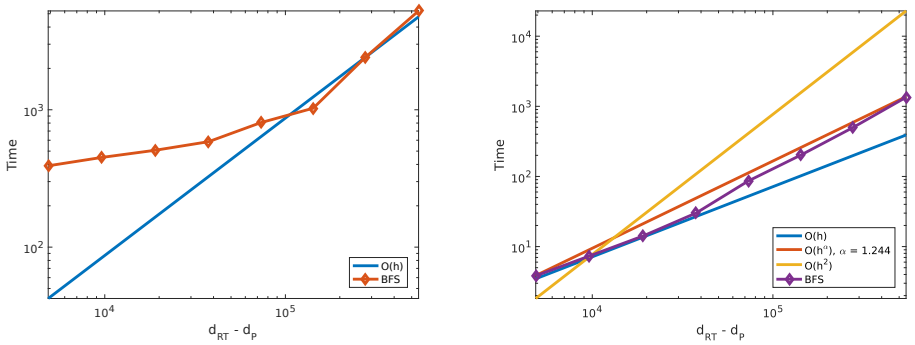

(a) Cube with a cube cavity. $p = 1$.

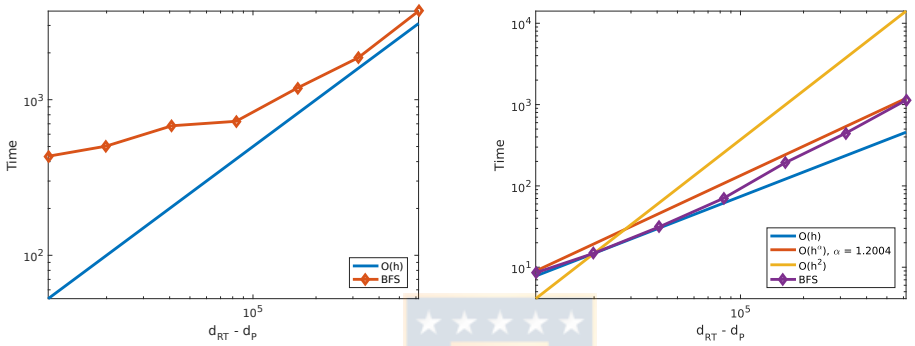

(b) Torus with toroidal cavity. $p = 1$.

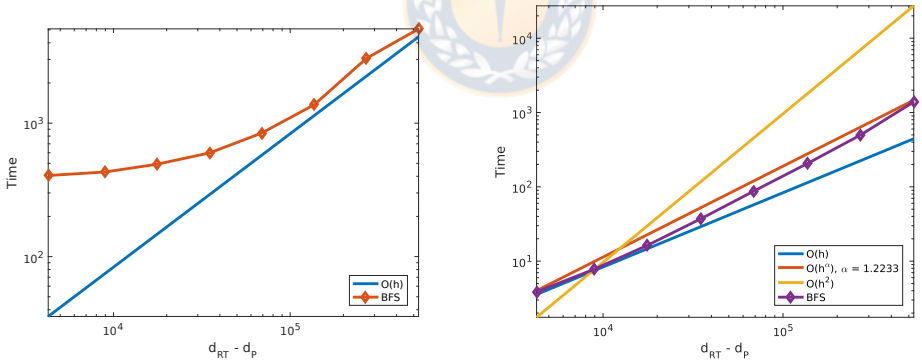

(c) Cube with two cubic cavities. $p = 2$.

Figure 1.5: Total computational time (left), and time for solving the linear systems (right) in the three test cases with not connected boundary, ($r = 1$) (figure produced by the author).

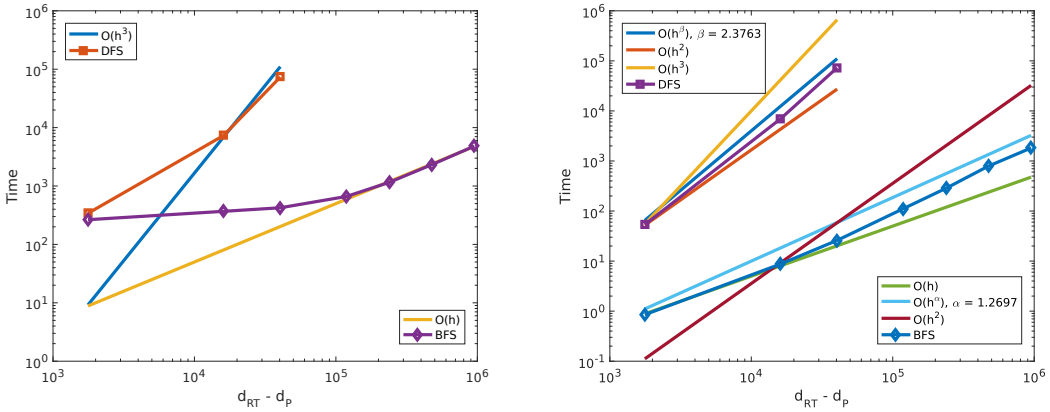

Figure 1.6: Total computational time (left), and time for solving the linear systems using breadth-first or a depth-first spanning tree (right) in the sphere test case, ($r = 2$) (figure produced by the author).

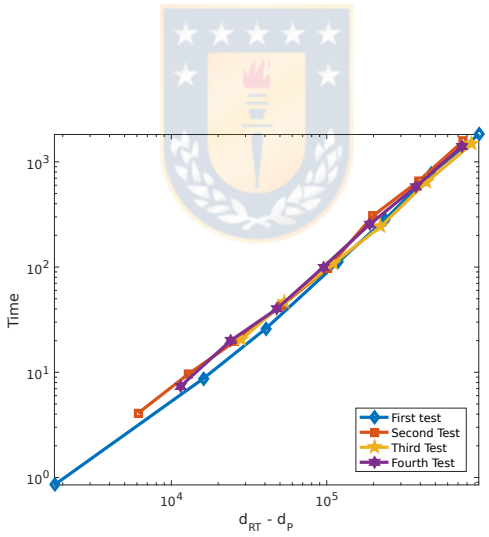

Figure 1.7: Time for solving the linear systems using breadth-first spanning tree in the four test cases, ($r = 2$) (figure produced by the author).

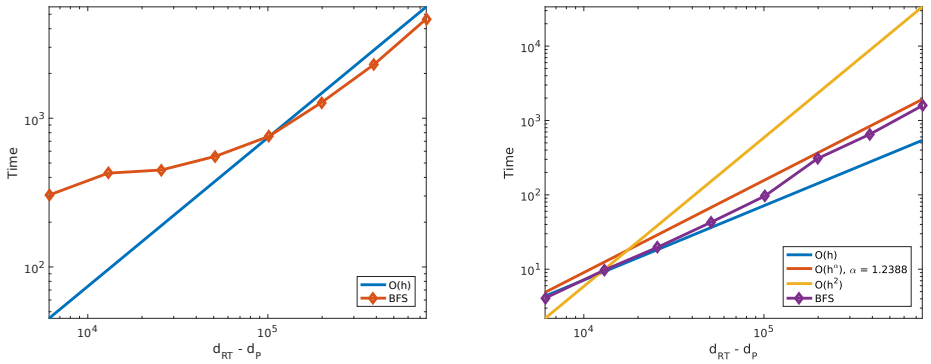

(a) Cube with a cube cavity. $p = 1$.

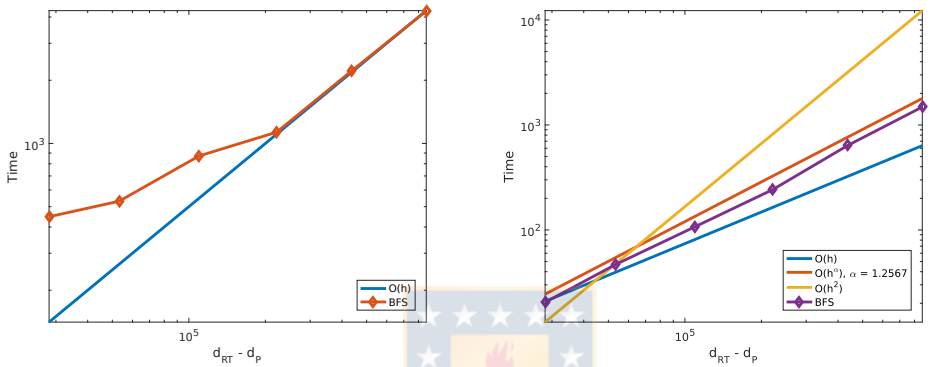

(b) Torus with toroidal cavity. $p = 1$.

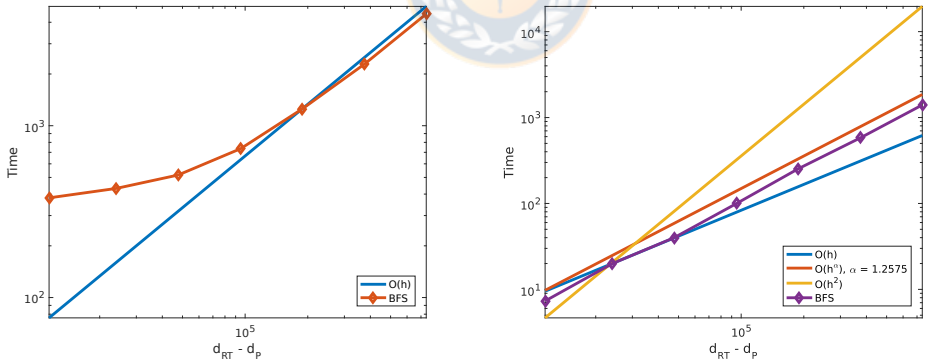

(c) Cube with two cubic cavities. $p = 2$.

Figure 1.8: Total computational time (left), and time for solving the linear systems (right) in the three test cases with not connected boundary, ($r = 2$) (figure produced by the author).

CHAPTER 2

A tree-cotree splitting for the construction of high order divergence-free Raviart-Thomas finite elements

2.1 Introduction

Let $\mathcal{T}$ be a tetrahedral mesh of a bounded polyhedral domain $\Omega \subset \mathbb{R}^3$. We will denote $\mathcal{P}^-_{r+1}\Lambda^k(\mathcal{T})$ the space of Whitney k-differential forms of degree $r+1$ (see e.g. [13]). They can be identified with

- Lagrange finite elements of degree $r+1$, L_{r+1}, if $k=0$.
- Nédélec finite elements (from the first Nédélec's family) of degree $r+1$, N_{r+1}, if $k=1$.
- Raviart-Thomas finite elements of degree $r+1$, RT_{r+1}, if $k=2$.
- The space of discontinuous piecewise polynomial functions of degree r, P_r, if $k=3$.

When using the lowest order Whitney elements on a simplicial complex $\mathcal{P}^-_1\Lambda^k(\mathcal{T})$, the degrees of freedom are supported on the vertices ($k=0$), edges ($k=1$), faces ($k=2$) and tetrahedra ($k=3$) of the mesh. It is well known (see e.g. [26]) that given an orientation to edges, faces and tetrahedra of the mesh, the matrix describing the differential operator $\mathrm{d}_k : \mathcal{P}^-_1\Lambda^k(\mathcal{T}) \to \mathcal{P}^-_1\Lambda^{k+1}(\mathcal{T})$ in terms of the degrees of freedom is the transpose of the matrix of the boundary operator $\partial_{k+1} : \mathcal{C}_{k+1}(\mathcal{T},\mathbb{Z}) \to \mathcal{C}_k(\mathcal{T},\mathbb{Z})$, being $\mathcal{C}_k(\mathcal{T},\mathbb{Z})$ the space of k-chains in $\mathcal{T}$ (see, e.g. [26]), for each $k \in \{0,\dots,2\}$.

Since the boundary of an edge consists in two vertices, and any face belongs to the boundary of one or two tetrahedra, from the point of view of graph theory we observe, still

for the lowest order case, that: i) the matrix associated to the gradient is the transpose of the all-nodes incidence matrix of a directed, connected and without self-loop graph having a node for each vertex and an arc for each (oriented) edge of the mesh; ii) the matrix associated to the divergence operator is an incidence matrix of a directed, connected and without self-loop graph having a node for each tetrahedron plus an additional node associated to the exterior of the domain, and an arc for each (oriented) face. This fact is used in different contexts as tree-cotree gauge (see [3], [4], [63], [52]), construction of bases of the space of divergence-free Raviart-Thomas finite elements (see [10], [66], [8]) or the construction of discrete potentials (see [70], [9]).

These two properties hold true also for $r > 0$ when using as degrees of freedom for $u \in \mathcal{P}^-_{r+1}\Lambda^k(\mathcal{T})$ a particular realizations of the moments (see e.g. [13])

$$m_S(u) = \int_S \mathrm{Tr}_S(u) \wedge \eta, \quad \eta \in \mathcal{P}_{r+k-\dim S}\Lambda^{\dim S-k}(S)\,,$$

being S any subsimplex of the mesh such that $\dim S \geq k$. The key point is to use Bernstein polynomials to identify a basis of $\mathcal{P}_{r+k-\dim S}\Lambda^{\dim S-k}(S)$, following the approach in [1] (see also [2] where Bernstein polynomials are used to express a subset of the basis of $\mathcal{P}^-_{r+1}\Lambda^k(\mathcal{T})$).

In particular this result allows to extend to the high order case ($r > 0$) the two approaches presented in [8] for the construction of a basis of the space of divergence-free Raviart-Thomas finite elements, RT^0_{r+1}, in a general topological domain: to compute directly a basis of the kernel of the matrix associated to the divergence operator, or to compute it starting from a basis of the range of the matrix associated to the curl operator. In this second approach, if the boundary of the domain has $p+1$ connected components with $p > 0$, it is necessary to complete this set with p discrete representatives of a basis of the second de Rham cohomology group (divergence-free functions that are not curls).

The extension of the first approach has been analyzed in the previous chapter. The main idea is to identify a maximal invertible submatrix of the matrix D associated to the divergence operator. Following the method proposed in [10] for a triangular mesh in $\mathbb{R}^2$ and with $r = 0$, this can be done choosing the columns in D corresponding to the arcs in a spanning tree of the graph associated to D. If we decompose $D = [D_{st}, D_{ct}]$ being D_{st} the columns corresponding to the spanning tree and D_{ct} those of the co-tree, then D_{st} is invertible. Let us set $d_P = \dim P_r$ and $d_{RT} = \dim RT_{r+1}$. For any vector $\mathbf{m}_{ct} \in \mathbb{R}^{d_{RT}-d_P}$, solving $D_{st}\mathbf{m}_{st} = -D_{ct}\mathbf{m}_{ct}$, the entries of the vector $\begin{bmatrix} \mathbf{m}_{st} \\ \mathbf{m}_{ct} \end{bmatrix}$ are the degrees of freedom of a discrete function that is divergence-free. Then it is easy to prove that the columns of $\begin{bmatrix} -D_{st}^{-1}D_{ct} \\ I \end{bmatrix}$, being I the identity matrix in $\mathbb{R}^{(d_{RT}-d_P)\times(d_{RT}-d_P)}$, are the degrees of

freedom of the elements of a basis of divergence-free Raviart-Thomas finite elements.

In this chapter we analyze the second approach, where if the boundary of the domain is connected, provides the moments of the elements of a basis of RT^0_{r+1} by selectig some elements of a cardinal (dual) basis of N_{r+1} and computing their curls. More precisely the elements corresponding to the moments out of a *belted* tree (a spanning tree if the domain is simply connected) of the graph associated to $G^\top$, where G is the matrix associated to the gradient operator. A belted tree is an augmented spanning tree, that in rigor is not longer a tree, this concept is recalled for the lowest order case and extended to the high order case in Section 2.4 .

For the case $r = 0$, the use of a spanning tree of the graph associated to $G^\top$ to identify a maximal set of linearly independent columns in the matrix associated to the curl operator C has been first proposed by Scheichl in a simply connected polyhedral domain Ω without cavities (see [66] and [65]) and extended to domains with an arbitrary topology in [8]. In $\mathbb{R}^2$, where the kernel of the curl operator reduces to constant functions, a basis of RT^0_{r+1} for $r \geq 0$, can be obtained computing the curl of a nodal basis of the space of continuous piecewise polynomial finite elements like in [69].

This chapter is organized as follows. In Section 2.2 we introduce the notation and some preliminary results. In Section 2.3 we choose the degrees of freedom that will be used in the sequel. For this choice of degrees of freedom, we compute the matrix associated to the gradient and we realize that it is the transpose of the all-nodes incidence matrix of a directed, connected and without self-loop graph $\mathcal{M}^G$. In Section 2.4, using a spanning tree of this graph, we identify a maximal set of linearly independent divergence-free Raviart-Thomas functions that are the curl of Nédélec functions and, if the boundary of Ω is not connected, we complete it to obtain a basis. Section 2.5 contains some remarks on implementation.

2.2 Notation

Let $\mathcal{T} = (V, E, F, T)$ be a tetrahedral mesh of Ω, where V is the set of vertices, E is the set of edges, F is the set of faces, and T is the set of tetrahedra of $\mathcal{T}$. If $\Delta_d(\mathcal{T})$ denotes, for $d \in \{0, 1, 2, 3\}$, the set of d-simplices of the mesh $\mathcal{T}$, then $\Delta_0(\mathcal{T}) = V$, $\Delta_1(\mathcal{T}) = E$, $\Delta_2(\mathcal{T}) = F$, and $\Delta_3(\mathcal{T}) = T$. Let us fix an orientation (namely, an ordering of vertices) of each edge, face, and tetrahedron of $\mathcal{T}$. This can be done choosing a total ordering of the elements of $V = \{\mathbf{v}_i\}_{i=1}^{n_V}$ and associating to each d-simplex of the mesh, $S \in \Delta_d(\mathcal{T})$, an increasing function $m_S : \{0, 1, \ldots, d\} \to \{1, \ldots, n_V\}$, hence the oriented d-simplex, denoted by an abuse of notation also as S, is given by $S = [\mathbf{v}_{m_S(0)}, \ldots, \mathbf{v}_{m_{S(d)}}]$.

Analogously, if $S \in \Delta_d(\mathcal{T})$ we denote by $\Delta_l(S)$, for $l \in \{0,\dots,d\}$, the set of l-subsimplices of S. When $\Sigma \in \Delta_l(S)$, then we can write $\Sigma = S - \sigma$, being σ the (oriented) $(d-l)$-subsimplex of S such that $\Delta_1(\Sigma) \cap \Delta_1(\sigma) = \emptyset$. Moreover, there exists a unique increasing map $m_\Sigma^S : \{0,\dots,l\} \to \{0,\dots,d\}$ such that, for each $i \in \{0,\dots,l\}$, $m_\Sigma(i) = m_S(m_\Sigma^S(i))$.

For any $t \in T$ we denote by $\mathbf{n}_{\partial t}$ the outward unit vector normal to the boundary of t. For any $f \in F$ we define $\mathbf{n}_f := \frac{(\mathbf{v}_{m_f(1)}-\mathbf{v}_{m_f(0)})\times(\mathbf{v}_{m_f(2)}-\mathbf{v}_{m_f(0)})}{|(\mathbf{v}_{m_f(1)}-\mathbf{v}_{m_f(0)})\times(\mathbf{v}_{m_f(2)}-\mathbf{v}_{m_f(0)})|}$ and we denote by $\boldsymbol{\nu}_{\partial f}$ the unit vector normal to the boundary of f in the plane containing f and pointing outward of f. We define $\mathbf{t}_{\partial f} := \mathbf{n}_f \times \boldsymbol{\nu}_{\partial f}$. For any $e \in E$ we define $\boldsymbol{\tau}_e := \frac{\mathbf{v}_{m_e(1)}-\mathbf{v}_{m_e(0)}}{|\mathbf{v}_{m_e(1)}-\mathbf{v}_{m_e(0)}|}$.

For ℓ, $d \in \mathbb{N}$ let us set

$$\mathcal{I}(\ell, d+1) := \{\boldsymbol{\eta} = (\eta_0,\dots,\eta_d) \in \mathbb{N}^{d+1} \,:\, |\boldsymbol{\eta}| = \ell\}\,,$$

being $|\boldsymbol{\eta}| := \sum_{i=0}^d \eta_i$. The cardinality of $\mathcal{I}(l, d+1)$ is equal to $\begin{pmatrix} l+d \\ d \end{pmatrix}$.

For $\boldsymbol{\zeta} \in \mathcal{I}(\ell+1, d+1)$ and $j \in \{0,1,\dots,d\}$ we denote by $\boldsymbol{\zeta} - \mathbf{e}_j$ the vector in $\mathbb{Z}^{d+1}$ with components $(\boldsymbol{\zeta} - \mathbf{e}_j)_i = \zeta_i - \delta_{j,i}$, for $i \in \{0,1,\dots,d\}$, namely

$$(\boldsymbol{\zeta} - \mathbf{e}_j)_i = \begin{cases} \zeta_i & \text{if } i \neq j \\ \zeta_i - 1 & \text{if } i = j\,. \end{cases} \tag{2.1}$$

Note that $\boldsymbol{\zeta} - \mathbf{e}_j \in \mathcal{I}(\ell, d+1)$ if and only if $\zeta_j > 0$. So we also consider the following set of vectors in $\mathbb{Z}^{d+1}$:

$$\mathcal{J}(\ell, d+1) := \{\widetilde{\boldsymbol{\eta}} \in \mathbb{Z}^{d+1} \,:\, \widetilde{\boldsymbol{\eta}} = \boldsymbol{\zeta} - \mathbf{e}_j \text{ for some } \boldsymbol{\zeta} \in \mathcal{I}(\ell+1, d+1) \text{ and } j \in \{0,1,\dots,d\}\}\,.$$

Clearly $\mathcal{I}(\ell, d+1) \subset \mathcal{J}(\ell, d+1)$. For each $\widetilde{\boldsymbol{\eta}} \in \mathcal{J}(\ell, d+1)$ we define

$$a_{\widetilde{\boldsymbol{\eta}}} = \begin{cases} \dfrac{\ell!}{\Pi_{i=0}^d \widetilde{\eta}_i!} = \begin{pmatrix} \ell \\ \widetilde{\boldsymbol{\eta}} \end{pmatrix} & \text{if } \widetilde{\boldsymbol{\eta}} \in \mathcal{I}(\ell, d+1) \\ 0 & \text{otherwise.} \end{cases}$$

In this way for each $\boldsymbol{\zeta} \in \mathcal{I}(\ell+1, d+1)$ we have

$$a_{\boldsymbol{\zeta}}\zeta_j = (\ell+1) a_{\boldsymbol{\zeta}-\mathbf{e}_j} \text{ for each } j \in \{0,1,\dots,d\}\,. \tag{2.2}$$

The barycentric coordinates of a point $\mathbf{x} \in t$ with respect to $t \in T$ are given by the unique vector $\boldsymbol{\lambda}_t(\mathbf{x}) = (\lambda_{t,0}(\mathbf{x}), \lambda_{t,1}(\mathbf{x}), \lambda_{t,2}(\mathbf{x}), \lambda_{t,3}(\mathbf{x}))$, with components the unique linear functions $\lambda_{t,j}$ in t satisfying

$$\mathbf{x} = \sum_{j=0}^3 \lambda_{t,j}(\mathbf{x}) \mathbf{v}_{m_t(j)} \text{ and } \sum_{j=0}^3 \lambda_{t,j}(\mathbf{x}) = 1\,.$$

For each $i \in \{1, \ldots, n_V\}$, $\lambda_i : \overline{\Omega} \to \mathbb{R}$ denotes the continuous function

$$\lambda_i(\mathbf{x}) = \begin{cases} \lambda_{t,j}(\mathbf{x}) & \text{if } \mathbf{x} \in t \text{ and } i = m_t(j) \text{ for some } j \in \{0,1,2,3\} \\ 0 & \text{otherwise}\,; \end{cases}$$

and for $S \in \Delta_d(\mathcal{T})$ and $\widetilde{\boldsymbol{\eta}} \in \mathcal{J}(\ell, d+1)$, $\lambda_S^{\widetilde{\boldsymbol{\eta}}} : \overline{\Omega} \to \mathbb{R}$ denotes the continuous function

$$\lambda_S^{\widetilde{\boldsymbol{\eta}}}(\mathbf{x}) = \begin{cases} \Pi_{j=0}^d \left[\lambda_{m_S(j)}(\mathbf{x})\right]^{\widetilde{\eta}_j} & \text{if } \widetilde{\boldsymbol{\eta}} \in \mathcal{I}(\ell, d+1) \\ 1 & \text{otherwise.} \end{cases}$$

For each $\ell \in \mathbb{N}$, $S \in \Delta_d(\mathcal{T})$ and $\mathbf{x} \in S$

$$1 = \left(\sum_{j=0}^d \lambda_{m_S(j)}(\mathbf{x})\right)^\ell = \sum_{\boldsymbol{\eta} \in \mathcal{I}(\ell, d+1)} a_{\boldsymbol{\eta}} \lambda_S^{\boldsymbol{\eta}}(\mathbf{x})\,. \tag{2.3}$$

For each $\boldsymbol{\eta} \in \mathcal{I}(\ell, d+1)$, $B_S^{\boldsymbol{\eta}} := a_{\boldsymbol{\eta}} \lambda_S^{\boldsymbol{\eta}}$ is a Bernstein polynomial of degree ℓ associated with S, (see, e.g., [1]).

For $t \in T$, $S \in \Delta_d(t)$ and $\mathbf{x} \in \mathring{t}$, interior of t, then

$$\begin{aligned} \operatorname{grad} B_S^{\boldsymbol{\eta}}(\mathbf{x}) = a_{\boldsymbol{\eta}} \operatorname{grad} \lambda_S^{\boldsymbol{\eta}}(\mathbf{x}) &= \textstyle\sum_{j=0}^d a_{\boldsymbol{\eta}} \eta_j \lambda_S^{\boldsymbol{\eta}-\mathbf{e}_j}(\mathbf{x}) \operatorname{grad} \lambda_{m_S(j)}(\mathbf{x}) \\ &= |\boldsymbol{\eta}| \textstyle\sum_{j=0}^d a_{\boldsymbol{\eta}-\mathbf{e}_j} \lambda_S^{\boldsymbol{\eta}-\mathbf{e}_j}(\mathbf{x}) \operatorname{grad} \lambda_{m_S(j)}(\mathbf{x}) \\ &= |\boldsymbol{\eta}| \textstyle\sum_{j=0}^d B_S^{\boldsymbol{\eta}-\mathbf{e}_j}(\mathbf{x}) \operatorname{grad} \lambda_{m_S(j)}(\mathbf{x})\,, \end{aligned}$$

being $B_S^{\boldsymbol{\eta}-\mathbf{e}_j} \equiv 0$ if $\eta_j = 0$.

If $\mathbf{x} \in \mathring{S}$ with $S \in \Delta_d(t)$, then $\mathbf{n}_S \times \operatorname{grad}[\lambda_{m_S(j)}]_{|t} \times \mathbf{n}_S$ (for $d = 2$) and $(\boldsymbol{\tau}_S \cdot \operatorname{grad}[\lambda_{m_S(j)}]_{|t})\,\boldsymbol{\tau}_S$ (for $d = 1$) are independent of t, so

$$\operatorname{grad}_S \lambda_{m_S(j)}(\mathbf{x}) := \begin{cases} \mathbf{n}_S \times \operatorname{grad}[\lambda_{m_S(j)}]_{|t} \times \mathbf{n}_S & (d=2) \\ (\boldsymbol{\tau}_S \cdot \operatorname{grad}[\lambda_{m_S(j)}]_{|t})\,\boldsymbol{\tau}_S & (d=1) \end{cases}$$

is well defined. Moreover, for $\mathbf{x} \in S$ we observe that $\sum_{j=0}^d \lambda_{m_S(j)}(\mathbf{x}) = 1$ and $\operatorname{grad}_S \lambda_{m_S(0)} = -\sum_{j=1}^d \operatorname{grad}_S \lambda_{m_S(j)}$. So for $\mathbf{x} \in \mathring{S}$ we have

$$\operatorname{grad}_S B_S^{\boldsymbol{\eta}}(\mathbf{x}) = a_{\boldsymbol{\eta}} \operatorname{grad}_S \lambda_S^{\boldsymbol{\eta}}(\mathbf{x}) = |\boldsymbol{\eta}| \textstyle\sum_{j=1}^d \left[B_S^{\boldsymbol{\eta}-\mathbf{e}_j}(\mathbf{x}) - B_S^{\boldsymbol{\eta}-\mathbf{e}_0}(\mathbf{x})\right] \operatorname{grad}_S \lambda_{m_S(j)}\,. \tag{2.4}$$

We denote by $R_{d,j} \in \mathbb{Z}^{d \times (d+1)}$ the matrix obtained from omitting the j-th row of the $(d+1) \times (d+1)$ identity matrix. Clearly, when $\boldsymbol{\eta} \in \mathcal{I}(\ell, d+1)$ if $\eta_j = 0$ for a particular

$j \in \{0,1,\dots,d\}$ we have $R_{d,j}\boldsymbol{\eta} \in \mathcal{I}(\ell,d)$ and $a_{\boldsymbol{\eta}} = a_{R_{d,j}\boldsymbol{\eta}}$. Notice that, if $\Sigma \in \Delta_{d-1}(S)$ then $\Sigma = S - [\mathbf{v}_{m_S(i)}]$ for a certain $i \in \{0,1,\dots,d\}$ and $[\lambda_S^{\boldsymbol{\eta}}]_{|\Sigma} = 0$ if $\eta_i \neq 0$, hence

$$[B_S^{\boldsymbol{\eta}}]_{|\Sigma} = \begin{cases} B_\Sigma^{\boldsymbol{\eta}'} \text{ with } \boldsymbol{\eta}' = R_{d,i}\boldsymbol{\eta} \in \mathcal{I}(\ell,d) & \text{if } \eta_i = 0 \\ 0 & \text{otherwise.} \end{cases}$$

2.3 Moments

Moments for $\mathbf{u}_h \in N_{r+1}$

Let us consider the following set of moments in the space N_{r+1}:

- $M^N_{\boldsymbol{\alpha},e}(\mathbf{u}_h) = \int_e \mathbf{u}_h \cdot \boldsymbol{\tau}_e\, B_e^{\boldsymbol{\alpha}}$, for each $e \in E$ and $\boldsymbol{\alpha} \in \mathcal{I}(r,2)$;
- $M^N_{\boldsymbol{\beta},f,i}(\mathbf{u}_h) = r\int_f (\mathbf{u}_h \times \mathbf{n}_f)\cdot B_f^{\boldsymbol{\beta}} \operatorname{grad}_f \lambda_{m_f(i)}$, for each $f \in F$, $\boldsymbol{\beta} \in \mathcal{I}(r-1,3)$ and $i = 1,2$;
- $M^N_{\boldsymbol{\gamma},t,i,j}(\mathbf{u}_h) = r(r-1)\int_t \mathbf{u}_h \cdot B_t^{\boldsymbol{\gamma}} \operatorname{grad}\lambda_{m_t(i)} \times \operatorname{grad}\lambda_{m_t(j)}$, for each $t \in T$, $\boldsymbol{\gamma} \in \mathcal{I}(r-2,4)$ and $1 \le i < j \le 3$.

It is worth noting that $\mathbf{n}_f \times \operatorname{grad}_f \lambda_{m_f(i)}$ is parallel to $\boldsymbol{\tau}_{f-[\mathbf{v}_{m_f(i)}]}$ ($\mathbf{n}_f \times \operatorname{grad}_f \lambda_{m_f(i)}$ has the same orientation of $(-1)^{i+1}\boldsymbol{\tau}_{f-[\mathbf{v}_{m_f(i)}]}$) while $\operatorname{grad}\lambda_{m_t(i)} \times \operatorname{grad}\lambda_{m_t(j)}$ is a parallel to $\boldsymbol{\tau}_{t-[\mathbf{v}_{m_t(i)},\mathbf{v}_{m_t(j)}]}$ ($\operatorname{grad}\lambda_{m_t(i)} \times \operatorname{grad}\lambda_{m_t(j)}$ has the same orientation of $(-1)^{i+j+1+s}\boldsymbol{\tau}_{t-[\mathbf{v}_{m_t(i)},\mathbf{v}_{m_t(j)}]}$, with $s = 0$ for t positively oriented, $s = 1$ for t negatively oriented and $i < j$).

If $\mathbf{u}_h = \operatorname{grad}\varphi_h$ with $\varphi_h \in L_{r+1}$ we obtain

- $$M^N_{\boldsymbol{\alpha},e}(\operatorname{grad}\varphi_h) = \int_e \operatorname{grad}\varphi_h \cdot \boldsymbol{\tau}_e\, B_e^{\boldsymbol{\alpha}}$$
$$= \varphi_h(\mathbf{v}_{m_e(1)})B_e^{\boldsymbol{\alpha}}(\mathbf{v}_{m_e(1)}) - \varphi_h(\mathbf{v}_{m_e(0)})B_e^{\boldsymbol{\alpha}}(\mathbf{v}_{m_e(0)}) - \int_e \varphi_h \operatorname{grad}_e B_e^{\boldsymbol{\alpha}} \cdot \boldsymbol{\tau}_e$$
$$= \varphi_h(\mathbf{v}_{m_e(1)})B_e^{\boldsymbol{\alpha}}(\mathbf{v}_{m_e(1)}) - \varphi_h(\mathbf{v}_{m_e(0)})B_e^{\boldsymbol{\alpha}}(\mathbf{v}_{m_e(0)}) - \frac{r}{|e|}\left[\int_e \varphi_h\, B_e^{\boldsymbol{\alpha}-\mathbf{e}_1} - \int_e \varphi_h\, B_e^{\boldsymbol{\alpha}-\mathbf{e}_0}\right]$$
where we have used (2.4) and that
$$\operatorname{grad}\lambda_{m_e(i)} \cdot \boldsymbol{\tau}_e = \begin{cases} -\frac{1}{|e|} & \text{if } i = 0 \\ \frac{1}{|e|} & \text{if } i = 1\,. \end{cases}$$

Since $\lambda_e^{\boldsymbol{\alpha}}(\mathbf{v}_{m_e(0)}) = \begin{cases} 0 & \text{if } \alpha_1 \neq 0 \\ 1 & \text{if } \alpha_1 = 0 \end{cases}$ and $\lambda_e^{\boldsymbol{\alpha}}(\mathbf{v}_{m_e(1)}) = \begin{cases} 0 & \text{if } \alpha_0 \neq 0 \\ 1 & \text{if } \alpha_0 = 0 \end{cases}$ we have

$$M^N_{\boldsymbol{\alpha},e}(\operatorname{grad}\varphi_h) = \begin{cases} -\varphi_h(\mathbf{v}_{m_e(0)}) + \frac{r}{|e|}\int_e \varphi_h\, B_e^{\boldsymbol{\alpha}-\mathbf{e}_0} & \text{if } \boldsymbol{\alpha} = (r,0) \\ \varphi_h(\mathbf{v}_{m_e(1)}) - \frac{r}{|e|}\int_e \varphi_h\, B_e^{\boldsymbol{\alpha}-\mathbf{e}_1} & \text{if } \boldsymbol{\alpha} = (0,r) \\ -\frac{r}{|e|}\left[\int_e \varphi_h\, B_e^{\boldsymbol{\alpha}-\mathbf{e}_1} - \int_e \varphi_h\, B_e^{\boldsymbol{\alpha}-\mathbf{e}_0}\right] & \text{otherwise.} \end{cases} \tag{2.5}$$

- $M^N_{\boldsymbol{\beta},f,i}(\operatorname{grad}\varphi_h) = r\displaystyle\int_f (\operatorname{grad}\varphi_h \times \mathbf{n}_f)\cdot B_f^{\boldsymbol{\beta}} \operatorname{grad}_f \lambda_{m_f(i)}$

$$= -r\int_f (\operatorname{grad}\varphi_h \times \operatorname{grad}_f\lambda_{m_f(i)})\cdot \mathbf{n}_f\, B_f^{\boldsymbol{\beta}} = -r\int_f \operatorname{div}_f(\varphi_h \operatorname{grad}_f\lambda_{m_f(i)} \times \mathbf{n}_f)\, B_f^{\boldsymbol{\beta}}$$

$$= -r\left[\int_{\partial f} (\varphi_h \operatorname{grad}_f\lambda_{m_f(i)} \times \mathbf{n}_f)\cdot \boldsymbol{\nu}_{\partial f}\, B_f^{\boldsymbol{\beta}} - \int_f (\varphi_h \operatorname{grad}_f\lambda_{m_f(i)} \times \mathbf{n}_f)\cdot \operatorname{grad}_f B_f^{\boldsymbol{\beta}}\right]$$

$$= -r\left[\int_{\partial f} \varphi_h \operatorname{grad}_f\lambda_{m_f(i)} \cdot (\mathbf{n}_f \times \boldsymbol{\nu}_{\partial f})\, B_f^{\boldsymbol{\beta}} - \int_f \varphi_h (\operatorname{grad}_f B_f^{\boldsymbol{\beta}} \times \operatorname{grad}_f\lambda_{m_f(i)})\cdot \mathbf{n}_f\right]$$

$$= -r\left[\int_{\partial f} \varphi_h \operatorname{grad}_f\lambda_{m_f(i)} \cdot \mathbf{t}_{\partial f}\, B_f^{\boldsymbol{\beta}} - \int_f \varphi_h (\operatorname{grad}_f B_f^{\boldsymbol{\beta}} \times \operatorname{grad}_f\lambda_{m_f(i)})\cdot \mathbf{n}_f\right]$$

$$= -r\left[\sum_{e\in\Delta_1(f)} ([\mathbf{t}_{\partial f}]_{|e}\cdot\boldsymbol{\tau}_e)\int_e \varphi_h \operatorname{grad}_f\lambda_{m_f(i)}\cdot\boldsymbol{\tau}_e\, [B_f^{\boldsymbol{\beta}}]_{|e}\right.$$
$$\left. -(r-1)\sum_{j=1}^{2}(\operatorname{grad}_f\lambda_{m_f(j)} \times \operatorname{grad}_f\lambda_{m_f(i)})\cdot\mathbf{n}_f \int_f \varphi_h \left(B_f^{\boldsymbol{\beta}-\mathbf{e}_j} - B_f^{\boldsymbol{\beta}-\mathbf{e}_0}\right)\right],$$

where in the last step we have used (2.4).

It is worth noting that $\operatorname{grad}_f \lambda_{m_f(i)}\cdot\boldsymbol{\tau}_e = 0$ if $\mathbf{v}_{m_f(i)} \notin \Delta_0(e)$. Moreover, for $i,j \in \{1,2\}$ we have

$$(\operatorname{grad}_f\lambda_{m_f(j)} \times \operatorname{grad}_f\lambda_{m_f(i)})\cdot\mathbf{n}_f = \begin{cases} 0 & \text{if } j = i \\ \frac{1}{2|f|} & \text{if } j < i \\ -\frac{1}{2|f|} & \text{if } j > i\,. \end{cases} \tag{2.6}$$

Hence, if $i = 1$ (and using the following notation $e_{lj} = [\mathbf{v}_{m_f(l)}, \mathbf{v}_{m_f(j)}]$),

$$M^N_{\boldsymbol{\beta},f,1}(\operatorname{grad}\varphi_h) = -r\left(\frac{1}{|e_{01}|}\int_{e_{01}} \varphi_h [B_f^{\boldsymbol{\beta}}]_{|e_{01}} - \frac{1}{|e_{12}|}\int_{e_{12}} \varphi_h [B_f^{\boldsymbol{\beta}}]_{|e_{12}}\right)$$
$$-\frac{r(r-1)}{2|f|}\int_f \varphi_h \left(B_f^{\boldsymbol{\beta}-\mathbf{e}_2} - B_f^{\boldsymbol{\beta}-\mathbf{e}_0}\right)$$

$$= \begin{cases} -\frac{r}{|e_{01}|}\int_{e_{01}} \varphi_h [B_f^{\boldsymbol{\beta}}]_{|e_{01}} + \frac{r}{|e_{12}|}\int_{e_{12}} \varphi_h [B_f^{\boldsymbol{\beta}}]_{|e_{12}} & \text{if } \boldsymbol{\beta} = (0, r-1, 0) \\ -\frac{r}{|e_{01}|}\int_{e_{01}} \varphi_h [B_f^{\boldsymbol{\beta}}]_{|e_{01}} + \frac{r(r-1)}{2|f|}\int_f \varphi_h B_f^{\boldsymbol{\beta}-\mathbf{e}_0} & \text{if } \boldsymbol{\beta} = (\beta_0, \beta_1, 0),\ \beta_0 \neq 0 \\ \frac{r}{|e_{12}|}\int_{e_{12}} \varphi_h [B_f^{\boldsymbol{\beta}}]_{|e_{12}} - \frac{r(r-1)}{2|f|}\int_f \varphi_h B_f^{\boldsymbol{\beta}-\mathbf{e}_2} & \text{if } \boldsymbol{\beta} = (0, \beta_1, \beta_2),\ \beta_2 \neq 0 \\ -\frac{r(r-1)}{2|f|}\int_f \varphi_h \left(B_f^{\boldsymbol{\beta}-\mathbf{e}_2} - B_f^{\boldsymbol{\beta}-\mathbf{e}_0} \right) & \text{otherwise.} \end{cases} \tag{2.7}$$

We recall that if $e = f - [\mathbf{v}_{m_f(i)}]$ then

$$[B_f^{\boldsymbol{\beta}}]_{|e} = \begin{cases} B_e^{R_{2,i}\boldsymbol{\beta}} & \text{if } \beta_i = 0 \\ 0 & \text{otherwise.} \end{cases}$$

Analogously if $i = 2$

$$M^N_{\boldsymbol{\beta},f,2}(\operatorname{grad}\varphi_h) = r\left(\frac{1}{|e_{02}|}\int_{e_{02}} \varphi_h [B_f^{\boldsymbol{\beta}}]_{|e_{02}} - \frac{1}{|e_{12}|}\int_{e_{12}} \varphi_h [B_f^{\boldsymbol{\beta}}]_{|e_{12}} \right) + \frac{r(r-1)}{2|f|}\int_f \varphi_h \left(B_f^{\boldsymbol{\beta}-\mathbf{e}_1} - B_f^{\boldsymbol{\beta}-\mathbf{e}_0} \right).$$

$$= \begin{cases} \frac{r}{|e_{02}|}\int_{e_{02}} \varphi_h [B_f^{\boldsymbol{\beta}}]_{|e_{02}} - \frac{r}{|e_{12}|}\int_{e_{12}} \varphi_h [B_f^{\boldsymbol{\beta}}]_{|e_{12}} & \text{if } \boldsymbol{\beta} = (0, 0, r-1) \\ \frac{r}{|e_{02}|}\int_{e_{02}} \varphi_h [B_f^{\boldsymbol{\beta}}]_{|e_{02}} - \frac{r(r-1)}{2|f|}\int_f \varphi_h B_f^{\boldsymbol{\beta}-\mathbf{e}_0} & \text{if } \boldsymbol{\beta} = (\beta_0, 0, \beta_2),\ \beta_0 \neq 0 \\ -\frac{r}{|e_{12}|}\int_{e_{12}} \varphi_h [B_f^{\boldsymbol{\beta}}]_{|e_{12}} + \frac{r(r-1)}{2|f|}\int_f \varphi_h B_f^{\boldsymbol{\beta}-\mathbf{e}_1} & \text{if } \boldsymbol{\beta} = (0, \beta_1, \beta_2),\ \beta_1 \neq 0 \\ \frac{r(r-1)}{2|f|}\int_f \varphi_h \left(B_f^{\boldsymbol{\beta}-\mathbf{e}_1} - B_f^{\boldsymbol{\beta}-\mathbf{e}_0} \right) & \text{otherwise.} \end{cases} \tag{2.8}$$

- $M^N_{\boldsymbol{\gamma},t,i,j}(\operatorname{grad}\varphi_h) = r(r-1)\int_t \operatorname{grad}\varphi_h \cdot B_t^{\boldsymbol{\gamma}} \operatorname{grad}\lambda_{m_t(i)} \times \operatorname{grad}\lambda_{m_t(j)}$

$$= r(r-1)\left[\int_{\partial t} \varphi_h\, B_t^{\boldsymbol{\gamma}} \operatorname{grad}\lambda_{m_t(i)} \times \operatorname{grad}\lambda_{m_t(j)} \cdot \mathbf{n}_{\partial t} - \int_t \varphi_h \operatorname{div}\left(B_t^{\boldsymbol{\gamma}} \operatorname{grad}\lambda_{m_t(i)} \times \operatorname{grad}\lambda_{m_t(j)} \right) \right]$$

$$= r(r-1)\left[\int_{\partial t} \varphi_h\, B_t^{\boldsymbol{\gamma}} \operatorname{grad}\lambda_{m_t(i)} \times \operatorname{grad}\lambda_{m_t(j)} \cdot \mathbf{n}_{\partial t} - \int_t \varphi_h \operatorname{grad} B_t^{\boldsymbol{\gamma}} \cdot \left(\operatorname{grad}\lambda_{m_t(i)} \times \operatorname{grad}\lambda_{m_t(j)} \right) \right]$$

$$= r(r-1)\left[\sum_{f\in\Delta_2(t)} ([\mathbf{n}_{\partial t}]_{|f} \cdot \mathbf{n}_f) \operatorname{grad}\lambda_{m_t(i)} \times \operatorname{grad}\lambda_{m_t(j)} \cdot \mathbf{n}_f \int_f \varphi_h\, [B_t^{\boldsymbol{\gamma}}]_{|f} - (r-2)\sum_{l=1}^{3} \operatorname{grad}\lambda_{m_t(l)} \cdot \left(\operatorname{grad}\lambda_{m_t(i)} \times \operatorname{grad}\lambda_{m_t(j)} \right) \int_t \varphi_h \left(B_t^{\boldsymbol{\gamma}-\mathbf{e}_l} - B_t^{\boldsymbol{\gamma}-\mathbf{e}_0} \right) \right].$$

It is worth noting that if $f = t-[\mathbf{v}_{m_t(l)}]$ for a certain $l \in \{0,1,2,3\}$ then $\mathbf{n}_f$ is parallel to $\operatorname{grad}\lambda_{m_t(l)}$ hence $\operatorname{grad}\lambda_{m_t(i)} \times \operatorname{grad}\lambda_{m_t(j)} \cdot \mathbf{n}_f = 0$ if $l = i$ or $l = j$. Moreover, for $i,l,j \in \{1,2,3\}$

$$(-1)^s \operatorname{grad}\lambda_{m_t(l)} \cdot \left(\operatorname{grad}\lambda_{m_t(i)} \times \operatorname{grad}\lambda_{m_t(j)}\right) = \begin{cases} 0 & \text{if } l = i \text{ or } l = j \\ \frac{1}{6|t|} & \text{if } l < i < j \text{ or } i < j < l \\ -\frac{1}{6|t|} & \text{if } i < l < j\,, \end{cases}$$

with $s = 0$ if t is positively oriented and $s = 1$ if t is negatively oriented.

For $i = 1$ and $j = 2$ (using (2.6) with the following notation $f_{lks} = [\mathbf{v}_{m_f(l)}, \mathbf{v}_{m_f(k)}, \mathbf{v}_{m_f(s)}]$),

$$\begin{aligned}(-1)^s M^N_{\boldsymbol{\gamma},t,1,2}(\operatorname{grad}\varphi_h) = r(r-1)\left(-\frac{1}{2|f_{012}|}\int_{f_{012}} \varphi_h \left[B_t^{\boldsymbol{\gamma}}\right]_{|f_{012}} + \frac{1}{2|f_{123}|}\int_{f_{123}} \varphi_h \left[B_t^{\boldsymbol{\gamma}}\right]_{|f_{123}}\right) \\ -\frac{r(r-1)(r-2)}{6|t|}\int_t \varphi_h \left(B_t^{\boldsymbol{\gamma}-\mathbf{e}_3} - B_t^{\boldsymbol{\gamma}-\mathbf{e}_0}\right)\end{aligned}$$

$$= \begin{cases} -\frac{r(r-1)}{2|f_{012}|}\int_{f_{012}} \varphi_h \left[B_t^{\boldsymbol{\gamma}}\right]_{|f_{012}} + \frac{r(r-1)}{2|f_{123}|}\int_{f_{123}} \varphi_h \left[B_t^{\boldsymbol{\gamma}}\right]_{|f_{123}} & \text{if } \boldsymbol{\gamma} = (0,\gamma_1,\gamma_2,0) \\ -\frac{r(r-1)}{2|f_{012}|}\int_{f_{012}} \varphi_h \left[B_t^{\boldsymbol{\gamma}}\right]_{|f_{012}} + \frac{r(r-1)(r-2)}{6|t|}\int_t \varphi_h B_t^{\boldsymbol{\gamma}-\mathbf{e}_0} & \text{if } \boldsymbol{\gamma} = (\gamma_0,\gamma_1,\gamma_2,0),\ \gamma_0 \neq 0 \\ \frac{r(r-1)}{2|f_{123}|}\int_{f_{123}} \varphi_h \left[B_t^{\boldsymbol{\gamma}}\right]_{|f_{123}} - \frac{r(r-1)(r-2)}{6|t|}\int_t \varphi_h B_t^{\boldsymbol{\gamma}-\mathbf{e}_3} & \text{if } \boldsymbol{\gamma} = (0,\gamma_1,\gamma_2,\gamma_3),\ \gamma_3 \neq 0 \\ -\frac{r(r-1)(r-2)}{6|t|}\int_t \varphi_h \left(B_t^{\boldsymbol{\gamma}-\mathbf{e}_3} - B_t^{\boldsymbol{\gamma}-\mathbf{e}_0}\right) & \text{otherwise.} \end{cases} \tag{2.9}$$

Analogously, if $i = 1$ and $j = 3$

$$\begin{aligned}(-1)^{s+1} M^N_{\boldsymbol{\gamma},t,1,3}(\operatorname{grad}\varphi_h) = r(r-1)\left(-\frac{1}{2|f_{013}|}\int_{f_{013}} \varphi_h \left[B_t^{\boldsymbol{\gamma}}\right]_{|f_{013}} + \frac{1}{2|f_{123}|}\int_{f_{123}} \varphi_h \left[B_t^{\boldsymbol{\gamma}}\right]_{|f_{123}}\right) \\ -\frac{r(r-1)(r-2)}{6|t|}\int_t \varphi_h \left(B_t^{\boldsymbol{\gamma}-\mathbf{e}_2} - B_t^{\boldsymbol{\gamma}-\mathbf{e}_0}\right).\end{aligned}$$

$$= \begin{cases} -\frac{r(r-1)}{2|f_{013}|}\int_{f_{013}} \varphi_h \left[B_t^{\boldsymbol{\gamma}}\right]_{|f_{013}} + \frac{r(r-1)}{2|f_{123}|}\int_{f_{123}} \varphi_h \left[B_t^{\boldsymbol{\gamma}}\right]_{|f_{123}} & \text{if } \boldsymbol{\gamma} = (0,\gamma_1,0,\gamma_3) \\ -\frac{r(r-1)}{2|f_{013}|}\int_{f_{013}} \varphi_h \left[B_t^{\boldsymbol{\gamma}}\right]_{|f_{013}} + \frac{r(r-1)(r-2)}{6|t|}\int_t \varphi_h B_t^{\boldsymbol{\gamma}-\mathbf{e}_0} & \text{if } \boldsymbol{\gamma} = (\gamma_0,\gamma_1,0,\gamma_3),\ \gamma_0 \neq 0 \\ +\frac{r(r-1)}{2|f_{123}|}\int_{f_{123}} \varphi_h \left[B_t^{\boldsymbol{\gamma}}\right]_{|f_{123}} - \frac{r(r-1)(r-2)}{6|t|}\int_t \varphi_h B_t^{\boldsymbol{\gamma}-\mathbf{e}_2} & \text{if } \boldsymbol{\gamma} = (0,\gamma_1,\gamma_2,\gamma_3),\ \gamma_2 \neq 0 \\ -\frac{r(r-1)(r-2)}{6|t|}\int_t \varphi_h \left(B_t^{\boldsymbol{\gamma}-\mathbf{e}_2} - B_t^{\boldsymbol{\gamma}-\mathbf{e}_0}\right) & \text{otherwise.} \end{cases} \tag{2.10}$$

If $i=2$ and $j=3$

$$(-1)^s M^N_{\boldsymbol{\gamma},t,2,3}(\operatorname{grad}\varphi_h) = r(r-1)\left(-\frac{1}{2|f_{023}|}\int_{f_{023}}\varphi_h\,[B_t^{\boldsymbol{\gamma}}]_{|f_{023}} + \frac{1}{2|f_{123}|}\int_{f_{123}}\varphi_h\,[B_t^{\boldsymbol{\gamma}}]_{|f_{123}}\right) - \frac{r(r-1)(r-2)}{6|t|}\int_t \varphi_h\left(B_t^{\boldsymbol{\gamma}-\mathbf{e}_1} - B_t^{\boldsymbol{\gamma}-\mathbf{e}_0}\right)$$

$$= \begin{cases} -\frac{r(r-1)}{2|f_{023}|}\int_{f_{023}}\varphi_h\,[B_t^{\boldsymbol{\gamma}}]_{|f_{023}} + \frac{r(r-1)}{2|f_{123}|}\int_{f_{123}}\varphi_h\,[B_t^{\boldsymbol{\gamma}}]_{|f_{123}} & \text{if } \boldsymbol{\gamma}=(0,0,\gamma_2,\gamma_3) \\ -\frac{r(r-1)}{2|f_{023}|}\int_{f_{023}}\varphi_h\,[B_t^{\boldsymbol{\gamma}}]_{|f_{023}} + \frac{r(r-1)(r-2)}{6|t|}\int_t\varphi_h B_t^{\boldsymbol{\gamma}-\mathbf{e}_0} & \text{if } \boldsymbol{\gamma}=(\gamma_0,0,\gamma_2,\gamma_3),\ \gamma_0\neq 0 \\ \frac{r(r-1)}{2|f_{123}|}\int_{f_{123}}\varphi_h\,[B_t^{\boldsymbol{\gamma}}]_{|f_{123}} - \frac{r(r-1)(r-2)}{6|t|}\int_t\varphi_h B_t^{\boldsymbol{\gamma}-\mathbf{e}_1} & \text{if } \boldsymbol{\gamma}=(0,\gamma_1,\gamma_2,\gamma_3),\ \gamma_1\neq 0 \\ -\frac{r(r-1)(r-2)}{6|t|}\int_t\varphi_h\left(B_t^{\boldsymbol{\gamma}-\mathbf{e}_1} - B_t^{\boldsymbol{\gamma}-\mathbf{e}_0}\right) & \text{otherwise.} \end{cases} \tag{2.11}$$

Moments for $\varphi_h \in L_{r+1}$

In view of these results, we consider the following set of moments for $\varphi_h \in L_{r+1}$:

- $M^L_{\boldsymbol{\alpha}',v}(\varphi_h) = (\varphi_h\, B_v^{\boldsymbol{\alpha}'})(v)$, for each $v\in V$ and $\boldsymbol{\alpha}'\in\mathcal{I}(r,1)$ (note that $B_v^{\boldsymbol{\alpha}'}(\tilde v)=1$ for $\tilde v = v$ and $B_v^{\boldsymbol{\alpha}'}(\tilde v)=0$ for $\tilde v\neq v$) ;
- $M^L_{\boldsymbol{\beta}',e}(\varphi_h) = \frac{r}{|e|}\int_e \varphi_h\, B_e^{\boldsymbol{\beta}'}$, for each $e\in E$ and $\boldsymbol{\beta}'\in\mathcal{I}(r-1,2)$;
- $M^L_{\boldsymbol{\gamma}',f}(\varphi_h) = \frac{r(r-1)}{2|f|}\int_f \varphi_h\, B_f^{\boldsymbol{\gamma}'}$, for each $f\in F$ and $\boldsymbol{\gamma}'\in\mathcal{I}(r-2,3)$;
- $M^L_{\boldsymbol{\delta}',t}(\varphi_h) = \frac{r(r-1)(r-2)}{6|t|}\int_t \varphi_h B_t^{\boldsymbol{\delta}'}$, for each $t\in T$ and $\boldsymbol{\delta}'\in\mathcal{I}(r-3,4)$.

In a more compact way, for $S\in\Delta_d(\mathcal{T})$ and $\boldsymbol{\eta}\in\mathcal{I}(r-d,d+1)$, if $r>d$

$$M^L_{\boldsymbol{\eta},S}(\varphi_h) = \frac{1}{|S|}\binom{r}{d}\int_S \varphi_h\, B_S^{\boldsymbol{\eta}}\,.$$

Remark 2.1. *It is well known (see [59] Proposition 3.5) that for any $S\in\Delta_d(\mathcal{T})$ and $\boldsymbol{\eta}\in\mathcal{I}(l,d+1)$ we have*

$$\int_S \lambda_S^{\boldsymbol{\eta}} = |S|\,\frac{\prod_{j=0}^d \eta_j!\, d!}{(l+d)!}\,, \tag{2.12}$$

hence the Lagrange moments of a constant function are constant, namely, $M^L_{\boldsymbol{\eta},S}(c)=c$ for any $S\in\Delta_d(\mathcal{T})$ and $\boldsymbol{\eta}\in\mathcal{I}(r-d,d+1)$.

We have defined $M^L_{\boldsymbol{\eta},S}(\varphi_h)$ for $d \in \{0,1,2,3\}$, $S \in \Delta_d(\mathcal{T})$ and $\boldsymbol{\eta} \in \mathcal{I}(r-d, d+1)$. When $d > 0$ we can extend the definition to $\mathcal{J}(r-d, d+1)$ in the following way: If $\widetilde{\boldsymbol{\eta}} \in \mathcal{J}(r-d, d+1) \setminus \mathcal{I}(r-d, d+1)$ then there exits $\boldsymbol{\zeta} \in \mathcal{I}(r-d+1, d+1)$ and $j \in \{0, 1, \ldots, d\}$ such that $\widetilde{\boldsymbol{\eta}} = \boldsymbol{\zeta} - \mathbf{e}_j$ and $\zeta_j = 0$ (hence $\widetilde{\eta}_j = -1$). Then

$$M^L_{\widetilde{\boldsymbol{\eta}},S}(\varphi_h) = M^L_{\boldsymbol{\zeta}-\mathbf{e}_j,S}(\varphi_h) = M^L_{R_{d,j}\boldsymbol{\zeta},S-[\mathbf{v}_{m_S(j)}]}(\varphi_h)\,.$$

With this notation we have proved that:

$$\begin{aligned}
M^N_{\boldsymbol{\alpha},e}(\operatorname{grad}\varphi_h) &= M^L_{\boldsymbol{\alpha}-\mathbf{e}_0,e}(\varphi_h) - M^L_{\boldsymbol{\alpha}-\mathbf{e}_1,e}(\varphi_h) \\
M^N_{\boldsymbol{\beta},f,1}(\operatorname{grad}\varphi_h) &= M^L_{\boldsymbol{\beta}-\mathbf{e}_0,f}(\varphi_h) - M^L_{\boldsymbol{\beta}-\mathbf{e}_2,f}(\varphi_h) \\
-M^N_{\boldsymbol{\beta},f,2}(\operatorname{grad}\varphi_h) &= M^L_{\boldsymbol{\beta}-\mathbf{e}_0,f}(\varphi_h) - M^L_{\boldsymbol{\beta}-\mathbf{e}_1,f}(\varphi_h) \\
(-1)^s M^N_{\boldsymbol{\gamma},t,1,2}(\operatorname{grad}\varphi_h) &= M^L_{\boldsymbol{\gamma}-\mathbf{e}_0,t}(\varphi_h) - M^L_{\boldsymbol{\gamma}-\mathbf{e}_3,t}(\varphi_h) \\
(-1)^{s+1} M^N_{\boldsymbol{\gamma},t,1,3}(\operatorname{grad}\varphi_h) &= M^L_{\boldsymbol{\gamma}-\mathbf{e}_0,t}(\varphi_h) - M^L_{\boldsymbol{\gamma}-\mathbf{e}_2,t}(\varphi_h) \\
(-1)^s M^N_{\boldsymbol{\gamma},t,2,3}(\operatorname{grad}\varphi_h) &= M^L_{\boldsymbol{\gamma}-\mathbf{e}_0,t}(\varphi_h) - M^L_{\boldsymbol{\gamma}-\mathbf{e}_1,t}(\varphi_h)\,.
\end{aligned} \tag{2.13}$$

2.4 A basis of the space divergence-free finite elements

We recall some basic definitions and results of graph theory that will be used in the sequel (they can be found, for instance, in [68]).

A graph $\mathcal{M} = (\mathcal{N}, \mathcal{A})$ consists of two sets: a finite set $\mathcal{N} = \{\mathfrak{n}_i\}_{i=1}^n$ of nodes and a finite set $\mathcal{A} = \{\mathfrak{a}_j\}_{j=1}^m$ of arcs. The end nodes of an arc need not be distinct. If the end nodes of the arc $\mathfrak{a}_j$ coincide with $\mathfrak{n}_i$, then it is called a self-loop at node $\mathfrak{n}_i$. If we choose an initial node and a final node between the extreme nodes of each arc of $\mathcal{M}$, then $\mathcal{M}$ is called a directed or an oriented graph. Otherwise $\mathcal{M}$ is called an undirected or a nonoriented graph.

The following definitions concern both directed and undirected graphs.

A walk is a finite alternating sequence of nodes and arcs $\mathfrak{n}_{i_0}$, $\mathfrak{a}_{j_1}$, $\mathfrak{n}_{i_1}$, $\mathfrak{a}_{j_2}$, $\mathfrak{n}_{i_2}, \ldots, \mathfrak{n}_{i_{K-1}}$, $\mathfrak{a}_{j_K}$, $\mathfrak{n}_{i_K}$ such that for $k \in \{1, \ldots, K\}$ the arc $\mathfrak{a}_{j_k}$ links the pair of nodes $\mathfrak{n}_{i_{k-1}}$, $\mathfrak{n}_{i_k}$. This walk is usually called a $\mathfrak{n}_{i_0} - \mathfrak{n}_{i_K}$ walk with $\mathfrak{n}_{i_0}$ and $\mathfrak{n}_{i_K}$ referred to as the end or terminal nodes of this walk. A walk is open if its end nodes, $\mathfrak{n}_{i_0}$, $\mathfrak{n}_{i_K}$ are distinct; otherwise it is closed. A walk is a trail if all its edges are distinct. An open trail is a path if all its nodes are distinct. A closed trail is a circuit if all its nodes except the end nodes are distinct. A graph is said to be acyclic if it has no circuits.

Two nodes $\mathfrak{n}_i$, $\mathfrak{n}_{i'}$ are said to be connected in a graph $\mathcal{M}$ if there exists a $\mathfrak{n}_i - \mathfrak{n}_{i'}$ path in $\mathcal{M}$. A graph $\mathcal{M}$ is connected if there exists a path between every pair of nodes in $\mathcal{M}$.

Proposition 2.1. *Let us set $d_N = \dim N_{r+1}$ and $d_L = \dim L_{r+1}$. Denoting by $G \in \mathbb{R}^{d_N \times d_L}$ the matrix that computes from the moments of φ_h, the moments of* $\operatorname{grad} \varphi_h$. *Then $G^\top$ is the all-nodes incidence matrix of a directed graph $\mathcal{M}^G$, with a node for each Lagrange moment and an arc for each Nédélec moment: $\mathcal{M}^G = (M^L, M^N)$. This graph is connected.*

Proof. We have proven in the previous section (and summarized in (2.13)) that the matrix $G \in \mathbb{R}^{d_N \times d_L}$ has two elements different from zero on each row, one equal to 1 and the other equal to -1, hence $G^\top$ is the all-nodes incidence matrix of the directed graph $\mathcal{M}^G = (M^L, M^N)$. To prove that it is connected we decompose it in edge, face and tetrahedra subgraphs (see Figure 2.1).

For all $e \in E$, $\mathcal{G}_e = (\mathcal{N}_e, \mathcal{A}_e)$ denotes the subgraph of $\mathcal{M}^G = (M^L, M^N)$ with nodes $\mathcal{N}_e = \{M^L_{\boldsymbol{\beta}',e} : \boldsymbol{\beta}' \in \mathcal{I}(r-1,2)\}$ and arcs $\mathcal{A}_e = \{M^N_{\boldsymbol{\alpha},e} : \boldsymbol{\alpha} \in \mathcal{I}(r,2) \text{ with } \alpha_0 \neq 0 \neq \alpha_1\}$. Using the third line in (2.5) it is easy to check that all the nodes of $\mathcal{N}_e$ are connected with the node $M^L_{(r-1,0),e}$. In fact if $\boldsymbol{\beta}' = (\beta'_0, \beta'_1)$ with $\beta'_1 \neq 0$, then the arc $M^N_{\boldsymbol{\alpha},e}$ with $\boldsymbol{\alpha} = (\beta'_0 + 1, \beta'_1)$ belongs to $\mathcal{A}_e$ and connects the node $M^L_{(\beta'_0,\beta'_1),e}$ with the node $M^L_{(\beta'_0+1,\beta'_1-1),e}$. Hence, it is possible to construct a path with β'_1 arcs connecting $M^L_{(\beta'_0,\beta'_1),e}$ with $M^L_{(\beta'_0+\beta'_1,0),e} = M^L_{(r-1,0),e}$.

Analogously, for all $f \in F$, $\mathcal{G}_f = (\mathcal{N}_f, \mathcal{A}_f)$ denotes the subgraph of $\mathcal{M}^G = (M^L, M^N)$ with nodes $\mathcal{N}_f = \{M^L_{\boldsymbol{\gamma}',f} : \boldsymbol{\gamma}' \in \mathcal{I}(r-2,3)\}$ and arcs $\mathcal{A}_f = \cup_{i=1}^2 \{M^N_{\boldsymbol{\beta},f,i} : \boldsymbol{\beta} \in \mathcal{I}(r-1,3) \text{ with } \beta_l \neq 0 \text{ if } l \neq i\}$. If $\gamma'_2 \neq 0$, from the last line in (2.7), taking $\boldsymbol{\beta}$ such that $\boldsymbol{\gamma}' = \boldsymbol{\beta} - e_0$, the arc $M^N_{\boldsymbol{\beta},f,1} \in \mathcal{A}_f$ connects the node $M^L_{(\gamma'_0,\gamma'_1,\gamma'_2),f}$ with the node $M^L_{(\gamma'_0+1,\gamma'_1,\gamma'_2-1),f}$. On the other hand if $\gamma'_1 \neq 0$, from the last line in (2.8), taking $\boldsymbol{\beta}$ such that $\boldsymbol{\gamma}' = \boldsymbol{\beta} - e_0$, the arc $M^N_{\boldsymbol{\beta},f,2} \in \mathcal{A}_f$ connects the node $M^L_{(\gamma'_0,\gamma'_1,\gamma'_2),f}$ with the node $M^L_{(\gamma'_0+1,\gamma'_1-1,\gamma'_2),f}$. Hence, if $\gamma'_1 + \gamma'_2 \neq 0$, it is possible to construct a path with $\gamma'_1 + \gamma'_2$ arcs connecting $M^L_{(\gamma'_0,\gamma'_1,\gamma'_2),f}$ with $M^L_{(\gamma'_0+\gamma'_1+\gamma'_2,0,0),f}$.

Finally, for all $t \in T$, $\mathcal{G}_t = (\mathcal{N}_t, \mathcal{A}_t)$ denotes the subgraph of $\mathcal{M}^G = (M^L, M^N)$ with nodes $\mathcal{N}_t = \{M^L_{\boldsymbol{\delta}',t} : \boldsymbol{\delta}' \in \mathcal{I}(r-3,4)\}$ and arcs $\mathcal{A}_t = \cup_{1 \leq i < j \leq 3} \{M^N_{\boldsymbol{\gamma},t,i,j} : \boldsymbol{\gamma} \in \mathcal{I}(r-2,4) \text{ with } \gamma_l \neq 0 \text{ if } l \notin \{i,j\}\}$. Using the last line in (2.9), (2.10) and (2.11) and proceeding as for edges and faces, it is easy to check that $\mathcal{G}_t$ is connected.

We consider also the subgraph $\mathcal{G}^*_e = (\mathcal{N}^*_e, \mathcal{A}^*_e)$ with nodes $\mathcal{N}^*_e = \mathcal{N}_e \cup_{i=0}^1 M^L_{\boldsymbol{\alpha}',\mathbf{v}_{m_e(i)}}$ $(\boldsymbol{\alpha}' \in \mathcal{I}(r,1))$ and arcs $\mathcal{A}^*_e = \{M^N_{\boldsymbol{\alpha},e} : \boldsymbol{\alpha} \in \mathcal{I}(r,2)\}$. The first line in (2.5) connects $M^L_{\boldsymbol{\alpha}',\mathbf{v}_{m_e(0)}}$ with a node of $\mathcal{G}_e$ while the second one connects $M^L_{\boldsymbol{\alpha}',\mathbf{v}_{m_e(1)}}$ with a node of $\mathcal{G}_e$,

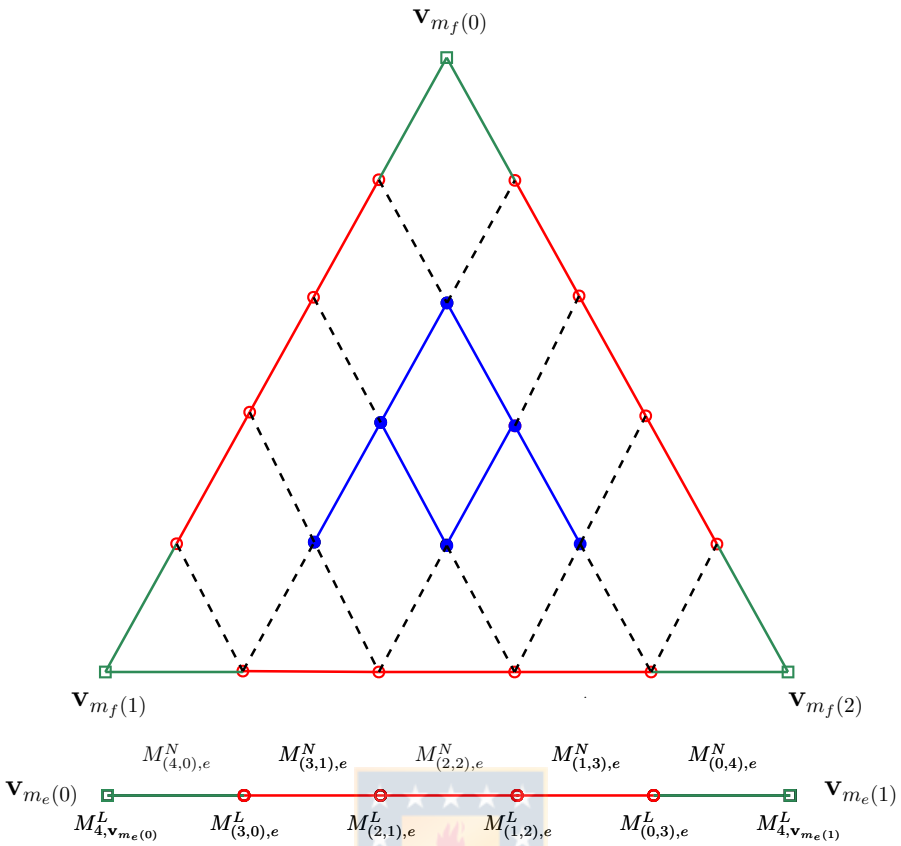

Figure 2.1: On the left an example of edge subgraph $\mathcal{G}_e$ in red and $\mathcal{G}_e^*$ (red and green). On the right, in blue, an example of face subgraph $\mathcal{G}_f$; in red and green the three subgraphs of the edges on the boundary of f.

hence $\mathcal{G}_e^*$ is connected. For each $e \in E$, $\mathcal{G}_e^*$ is a path connecting the Lagrange moments associated to the vertices of the mesh in $\Delta_0(e)$. Hence if Ω is connected the graph $\cup_{e\in E}\mathcal{G}_e^*$ is connected.

To conclude the proof we notice that, for instance, the second line of (2.7) corresponds to an arc of $\mathcal{M}^G = (M^L, M^N)$ that connects a node of $\mathcal{G}_f$ with a node of $\mathcal{G}_{f-[v_{m_f(2)}]}$ and the second line of (2.9) corresponds to an arc that connects a node of $\mathcal{G}_t$ with a node of $\mathcal{G}_{t-[v_{m_t(3)}]}$. Since each node of $\mathcal{M}^G$ belongs to a subgraph of the type $\mathcal{G}_e^*$, $\mathcal{G}_f$ or $\mathcal{G}_t$, the previous fact proves that $\mathcal{M}^G$ is connected. □

Let $\{M_i^N\}_{i=1}^{d_N}$ be the set of Nédélec moments and $\{\mathbf{\Phi}_i\}_{i=1}^{d_N}$ be a cardinal (dual) basis for those moments. Let $\mathcal{S}^G = (M^L, S^N)$ be a spanning tree of $\mathcal{M}^G$. We consider the set

of elements of the cardinal basis corresponding to Nédélec moments that are not in the spannig tree $\mathcal{S}^G$, namely, the set $\{\mathbf{\Phi}_i\}_{i\in K}$ being $K = \{i \in \mathbb{N}, 1 \le i \le d_N : M_i^N \notin S^N\}$. Clearly, denoting by d_K the number of elements in K, one has $d_K = d_N - (d_L - 1)$.

Proposition 2.2. *If Ω is simply connected, then the set $\{\operatorname{curl}\mathbf{\Phi}_i\}_{i\in K}$ is linearly independent.*

Proof. Let $A \in \mathbb{R}^{d_N\times d_N}$ be the matrix with entries

$$A_{i,j} = \int_\Omega \operatorname{curl}\mathbf{\Phi}_j \cdot \operatorname{curl}\mathbf{\Phi}_i$$

and $A^0 \in \mathbb{R}^{d_K\times d_K}$ the submatrix of A obtained by choosing those rows and columns of A that correspond to indices in K. We will prove that A^0 is nonsingular. Given $\mathbf{c} \in \mathbb{R}^{d_K}$, we denote $\mathbf{c}_h = \sum_{i\in K} c_i\mathbf{\Phi}_i$. If $A^0\mathbf{c} = \mathbf{0}$, then

$$\mathbf{c}^\top A^0\mathbf{c} = \int_\Omega \operatorname{curl}\mathbf{c}_h \cdot \operatorname{curl}\mathbf{c}_h = 0\,,$$

being Ω simply connected, it follows that $\mathbf{c}_h = \operatorname{grad}\phi_h$ for some $\phi_h \in L_{r+1}$.

On the other hand, all the Nédélec moments of $\mathbf{c}_h = \operatorname{grad}\phi_h$ in a spanning tree of $\mathcal{M}^G$ are equal to zero. It follows from (2.13) that all the moments of ϕ_h are equal to a constant. This means that ϕ_h is constant and that $\mathbf{c}_h = \operatorname{grad}\phi_h = 0$.

Now it is easy to see that $\{\operatorname{curl}\mathbf{\Phi}_i\}_{i\in K}$ is linearly independent. In fact, if $\mathbf{w}_h = \sum_{i\in K} c_i\operatorname{curl}\mathbf{\Phi}_i = 0$, then $\int_\Omega \mathbf{w}_h \cdot \operatorname{curl}\mathbf{\Phi}_l = 0$ for any $l \in K$. This means that $A^0\mathbf{c} = \mathbf{0}$ and also that $\mathbf{c} = \mathbf{0}$ because A^0 is not singular. □

If Ω is not simply connected, then its first Betti number $\beta_1(\Omega) := \dim\mathcal{H}_1(\overline{\Omega};\mathbb{Z}) = g$ is not zero. If $\{\sigma_j\}_{j=1}^g$ is a set of 1-cycles (the elements of $\ker\partial_1$) representing a basis of $\mathcal{H}_1(\overline{\Omega};\mathbb{Z})$ (the first homology group: 1-cycles in $\overline{\Omega}$ that do not bound any surface contained in $\overline{\Omega}$), then any curl-free function $\mathbf{u}_h$ with $\oint_{\sigma_j}\mathbf{u}_h = 0$ for $j = 1,\dots,g$, is a gradient. Our aim is to extend to the high order case the notion of belted tree (see e.g. [49], [63], [61]). To this end we assume that we know a set of g polygonal loops in $\mathcal{T}$, $\{\sigma_j\}_{j=1}^g$, mutually disjoint and without self-intersection, representing a basis of $\mathcal{H}_1(\overline{\Omega};\mathbb{Z})$. For each $j \in \{1,\dots,g\}$, σ_j is a 1-cycle of the form $\sigma_j = \sum_{e\in E} a_e^j e$ with $a_e^j \in \{-1,0,1\}$. We denote $\operatorname{supp}(\sigma_j) := \{e \in E : a_e^j \neq 0\}$. Then, using (2.3) we have

$$\oint_{\sigma_j}\mathbf{u}_h = \sum_{e\in\operatorname{supp}(\sigma_j)} a_e^j\int_e \mathbf{u}_h\cdot\boldsymbol{\tau}_e = \sum_{e\in\operatorname{supp}(\sigma_j)} a_e^j\sum_{\boldsymbol{\alpha}\in\mathcal{I}(r,2)}\int_e \mathbf{u}_h\cdot\boldsymbol{\tau}_e B_e^{\boldsymbol{\alpha}} = \sum_{e\in\operatorname{supp}(\sigma_j)} a_e^j\sum_{\boldsymbol{\alpha}\in\mathcal{I}(r,2)} M_{\boldsymbol{\alpha},e}^N\,. \tag{2.14}$$

We associate to each 1-cycle σ_j in $\mathcal{T}$ a circuit $\mathcal{G}_j$ of the graph $\mathcal{M}^G$ in the following natural way

$$\mathcal{G}_j = \cup_{e\in \mathrm{supp}(\sigma_j)} \mathcal{G}_e^* \,.$$

Each $\mathcal{G}_j$ is a circuit because σ_j has not self-intersections.

For each $j \in \{1,\dots,g\}$ we choose an arc $M^N_{\boldsymbol{\alpha}^*_j, e^*_j}$ of $\mathcal{G}_j$. The new trail $\mathcal{G}_j^-$, obtained from the circuit $\mathcal{G}_j$ removing the arc $M^N_{\boldsymbol{\alpha}^*_j, e^*_j}$, is a path. Since the cycles $\{\sigma_j\}_{j=1}^g$ are mutually disjoint, the subgraph of $\mathcal{M}^G$, given by the union of the paths $\mathcal{G}_j^-$ has g acyclic connected components, hence it is acyclic. So it is possible to construct a spanning tree $\mathcal{S}^G = (M^L, S^N)$ of $\mathcal{M}^G$ that contains the acyclic subgraph. We will refer to the subgraph $\mathcal{B}^G = (M^L, B^N)$ of $\mathcal{M}^G$, with $B^N = S^N \cup \{M^N_{\boldsymbol{\alpha}^*_1, e^*_1}, \dots M^N_{\boldsymbol{\alpha}^*_g, e^*_g}\}$, as a *belted tree*.

Proposition 2.3. *The set* $\{\operatorname{curl} \boldsymbol{\Phi}_i\}_{i\in K^*}$, *being* $K^* = \{i \in \mathbb{N}, 1 \le i \le d_N : M_i^N \notin B^N\}$, *is linearly independent.*

Proof. The procedure is similar to the one of Proposition 2.2. Denoting by d_{K^*} the cardinality of K^*, let $A^{0,*} \in \mathbb{R}^{d_{K^*}\times d_{K^*}}$ be the submatrix of A obtained by choosing those rows and columns of A that correspond to indices in K^*. It is easy to verify that $A^{0,*}$ is nonsingular. In fact, given $\mathbf{c} \in \mathbb{R}^{d_{K^*}}$ and denoting $\mathbf{c}_h = \sum_{i\in K^*} c_i \boldsymbol{\Phi}_i$. If $A^{0,*}\mathbf{c} = \mathbf{0}$, then

$$\mathbf{c}^\top A^{0,*}\mathbf{c} = \int_\Omega \operatorname{curl} \mathbf{c}_h \cdot \operatorname{curl} \mathbf{c}_h = 0\,,$$

hence $\operatorname{curl} \mathbf{c}_h = 0$. Moreover, since the Nédélec moments of $\mathbf{c}_h$ with indices in B^N are equal to zero, from (2.14) we have $\oint_{\sigma_j} \mathbf{c}_h = 0$ for all $j \in \{1,\dots,g\}$, so $\mathbf{c}_h = \operatorname{grad} \phi_h$ for some $\phi_h \in L_{r+1}$. Now the proof follows as in Proposition 2.2. □

In general $\dim RT^0_{r+1} = d_N - (d_L - 1) - g + p$, being p the number of connected components of the boundary of Ω minus one. Since $d_{K^*} = d_N - (d_L - 1) - g$, if the boundary of Ω is connected, the set $\{\operatorname{curl} \boldsymbol{\Phi}_i\}_{i\in K^*}$ is really a basis of RT^0_{r+1} in this case. However, for $p > 0$, the space of divergence-free Raviart-Thomas finite elements that are not the curl of Nédélec finite elements is non-trivial and has dimension p. So we have to add, for each $n = 1,\dots,p$, one solution $\mathbf{z}_{h,n} \in RT_{r+1}$ of

$$\begin{cases} \operatorname{div} \mathbf{z}_{h,n} &= 0 & \text{in } \Omega \\ \int_{(\partial\Omega)_l} \mathbf{z}_{h,n} \cdot \mathbf{n}_\Omega &= \delta_{n,l} & l = 1,\dots,p\,. \end{cases} \tag{2.15}$$

It is worth noting that each one of these problems has infinite solutions. However, it is clear that for any choice of $\mathbf{z}_{h,n}$ the set $\{\mathbf{z}_{h,n}\}_{n=1}^p$ is linearly independent.

A solution of (2.15) can be computed, for instance, as indicated in [7]. Consider the graph $\mathcal{M}^D$ that has $d_P + (p+1)$ nodes, one for each moment of P_r and one for each connected component of $\partial\Omega$, and d_{RT} arcs, one for each moment of RT_{r+1}; for which the divergence matrix is the incidence matrix of $\mathcal{M}^D$, with reference node the one corresponding to the external connected component of $\partial\Omega$. If we choose a spanning tree of this graph, for $n \in \{1, \ldots, p\}$, the corresponding column of the matrix $\widetilde{B}_1$ in [7] contains the moments of the unique solution of (2.15) that has all the moments corresponding to the arcs of the cotree (out of a spanning tree) equal to zero. This solution can be computed using a very efficient elimination procedure.

Another possibility is to consider the mixed finite element approximation of the problem

$$\begin{aligned} -\Delta\varphi_n &= 0 \quad \text{in } \Omega \\ \varphi_n &= 1 \quad \text{on } (\partial\Omega)_n \\ \varphi_n &= 0 \quad \text{on } (\partial\Omega)_l, \ \text{ for } l \neq n\,. \end{aligned}$$

Hence, we look for $(\widehat{\mathbf{z}}_{h,n}, \varphi_{n,h}) \in RT_{r+1} \times P_r$ such that

$$\begin{aligned} \int_\Omega \widehat{\mathbf{z}}_{h,n} \cdot \mathbf{v}_h + \int_\Omega \operatorname{div} \mathbf{v}_h \, \varphi_{n,h} &= \int_{(\partial\Omega)_n} \varphi_{n,h} (\mathbf{v}_h \cdot \mathbf{n}_\Omega) \quad \forall\, \mathbf{v}_h \in RT_{r+1} \\ \int_\Omega \operatorname{div} \widehat{\mathbf{z}}_{h,n} \, q_h &= 0 \qquad\qquad\qquad\qquad\quad \forall\, q_h \in P_r\,. \end{aligned} \tag{2.16}$$

2.5 Remarks on implementation

If $p = 0$ then the mass matrix corresponding to the divergence-free basis of RT_{r+1} constructed in Section 2.4 is obtained by choosing some rows and columns in the stiffness matrix of a cardinal basis of N_{r+1}, (those rows and columns corresponding to Nédélec moments that are not in a belted tree of the graph associated to the gradient operator). As usually this stiffness matrix is constructed by assembling the elementary matrices $A_t^{card} \in \mathbb{R}^{\mathtt{n}\times\mathtt{n}}$ with entries $[A_t^{card}]_{i,j} = \int_t \operatorname{curl} \boldsymbol{\Phi}_{t,i} \cdot \operatorname{curl} \boldsymbol{\Phi}_{t,j}$, being $\mathtt{n} = (r+1)\begin{pmatrix} r+4 \\ 2 \end{pmatrix}$ the dimension of $\mathcal{P}^-_{r+1}\Lambda^1(t)$. The explicit form of the elements of the local cardinal basis $\{\boldsymbol{\Phi}_{t,j}\}_{j=1}^{\mathtt{n}}$ is not known. However a well known basis of $\mathcal{P}^-_{r+1}\Lambda^1(t)$ is given by

$$\{\lambda_t^{\boldsymbol{\eta}(e')} \boldsymbol{\omega}_{e'} \ : e' \in \Delta_1(t) \text{ and } \boldsymbol{\eta}(e') \in \mathcal{I}^{e'}(r,4)\}, \tag{2.17}$$

being $\mathcal{I}^{e'}(r,4) := \{\boldsymbol{\eta} \in \mathcal{I}(r,4) \ : \ \eta_i = 0 \text{ if } i < m^t_{e'}(0)\}$. It is worth noting that the number of elements in $\mathcal{I}^{e'}(r,4)$ is equal to the number of elements in $\mathcal{I}(r, 4 - m^t_{e'}(0))$. We denote by $\{\boldsymbol{\zeta}_l\}_{l=1}^{\mathtt{n}}$ the elements of this basis, and by $\{M^N_{t,i}\}_{i=1}^{\mathtt{n}}$, the set of local Nédélec moments.

Since $\{\boldsymbol{\zeta}_l\}_{l=1}^{\mathtt{n}}$ is a basis, for each $j \in \{1,\dots,\mathtt{n}\}$ there are $\mathtt{n}$ coefficients $c_{j,l}$ (and they are unique) such that $\boldsymbol{\Phi}_{t,j} = \sum_{l=1}^{\mathtt{n}} c_{j,l}\boldsymbol{\zeta}_l$. Moreover

$$M_{t,i}^N(\boldsymbol{\Phi}_{t,j}) = \delta_{i,j} = \sum_{l=1}^{\mathtt{n}} c_{j,l} M_{t,i}^N(\boldsymbol{\zeta}_l)\,.$$

Following [59] we introduce the generalized Vandermonde matrix: $V \in \mathbb{R}^{\mathtt{n}\times\mathtt{n}}$ with entries $V_{i,l} = M_{t,i}^N(\boldsymbol{\zeta}_l)$. Since $\{\boldsymbol{\Phi}_{t,j}\}_{j=1}^{\mathtt{n}}$ is the local cardinal basis with respects to the moments introduced in Section 2.3, we have

$$M_{t,i}^N(\boldsymbol{\Phi}_j) = \delta_{i,j} = \sum_{l=1}^{\mathtt{n}} c_{j,l} M_{t,i}^N(\boldsymbol{\zeta}_l) = \sum_{l=1}^{\mathtt{n}} c_{j,l} V_{i,l} = [VC^\top]_{i,j}\,,$$

being $C \in \mathbb{R}^{\mathtt{n}\times\mathtt{n}}$ the matrix with entries $c_{j,l}$. This means that $VC^\top = I$ and then $C^\top = V^{-1}$. So, it is possible to compute A_t^{card} from the elementary matrices $A_t \in \mathbb{R}^{\mathtt{n}\times\mathtt{n}}$ with entries $[A_t]_{i,j} = \int_t \operatorname{curl}\boldsymbol{\zeta}_i \cdot \operatorname{curl}\boldsymbol{\zeta}_j$ because they are linked by V in the following way.

$$A_t^{card} = C A_t\, C^\top = V^{-\top} A_t V^{-1}\,.$$

Moreover it is enough to compute V for the reference element because it is, in fact, independent of the physical element (see [25] *Property 1*).

Proposition 2.4. *The generalized Vandermonde matrix V is independent of the tetrahedra t (up to its orientation).*

Proof. For the moments defined in (2.3) we have:

- $M_{\boldsymbol{\alpha},e}^N(\lambda^{\boldsymbol{\eta}}\boldsymbol{\omega}_{e'}) = \int_e \lambda^{\boldsymbol{\eta}}\boldsymbol{\omega}_{e'}\cdot\boldsymbol{\tau}_e B_e^{\boldsymbol{\alpha}} = (\boldsymbol{\omega}_{e'}\cdot\boldsymbol{\tau}_e)_{|e}\int_e \lambda^{\boldsymbol{\eta}}\, B_e^{\boldsymbol{\alpha}}$ and

$$(\boldsymbol{\omega}_{e'}\cdot\boldsymbol{\tau}_e)_{|e} = \begin{cases} 0 & \text{if } e' \neq e \\ \frac{1}{|e|} & \text{if } e' = e\,. \end{cases}$$

- $M_{\boldsymbol{\beta},f,i}^N(\lambda^{\boldsymbol{\eta}}\boldsymbol{\omega}_{e'}) = r\int_f(\lambda^{\boldsymbol{\eta}}\boldsymbol{\omega}_{e'}\times\mathbf{n}_f)\cdot B_f^{\boldsymbol{\beta}}\operatorname{grad}_f\lambda_{m_f(i)}$.

  First we notice that $(\boldsymbol{\omega}_{e'}\times\mathbf{n}_f)_{|f} = \mathbf{0}$ if $e' \notin \Delta_1(f)$ because if $\mathbf{v}_i \notin \Delta_0(f)$ then $\lambda_{i|f} = 0$ and $(\operatorname{grad}\lambda_i \times \mathbf{n}_f)_{|f} = \mathbf{0}$.

  Otherwise $e' = f - [\mathbf{v}_{m_f(k)}]$ and using that $\operatorname{grad}_f\lambda_{m_f(0)} = -\operatorname{grad}_f\lambda_{m_f(1)} - \operatorname{grad}_f\lambda_{m_f(2)}$ we have

– $k=0$

$$(\boldsymbol{\omega}_{e'}\times\mathbf{n}_f)\cdot\operatorname{grad}_f\lambda_{m_f(i)} = [\operatorname{grad}_f\lambda_{m_f(i)}\times(\lambda_{m_f(1)}\operatorname{grad}\lambda_{m_f(2)}-\lambda_{m_f(2)}\operatorname{grad}\lambda_{m_f(1)})]\cdot\mathbf{n}_f$$

$$= \lambda_{m_f(i)}(\operatorname{grad}\lambda_{m_f(1)}\times\operatorname{grad}\lambda_{m_f(2)})\cdot\mathbf{n}_f = \lambda_{m_f(i)}\frac{1}{2|f|}$$

– $k=1$

$$(\boldsymbol{\omega}_{e'}\times\mathbf{n}_f)\cdot\operatorname{grad}_f\lambda_{m_f(i)} = [\operatorname{grad}_f\lambda_{m_f(i)}\times(\lambda_{m_f(0)}\operatorname{grad}\lambda_{m_f(2)}-\lambda_{m_f(2)}\operatorname{grad}\lambda_{m_f(0)})]\cdot\mathbf{n}_f$$

$$= [\operatorname{grad}_f\lambda_{m_f(i)}\times((\lambda_{m_f(0)}+\lambda_{m_f(2)})\operatorname{grad}\lambda_{m_f(2)}+\lambda_{m_f(2)}\operatorname{grad}\lambda_{m_f(1)})]\cdot\mathbf{n}_f$$

$$= \begin{cases} (\lambda_{m_f(0)}+\lambda_{m_f(2)})\frac{1}{2|f|} & \text{if } i=1 \\ -\lambda_{m_f(2)}\frac{1}{2|f|} & \text{if } i=2 \end{cases}$$

– $k=2$

$$(\boldsymbol{\omega}_{e'}\times\mathbf{n}_f)\cdot\operatorname{grad}_f\lambda_{m_f(i)} = [\operatorname{grad}_f\lambda_{m_f(i)}\times(\lambda_{m_f(0)}\operatorname{grad}\lambda_{m_f(1)}-\lambda_{m_f(1)}\operatorname{grad}\lambda_{m_f(0)})]\cdot\mathbf{n}_f$$

$$= [\operatorname{grad}_f\lambda_{m_f(i)}\times((\lambda_{m_f(0)}+\lambda_{m_f(1)})\operatorname{grad}\lambda_{m_f(1)}+\lambda_{m_f(1)}\operatorname{grad}\lambda_{m_f(2)})]\cdot\mathbf{n}_f$$

$$= \begin{cases} \lambda_{m_f(1)}\frac{1}{2|f|} & \text{if } i=1 \\ -(\lambda_{m_f(0)}+\lambda_{m_f(1)})\frac{1}{2|f|} & \text{if } i=2 \end{cases}$$

- $M^N_{\boldsymbol{\gamma},t,i,j}(\lambda^{\boldsymbol{\eta}}\boldsymbol{\omega}_{e'}) = r(r-1)\int_t \lambda^{\boldsymbol{\eta}}\boldsymbol{\omega}_{e'}\cdot B_t^{\gamma}\operatorname{grad}\lambda_{m_t(i)}\times\operatorname{grad}\lambda_{m_t(j)}$.
  Clearly $\boldsymbol{\omega}_{e'}\cdot\operatorname{grad}\lambda_{m_t(i)}\times\operatorname{grad}\lambda_{m_t(j)}=0$ if $e'=[\mathbf{v}_{m_t(i)},\mathbf{v}_{m_t(j)}]$. Otherwise

  $$\boldsymbol{\omega}_{e'}\cdot\operatorname{grad}\lambda_{m_t(i)}\times\operatorname{grad}\lambda_{m_t(j)} = (\lambda_{m_t(0)}\operatorname{grad}\lambda_{m_t(k)}-\lambda_{m_t(k)}\operatorname{grad}\lambda_{m_t(0)})\cdot\operatorname{grad}\lambda_{m_t(i)}\times\operatorname{grad}\lambda_{m_t(j)}$$

  with $k\in\{1,2,3\}$. Using that $\operatorname{grad}\lambda_{m_t(0)} = -\operatorname{grad}\lambda_{m_t(1)}-\operatorname{grad}\lambda_{m_t(2)}-\operatorname{grad}\lambda_{m_t(3)}$ we have

  $$\boldsymbol{\omega}_{e'}\cdot\operatorname{grad}\lambda_{m_t(i)}\times\operatorname{grad}\lambda_{m_t(j)} = (\lambda_{m_t(0)}+\lambda_{m_t(k)})\operatorname{grad}\lambda_{m_t(k)}\cdot\operatorname{grad}\lambda_{m_t(i)}\times\operatorname{grad}\lambda_{m_t(j)}$$

  with $k\in\{1,2,3\}$, $i\neq k\neq j$ and

  $$\operatorname{grad}\lambda_{m_t(k)}\cdot\operatorname{grad}\lambda_{m_t(i)}\times\operatorname{grad}\lambda_{m_t(j)} = \begin{cases} \frac{(-1)^s}{6|t|} & \text{if } k<i<j \text{ or } i<j<k \\ \frac{(-1)^{s+1}}{6|t|} & \text{if } i<k<j\,, \end{cases}$$

  being $s=0$ if t is positive oriented and $s=1$ otherwise.

Hece all the entries are of the form $\pm\frac{1}{d!|S|}\int_S \lambda_t^{\boldsymbol{\eta}} B_S^{\widetilde{\boldsymbol{\eta}}}$ or $\pm\frac{1}{d!|S|}\int_S \lambda_{m_S(i)}\lambda_t^{\boldsymbol{\eta}} B_S^{\widetilde{\boldsymbol{\eta}}}$ for $S\in\Delta_d(t)$, $d\in\{1,2,3\}$. It is worth noting that

$$[\lambda_t^{\boldsymbol{\eta}}]_{|S} = \begin{cases} 0 & \text{if } \eta_i\neq 0 \text{ and } \mathbf{v}_{m_t(i)}\notin\Delta_1(S) \\ \lambda_S^{R\boldsymbol{\eta}} & \text{otherwise,}\end{cases}$$

being $R\boldsymbol{\eta}\in\mathcal{I}(r,d)$. From (2.12) these integrals are equal to $|S|F(i,d,\boldsymbol{\eta},\widetilde{\boldsymbol{\eta}})$ with F independent of $|S|$, hence the entries of the Vandermonde matrix are independent of t. □

If $\beta_2(\Omega)\neq 0$ then the mass matrix correspondig the divergence-free basis of RT_{r+1} has also entries of the form $\int_t \mathbf{w}_{h,n}\cdot\operatorname{curl}\boldsymbol{\Phi}_i$ and $\int_t \mathbf{w}_{h,n}\cdot\mathbf{w}_{h,n'}$ being $\{\mathbf{w}_{h,n}\}_{n=1}^p$ a basis of the space of divergence-free Raviart-Thomas finite elements that are not a curl. Taking in particular the basis construted solving (2.16), namely, $\{\widehat{\mathbf{z}}_{h,n}\}_{n=1}^p$, the mass matrix is block diagonal because taking $\operatorname{curl}\boldsymbol{\Phi}_i$ as test function in the first equation of (2.16) one has

$$\int_\Omega \widehat{\mathbf{z}}_{h,n}\cdot\operatorname{curl}\boldsymbol{\Phi}_i = \int_{(\partial\Omega)_n}\operatorname{curl}\boldsymbol{\Phi}_i\cdot\mathbf{n} = 0\,.$$

CHAPTER 3

Divergence-free finite elements for the numerical solution of a hydroelastic vibration problem

3.1 Introduction

Fluid-structure interaction involves the motion of a deformable structure in contact with an internal or surrounding fluid. These kind of interactions are a crucial consideration in the design of many engineering systems, e.g., aircraft, engines and bridges. Another example where it has also to be taken into account is for the analysis of aneurysms in large arteries and artificial heart valves. As a result, much effort has gone into the development of general finite element methods for fluid-structure systems.

In this chapter we are concerned with the interaction between a fluid and an elastic structure. We will consider the problem that consists of a bounded domain completely filled by the fluid and limited by the solid. Different formulations have been proposed to solve this problem (see, for instance, [20] and references therein).

Pure displacement formulations are very much used in applications. Indeed, they lead to simple well-posed generalized eigenvalue problems and are convenient to handle more complex interactions between fluids and structures (for instance, in presence of wall dissipation [18]). However, it is well-known that standard discretizations with Lagrange elements lead to spurious vibration frequencies interspersed among the physical ones [43]. In [17] (see also [15]) a finite element method for a 2D (two-dimensional) domain that does not present spurious modes has been introduced. It is based on using displacement variables for both the fluid and the solid. The pressure of the fluid is also used for the theoretical analysis. The displacements are approximated by piecewise linear elements for the solid

and Raviart–Thomas elements of lowest order for the fluid. The interface coupling of both discretization is achieved in a non-conforming way. In the case of an incompressible fluid, the fluid displacement variables can be eliminated by using the so-called *added mass* formulation (see, for instance, [55]). This consists of taking into account the effect of the fluid by means of a Neumann-to-Dirichlet operator (also called Steklov-Poincaré operator) on the fluid-solid interface. The finite element discretization of this problem has been treated, for instance, in [14], [22].

Another strategy was presented in [16, 17]. It consists of using divergence-free fields for describing the fluid displacements. This is theoretically analyzed and conveniently implemented in the 2D case by means of curls of piecewise linear elements. However, its extension to 3D (three-dimensional case) is not straightforward. In particular, in order to use a similar approach in 3D, we would need to construct a basis of the divergence-free discrete fields. Two approaches have been recently proposed in [8] to this end. The first one consists in finding a suitable selection of curls of NéÌĄdélec finite elements. The second one, is based on an efficient algebraic procedure which is inspired by [10, 11] and consists of writing the basis functions as linear combinations of lowest-order Raviart–Thomas elements. We perform the numerical analysis of the proposed method and report numerical results by considering both sets of basis functions which illustrate the good performance of the method.

The outline of the chapter is as follows. In Section 3.2 we introduce the model problem. Next, in Section 3.3, we recall the mixed formulation proposed in [17], introduce the solution operator and characterize its spectrum. In Section 3.4 we introduce the numerical approach based on standard piecewise linear finite elements for the displacement in the solid, divergence-free Raviart–Thomas elements for the displacement of the fluid and piecewise constant functions for the pressure on the interface. In addition, we introduce the discrete solution operator. Next, in Section 3.5 we prove convergence of the method and optimal-order error estimates for eigenfunctions and eigenvalues. Finally, in Section 3.6, we report some numerical experiments.

3.2 The model problem

We consider the problem of determining the vibration modes of a linear elastic structure containing an incompressible, inviscid and homogeneous fluid. We focus on the three-dimensional (3D) case and assume polygonal boundaries and interfaces.

Let Ω_F and Ω_S be polyhedral Lipschitz bounded domains occupied by the fluid and the

solid, respectively, as shown in Figure 3.1. We assume Ω_F to be a connected domain with boundary $\Gamma_I = \overline{\Omega_S} \cap \overline{\Omega_F}$ and $\boldsymbol{\nu}$ its unit normal vector pointing toward Ω_S. We assume that $\Gamma_I = \bigcup_{j=1}^{J} \Gamma_j$, where Γ_j, $j = 1, ..., J$ are the faces of the polyhedral interface Γ_I.

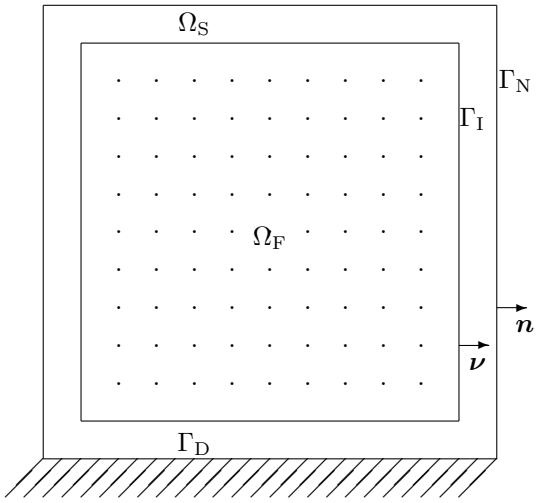

Figure 3.1: Vertical sections of fluid and solid domains (figure produced by the author).

The exterior boundary of the solid is the union of polyhedral surfaces Γ_D and Γ_N, the structure being fixed on Γ_D and free of stress on Γ_N. The outward unit normal vector to $\partial\Omega_S \setminus \Gamma_I$ is denoted by $\boldsymbol{n}$.

Thought this chapter we use the standard notation for Sobolev spaces, norms and seminorms. The space $H(\mathrm{div}; \Omega_F) := \{\mathbf{u} \in [L^2(\Omega_F)]^3 \,:\, \mathrm{div}\ \mathbf{u} \in L^2(\Omega_F)\}$ is endowed with the norm defined by

$$\|\mathbf{u}\|^2_{\mathrm{div},\Omega_F} := \|\mathbf{u}\|^2_{0,\Omega_F} + \|\,\mathrm{div}\ \mathbf{u}\|^2_{0,\Omega_F}.$$

We also introduce the spaces:

$$\begin{aligned} H(\mathrm{div}^0; \Omega_F) &:= \{\mathbf{u} \in H(\mathrm{div}; \Omega_F) \,:\, \mathrm{div}\ \mathbf{u} = 0 \text{ in } \Omega_F\}\,, \\ H_0(\mathrm{div}; \Omega_F) &:= \{\mathbf{u} \in H(\mathrm{div}, \Omega_F) \,:\, \mathbf{u} \cdot \boldsymbol{\nu} = 0 \text{ on } \Gamma_I\}\,, \\ H_0(\mathrm{div}^0; \Omega_F) &:= H(\mathrm{div}^0; \Omega_F) \cap H_0(\mathrm{div}, \Omega_F)\,. \end{aligned}$$

In what follows, we employ $\mathbf{0}$ to denote a generic null vector and C, with or without subscripts, bars, tildes or hats, to denote a generic positive constant independent of the discretization parameters, which may take different values at different places.

In the case of an incompressible fluid, the classical elastoacoustics approximation for small amplitude motions yields the following eigenvalue problem for the vibration modes of the coupled system and their corresponding frequencies ω (see, for instance, [55]).

Problem 1. Find $\omega \geq 0$, $\mathbf{u} \in H(\mathrm{div};\Omega_F)$, $\mathbf{v} \in H^1(\Omega_S)^3$ and $p \in H^1(\Omega_F)$, $(\mathbf{u}, \mathbf{v}, p) \neq (\mathbf{0}, \mathbf{0}, 0)$, such that

$$\nabla p - \omega^2 \rho_F \mathbf{u} = \mathbf{0} \quad \text{in} \quad \Omega_F, \tag{3.1a}$$

$$\mathrm{div}\ \mathbf{u} = 0 \quad \text{in} \quad \Omega_F, \tag{3.1b}$$

$$\mathrm{div}\ \boldsymbol{\sigma}(\mathbf{v}) + \omega^2 \rho_S \mathbf{v} = \mathbf{0} \quad \text{in} \quad \Omega_S, \tag{3.1c}$$

$$\boldsymbol{\sigma}(\mathbf{v})\boldsymbol{\nu} + p\boldsymbol{\nu} = \mathbf{0} \quad \text{on} \quad \Gamma_I, \tag{3.1d}$$

$$\mathbf{u} \cdot \boldsymbol{\nu} - \mathbf{v} \cdot \boldsymbol{\nu} = 0 \quad \text{on} \quad \Gamma_I, \tag{3.1e}$$

$$\boldsymbol{\sigma}(\mathbf{v})\boldsymbol{n} = \mathbf{0} \quad \text{on} \quad \Gamma_N, \tag{3.1f}$$

$$\mathbf{v} = \mathbf{0} \quad \text{on} \quad \Gamma_D, \tag{3.1g}$$

where $\mathbf{u}$ and $\mathbf{v}$ are the displacements in the fluid and the solid, respectively, and ρ_F and ρ_S are the respective densities. The variable $\boldsymbol{\sigma}$ is the 3×3 stress tensor defined as follows

$$\boldsymbol{\sigma}(\mathbf{v}) := \mathcal{C}\boldsymbol{\varepsilon}(\mathbf{v}),$$

where the elasticity operator $\mathcal{C} : \mathbb{R}^{3\times 3} \longrightarrow \mathbb{R}^{3\times 3}$ is given by Hooke's law,

$$\mathcal{C}\boldsymbol{\tau} := \lambda_S (\mathrm{tr}\,\boldsymbol{\tau})\, I + 2\mu_S \boldsymbol{\tau}$$

with λ_S and μ_S being the Lamé coefficients, and $\boldsymbol{\varepsilon}(\mathbf{v}) := \frac{1}{2}(\nabla \mathbf{v} + (\nabla \mathbf{v})^t)$ is the linearized strain tensor. In spite of the fact that equations (3.1c)-(3.1f) of Problem 1 must be understood in the sense of distributions, since $p \in H^1(\Omega_F)$ and $\mathbf{v} \in [H^1(\Omega_S)]^3$, these interface conditions are valid in the $L^2(\Gamma_I)$ sense. Let us remark that the actual vibration modes of the coupled system are the solutions of Problem 1 with $\omega > 0$. However, $\omega = 0$ is an eigenvalue of Problem 1 with corresponding eigenspace $H_0(\mathrm{div}^0;\Omega_F) \times \{\mathbf{0}\} \times \{0\}$, which, from the physical point of view, is a spurious solution of the model given by equations (3.1).

3.3 Variational formulation and spectral characterization

Let us define some function spaces that we will use to pose a variational formulation of Problem 1. Let $P := L^2(\Gamma_I)$, $\mathbf{H} := [L^2(\Omega_F)]^3 \times [L^2(\Omega_S)]^3$, $\mathbf{X} := H(\mathrm{div};\Omega_F) \times [H^1_{\Gamma_D}(\Omega_S)]^3$ where $H^1_{\Gamma_D}(\Omega_S) := \{v \in H^1(\Omega_S) : v|_{\Gamma_D} = 0\}$ and

$$\mathbf{Y} := \left\{ (\mathbf{u}, \mathbf{v}) \in \mathbf{X} : \quad \mathrm{div}\ \mathbf{u} = 0 \text{ in } \Omega_F \text{ and } \mathbf{u} \cdot \boldsymbol{\nu}\big|_{\Gamma_I} \in L^2(\Gamma_I) \right\}.$$

We denote by $\|\cdot\|_{\mathbf{X}}$ the natural norm on $\mathbf{X}$, by $\|\cdot\|_{\mathbf{H}}$ the L^2 norm on $\mathbf{H}$ and by $\|(\mathbf{u},\mathbf{v})\|^2_{\mathbf{Y}} := \|(\mathbf{u},\mathbf{v})\|^2_{\mathbf{X}} + \|\mathbf{u}\cdot\boldsymbol{\nu}\|^2_{0,\Gamma_I}$ the norm on $\mathbf{Y}$.

Let us now define an additional unknown, $\mu := p|_{\Gamma_I}$. Multiplying by $\boldsymbol{\phi}$ in (3.1a) and $\boldsymbol{\psi}$ in (3.1c) such that $(\boldsymbol{\phi},\boldsymbol{\psi}) \in \mathbf{Y}$ and by $\zeta \in P$ in (3.1e), we obtain the following variational formulation of Problem 1, where $\lambda = \omega^2$:

Problem 2. Find $\lambda \in \mathbb{R}$ and $(\mathbf{u},\mathbf{v},\mu) \in \mathbf{Y} \times P$, $(\mathbf{u},\mathbf{v},\mu) \neq (\mathbf{0},\mathbf{0},0)$, such that

$$\int_{\Omega_S} \boldsymbol{\sigma}(\mathbf{v}) : \boldsymbol{\varepsilon}(\boldsymbol{\psi}) + \int_{\Gamma_I} \mu\,(\boldsymbol{\phi}\cdot\boldsymbol{\nu} - \boldsymbol{\psi}\cdot\boldsymbol{\nu}) = \lambda\left(\int_{\Omega_F} \rho_F \mathbf{u}\cdot\boldsymbol{\phi} + \int_{\Omega_S} \rho_S \mathbf{v}\cdot\boldsymbol{\psi}\right), \tag{3.2a}$$

$$\int_{\Gamma_I} \zeta\,(\mathbf{u}\cdot\boldsymbol{\nu} - \mathbf{v}\cdot\boldsymbol{\nu}) = 0, \tag{3.2b}$$

for all $(\boldsymbol{\phi},\boldsymbol{\psi}) \in \mathbf{Y}$ and $\zeta \in P$, where $\boldsymbol{\sigma}(\mathbf{v}) : \boldsymbol{\varepsilon}(\boldsymbol{\psi}) := \sum_{i,j=1}^{3} \boldsymbol{\sigma}_{ij}(\mathbf{v})\boldsymbol{\varepsilon}_{ij}(\boldsymbol{\psi})$ denotes the usual inner product. In principle, for Problem 1 and 2 to be equivalent, in the latter λ should be sought in $[0,+\infty)$. However, it is easy to check that, for any solution of Problem 2, $\lambda \geq 0$.

Let us now consider the following continuous bilinear forms:

$$\begin{aligned}
a((\mathbf{u},\mathbf{v}),(\boldsymbol{\phi},\boldsymbol{\psi})) &:= \int_{\Omega_S} \boldsymbol{\sigma}(\mathbf{v}) : \boldsymbol{\varepsilon}(\boldsymbol{\psi}), \quad (\mathbf{u},\mathbf{v}),\,(\boldsymbol{\phi},\boldsymbol{\psi}) \in \mathbf{Y},\\
b((\mathbf{u},\mathbf{v}),\zeta) &:= \int_{\Gamma_I} \zeta\,(\mathbf{u}\cdot\boldsymbol{\nu} - \mathbf{v}\cdot\boldsymbol{\nu}), \quad (\mathbf{u},\mathbf{v}) \in \mathbf{Y}, \quad \zeta \in P,\\
d((\mathbf{u},\mathbf{v}),(\boldsymbol{\phi},\boldsymbol{\psi})) &:= \int_{\Omega_F} \rho_F \mathbf{u}\cdot\boldsymbol{\phi} + \int_{\Omega_S} \rho_S \mathbf{v}\cdot\boldsymbol{\psi}, \quad (\mathbf{u},\mathbf{v}),\,(\boldsymbol{\phi},\boldsymbol{\psi}) \in \mathbf{Y}.
\end{aligned}$$

Next step would be to prove Brezzi's conditions for the source problem associated to Problem 2, i.e.,

H1: there exists $\alpha > 0$ such that

$$a((\mathbf{u},\mathbf{v}),(\mathbf{u},\mathbf{v})) \geq \alpha \|(\mathbf{u},\mathbf{v})\|^2_{\mathbf{Y}} \qquad \forall\,(\mathbf{u},\mathbf{v}) \in \mathbf{W},$$

where

$$\mathbf{W} := \{(\mathbf{u},\mathbf{v}) \in \mathbf{Y} \,:\, b((\mathbf{u},\mathbf{v}),\zeta) = 0 \;\; \forall\,\zeta \in P\} = \{(\mathbf{u},\mathbf{v}) \in \mathbf{Y} \,:\, \mathbf{u}\cdot\boldsymbol{\nu} = \mathbf{v}\cdot\boldsymbol{\nu} \text{ on } \Gamma_I\}.$$

H2: b satisfies the inf-sup condition

$$\inf_{\zeta\in P}\left[\sup_{\substack{(\mathbf{u},\mathbf{v})\in\mathbf{Y}\\(\mathbf{u},\mathbf{v})\neq(\mathbf{0},\mathbf{0})}} \frac{b((\mathbf{u},\mathbf{v}),\zeta)}{\|(\mathbf{u},\mathbf{v})\|_{\mathbf{Y}}\|\zeta\|_{0,\Gamma_I}}\right] \geq \beta.$$

For the proof of **H2**, we refer to [17, Lemma 8.1] where the condition is proved in 2D; its extension to 3D is straightforward. In particular, as in that reference, the proof relies on the fact that for each $\zeta \in P$, there exists $(\mathbf{u}, \mathbf{v}) \in \mathbf{Y}$, satisfying

$$\mathbf{u}\cdot\boldsymbol{\nu} - \mathbf{v}\cdot\boldsymbol{\nu} = \zeta \quad \text{on} \quad \Gamma_I, \qquad \mathbf{v} = \mathbf{0} \quad \text{on} \quad \Gamma_D \cup \Gamma_N \qquad \text{and} \qquad \|(\mathbf{u}, \mathbf{v})\|_{\mathbf{Y}} \leq C\|\zeta\|_{0,\Gamma_I}. \tag{3.3}$$

Concerning **H1**, it is clear that the form a is not coercive on $\mathbf{W}$, since for all $\mathbf{u} \in H_0(\mathrm{div}^0; \Omega_F)$, $(\mathbf{u}, \mathbf{0}) \in \mathbf{W}$ and $a((\mathbf{u}, \mathbf{0}), (\mathbf{u}, \mathbf{0})) = 0$. However, following the ideas from [17] and considering $a^* := a + d$ instead of a, we obtain a coercive bilinear form on $\mathbf{W}$:

Lemma 3.1. *There exists $\alpha > 0$ such that*

$$a^*((\mathbf{u}, \mathbf{v}), (\mathbf{u}, \mathbf{v})) \geq \alpha\|(\mathbf{u}, \mathbf{v})\|_{\mathbf{Y}} \qquad \forall\, (\mathbf{u}, \mathbf{v}) \in \mathbf{W}.$$

Proof. Notice that for all $(\mathbf{u}, \mathbf{v}) \in \mathbf{X}$ such that $\mathrm{div}\ \mathbf{u} = 0$,

$$a^*((\mathbf{u}, \mathbf{v}), (\mathbf{u}, \mathbf{v})) = \int_{\Omega_S} \boldsymbol{\sigma}(\mathbf{v}) : \boldsymbol{\varepsilon}(\mathbf{v}) + \int_{\Omega_F} \rho_F|\mathbf{u}|^2 + \int_{\Omega_S} \rho_S|\mathbf{v}|^2 \geq \alpha\|(\mathbf{u}, \mathbf{v})\|^2_{\mathbf{X}},$$

with $\alpha = \min\{\rho_F, \kappa\}$ where κ is the constant in Korn's inequality (see, for instance, [37]). Hence, from the fact that for all $(\mathbf{u}, \mathbf{v}) \in \mathbf{W}$, $\|\mathbf{u}\cdot\boldsymbol{\nu}\|_{0,\Gamma_I} = \|\mathbf{v}\cdot\boldsymbol{\nu}\|_{0,\Gamma_I} \leq C\|\mathbf{v}\|_{1,\Omega_S} \leq \widetilde{C}\|(\mathbf{u}, \mathbf{v})\|_{\mathbf{X}}$ we conclude the claimed result. □

Thus, we consider this modified eigenvalue problem:

Problem 3. Find $\widehat{\lambda} \in \mathbb{R}$ and $(\mathbf{u}, \mathbf{v}, \mu) \in \mathbf{Y} \times P$, $(\mathbf{u}, \mathbf{v}, \mu) \neq (\mathbf{0}, \mathbf{0}, 0)$, such that

$$a^*((\mathbf{u}, \mathbf{v}), (\boldsymbol{\phi}, \boldsymbol{\psi})) + b((\boldsymbol{\phi}, \boldsymbol{\psi}), \mu) = \widehat{\lambda}\, d((\mathbf{u}, \mathbf{v}), (\boldsymbol{\phi}, \boldsymbol{\psi})), \tag{3.4a}$$

$$b((\mathbf{u}, \mathbf{v}), \zeta) = 0, \tag{3.4b}$$

for all $(\boldsymbol{\phi}, \boldsymbol{\psi}) \in \mathbf{Y}$ and $\zeta \in P$. Notice that λ is an eigenvalue of Problem 2 if and only if $\widehat{\lambda} = 1 + \lambda$ is an eigenvalue of Problem 3 and the eigenfunctions for both problems coincide.

Theorem 3.2. *Problems 1 and 3 are equivalents. In particular, $\mu = p|_{\Gamma_I}$.*

Proof. We have just shown that if $(\lambda, \mathbf{u}, \mathbf{v}, p)$ is a solution of Problem 1, then $(\widehat{\lambda} = \lambda + 1, \mathbf{u}, \mathbf{v}, p|_{\Gamma_I})$ is a solution of Problem 3. Now, let $(\widehat{\lambda}, \mathbf{u}, \mathbf{v}, \mu)$ be an eigenpair of Problem 3. First, it is immediate to check that $\widehat{\lambda} \geq 1$, so that $\lambda \geq 0$. Since $(\mathbf{u}, \mathbf{v}) \in \mathbf{Y}$ and satisfies (3.4b), then (3.1b), (3.1g) and (3.1e) are automatically satisfied. Moreover, taking $(\mathbf{0}, \boldsymbol{\psi})$,

with $\boldsymbol{\psi} \in [\mathcal{D}(\Omega_S)]^3$ in (3.4a), we obtain (3.1c), while considering $\boldsymbol{\psi} \in [H^1_{\Gamma_D}(\Omega_S)]^3$ together with (3.1c) it follows that

$$\boldsymbol{\sigma}(\mathbf{v})\boldsymbol{\nu} + \mu\boldsymbol{\nu} = \mathbf{0} \quad \text{on} \quad \Gamma_I \tag{3.5}$$

and (3.1f).

On the other hand, let $p \in H^1(\Omega_F)$ be the solution of the following compatible Neumann problem:

$$\Delta p = 0 \quad \text{in} \quad \Omega_F, \qquad \nabla p \cdot \boldsymbol{\nu} = \lambda \rho_F \mathbf{u} \cdot \boldsymbol{\nu} \quad \text{on} \quad \Gamma_I, \qquad \int_{\Gamma_I} p = \int_{\Gamma_I} \mu. \tag{3.6}$$

Hence, from (3.1b), we have that $(\nabla p - \lambda \rho_F \mathbf{u}) \in H_0(\mathrm{div}^0; \Omega_F)$. Now, taking as test function $(\boldsymbol{\phi}, \mathbf{0})$ with $\boldsymbol{\phi} = \nabla p - \lambda \rho_F \mathbf{u}$ in (3.4a), it follows that $\lambda \displaystyle\int_{\Omega_F} \rho_F \mathbf{u} \cdot (\nabla p - \lambda \rho_F \mathbf{u}) = 0$. Subtracting this equation to $\displaystyle\int_{\Omega_F} \nabla p \cdot (\nabla p - \lambda \rho_F \mathbf{u}) = 0$, we conclude (3.1a).

Now, let $s \in L^2_0(\Gamma_I) := \{r \in L^2(\Gamma_I) \ : \ \int_{\Gamma_I} r = 0\}$. Let $r \in H^1(\Omega)/\mathbb{R}$ be the solution of the compatible Neumann problem

$$\Delta r = 0 \quad \text{in} \quad \Omega_F, \qquad \nabla r \cdot \boldsymbol{\nu} = s \quad \text{on} \quad \Gamma_I. \tag{3.7}$$

Then, testing (3.4a) with $(\boldsymbol{\phi}, \boldsymbol{\psi}) = (\nabla r, \mathbf{0})$ we obtain

$$\int_{\Gamma_I} \mu s = \lambda \int_{\Omega_F} \rho_F \mathbf{u} \cdot \nabla r.$$

On the other hand, using again that $(\nabla p - \lambda \rho_F \mathbf{u}) \in H_0(\mathrm{div}^0; \Omega_F)$, we have that

$$0 = \int_{\Omega_F} (\nabla p - \lambda \rho_F \mathbf{u}) \cdot \nabla r = \int_{\Gamma_I} p \nabla r \cdot \boldsymbol{\nu} - \lambda \int_{\Omega_F} \rho_F \mathbf{u} \cdot \nabla r.$$

Therefore,

$$\int_{\Gamma_I} \mu\, s = \int_{\Gamma_I} p \nabla r \cdot \boldsymbol{\nu} = \int_{\Gamma_I} p\, s$$

for all $s \in L^2_0(\Gamma_I)$. Hence, $p = \mu + C$, with C a constant. However, thanks to the third equation of problem (3.6), we conclude that $p = \mu$ on Γ_I, which together with (3.5) yields (3.1d). This fact completes the proof. □

The following theorem gives a characterization of the eigenspace associated to the eigenvalue $\widehat{\lambda} = 1$ in Problem 3.

Theorem 3.3. *The eigenspace corresponding to* $\widehat{\lambda} = 1$ *in Problem 3 is* $\mathbf{K} \times \{0\}$ *with* $\mathbf{K} := H_0(\mathrm{div}^0; \Omega_F) \times \{\mathbf{0}\}$.

Proof. Let $(\mathbf{u}, \mathbf{0}) \in \mathbf{K}$. Clearly, $(\mathbf{u}, \mathbf{0}) \in \mathbf{W}$ and $(\mathbf{u}, \mathbf{0}, 0)$ satisfies Problem 3 with $\widehat{\lambda} = 1$. Therefore, $(\mathbf{u}, \mathbf{0}, 0)$ is an eigenfunction of Problem 3 with associated eigenvalue $\widehat{\lambda} = 1$. Conversely, let $(\mathbf{u}, \mathbf{v}, \mu) \in \mathbf{Y} \times P$, $(\mathbf{u}, \mathbf{v}, \mu) \neq (\mathbf{0}, \mathbf{0}, 0)$, such that

$$\begin{aligned} a((\mathbf{u}, \mathbf{v}), (\boldsymbol{\phi}, \boldsymbol{\psi})) + b((\boldsymbol{\phi}, \boldsymbol{\psi}), \mu) &= 0, \\ b((\mathbf{u}, \mathbf{v}), \zeta) &= 0, \end{aligned}$$

for all $(\boldsymbol{\phi}, \boldsymbol{\psi}) \in \mathbf{Y}$ and $\zeta \in P$. From the second equation we obtain $\mathbf{u} \cdot \boldsymbol{\nu} = \mathbf{v} \cdot \boldsymbol{\nu}$ on Γ_I. By using $(\boldsymbol{\phi}, \boldsymbol{\psi}) = (\mathbf{u}, \mathbf{v})$ in the first equation and Korn's inequality, we obtain that $\mathbf{v} = \mathbf{0}$ in Ω_S. Since $\mathrm{div}\, \mathbf{u} = 0$ in Ω_F and $\mathbf{u} \cdot \boldsymbol{\nu} = \mathbf{v} \cdot \boldsymbol{\nu} = 0$ on Γ_I, then $\mathbf{u} \in H_0(\mathrm{div}^0; \Omega_F)$. Finally, the inf-sup condition **H2** allow us to conclude that $\mu = 0$ on Γ_I. □

In order to obtain a spectral characterization of Problem 3, we introduce the solution operator:

$$\begin{aligned} \mathbf{T} : \mathbf{H} &\longrightarrow \mathbf{Y} \subseteq \mathbf{H}, \\ (\mathbf{f}, \mathbf{g}) &\longmapsto \mathbf{T}(\mathbf{f}, \mathbf{g}) := (\mathbf{u}, \mathbf{v}) \end{aligned}$$

with $(\mathbf{u}, \mathbf{v}, \mu) \in \mathbf{Y} \times P$ being the solution of the following source problem: Find $(\mathbf{u}, \mathbf{v}, \mu) \in \mathbf{Y} \times P$ such that

$$a^*((\mathbf{u}, \mathbf{v}), (\boldsymbol{\phi}, \boldsymbol{\psi})) + b((\boldsymbol{\phi}, \boldsymbol{\psi}), \mu) = d((\mathbf{f}, \mathbf{g}), (\boldsymbol{\phi}, \boldsymbol{\psi})), \tag{3.8a}$$

$$b((\mathbf{u}, \mathbf{v}), \zeta) = 0, \tag{3.8b}$$

for all $(\boldsymbol{\phi}, \boldsymbol{\psi}) \in \mathbf{Y}$ and $\zeta \in P$. By virtue of the following theorem, $\mathbf{T}$ is well-defined and bounded. In addition, $(\gamma, (\mathbf{u}, \mathbf{v}))$ with $\gamma \neq 0$ is an eigenpair of $\mathbf{T}$ if and only if there exists $\mu \in P$ such that $(1/\gamma, (\mathbf{u}, \mathbf{v}, \mu))$ is a solution of Problem 3.

Theorem 3.4. *Given* $(\mathbf{f}, \mathbf{g}) \in \mathbf{H}$*, there exists a unique solution* $(\mathbf{u}, \mathbf{v}, \mu) \in \mathbf{Y} \times P$ *of the source problem*

$$a^*((\mathbf{u}, \mathbf{v}), (\boldsymbol{\phi}, \boldsymbol{\psi})) + b((\boldsymbol{\phi}, \boldsymbol{\psi}), \mu) = d((\mathbf{f}, \mathbf{g}), (\boldsymbol{\phi}, \boldsymbol{\psi})),$$

$$b((\mathbf{u}, \mathbf{v}), \zeta) = 0,$$

for all $(\boldsymbol{\phi}, \boldsymbol{\psi}) \in \mathbf{Y}$ *and* $\zeta \in P$*. Moreover, there exists* $C > 0$ *such that*

$$\|(\mathbf{u}, \mathbf{v})\|_{\mathbf{Y}} + \|\mu\|_{0,\Gamma_I} \leq C \|(\mathbf{f}, \mathbf{g})\|_{\mathbf{H}}. \tag{3.10}$$

Proof. Since the bilinear forms a^* and b satisfy the Brezzi's conditions, the mixed source problem above is well-posed. See, for instance, [28]. □

Notice that it is easy to prove that Problem 3 is equivalent to the following:

Problem 3*. Find $\widehat{\lambda} \in \mathbb{R}$ and $(\mathbf{u}, \mathbf{v}) \in \mathbf{W}$, $(\mathbf{u}, \mathbf{v}) \neq (\mathbf{0}, \mathbf{0})$, such that

$$a^*((\mathbf{u}, \mathbf{v}), (\boldsymbol{\phi}, \boldsymbol{\psi})) = \widehat{\lambda}\, d((\mathbf{u}, \mathbf{v}), (\boldsymbol{\phi}, \boldsymbol{\psi})), \quad \forall (\boldsymbol{\phi}, \boldsymbol{\psi}) \in \mathbf{W}. \tag{3.11}$$

In fact, any solution of Problem 3 gives a solution of Problem 3*. Conversely, let $(\widehat{\lambda}, (\mathbf{u}, \mathbf{v}))$ be an eigenpair of Problem 3*. Thanks to Theorem 3.4, we know that there exists a unique solution $(\widetilde{\mathbf{u}}, \widetilde{\mathbf{v}}, \widetilde{\mu}) \in \mathbf{Y} \times P$ of the following source problem:

$$a^*((\widetilde{\mathbf{u}}, \widetilde{\mathbf{v}}), (\boldsymbol{\phi}, \boldsymbol{\psi})) + b((\boldsymbol{\phi}, \boldsymbol{\psi}), \widetilde{\mu}) = d(\widehat{\lambda}(\mathbf{u}, \mathbf{v}), (\boldsymbol{\phi}, \boldsymbol{\psi})),$$

$$b((\widetilde{\mathbf{u}}, \widetilde{\mathbf{v}}), \zeta) = 0,$$

for all $(\boldsymbol{\phi}, \boldsymbol{\psi}) \in \mathbf{Y}$ and $\zeta \in P$. Hence, $(\widetilde{\mathbf{u}}, \widetilde{\mathbf{v}}) \in \mathbf{W}$ and it satisfies $a^*((\widetilde{\mathbf{u}}, \widetilde{\mathbf{v}}), (\boldsymbol{\phi}, \boldsymbol{\psi})) = d(\widehat{\lambda}(\mathbf{u}, \mathbf{v}), (\boldsymbol{\phi}, \boldsymbol{\psi}))$ for all $(\boldsymbol{\phi}, \boldsymbol{\psi}) \in \mathbf{W}$. Since a^* is elliptic in $\mathbf{W}$, because of (3.11) $(\mathbf{u}, \mathbf{v})$ is the unique solution of this equation. Then, $(\widehat{\lambda}, (\mathbf{u}, \mathbf{v}, \mu))$ is an eigenpair of Problem 3.

Because of (3.8b), notice that $\mathbf{T}(\mathbf{H})$ is actually included into $\mathbf{W} \subseteq \mathbf{Y}$. We will focus on studying $\mathbf{T}|_{\mathbf{W}}$. Since the bilinear forms a^* and d are symmetric, $\mathbf{T}$ is self-adjoint with respect to both. Hence all of its eigenvalues are real and by virtue of (3.11) non negative. In addition, because of Theorem 3.3, $\mathbf{T}|_{\mathbf{K}}$ is the identity on the infinite dimensional subspace $\mathbf{K} \subseteq \mathbf{W}$. Therefore, $\mathbf{T}|_{\mathbf{W}}$ is not compact. However, the restriction of $\mathbf{T}$ to the orthogonal complement of $\mathbf{K}$ is compact. We will use this to characterize the spectrum of $\mathbf{T}$. To this end, we start recalling the classical Helmholtz decomposition (cf. [37, Theorem I.2.7]):

$$[L^2(\Omega_F)]^3 = H_0(\overset{0}{\text{div}}; \Omega_F) \overset{\perp}{\oplus} \nabla H^1(\Omega_F).$$

As a consequence of this result and Theorem 3.3, we obtain that

$$\mathbf{K}^{\perp_{\mathbf{H}}} := \left\{ (\nabla q, \mathbf{v}) \,:\, q \in H^1(\Omega_F),\, \mathbf{v} \in [L^2(\Omega_S)]^3 \right\}.$$

In addition, it can be easily proved that $\mathbf{K}^{\perp_{\mathbf{W}}} = \mathbf{K}^{\perp_{\mathbf{H}}} \cap \mathbf{W}$ and that $\mathbf{K}$ and $\mathbf{K}^{\perp_{\mathbf{W}}}$ are also orthogonal with respect to a^*. Moreover, we have the following result.

Lemma 3.5. *The operator* $\mathbf{T}$ *satisfies* $\mathbf{T}(\mathbf{K}^{\perp_{\mathbf{H}}}) \subseteq \mathbf{K}^{\perp_{\mathbf{W}}}$. *Moreover, there exist* $s > 1/2$, $t > 0$ *and* $C > 0$ *such that if* $(\mathbf{u}, \mathbf{v}, \mu) \in \mathbf{Y} \times P$ *is the solution of problem* (3.8) *with* $(\mathbf{f}, \mathbf{g}) \in \mathbf{K}^{\perp_{\mathbf{W}}}$, *then* $\mathbf{u} \in [H^s(\Omega_F)]^3$, $\mathbf{v} \in [H^{1+t}(\Omega_S)]^3$, $\mu \in H^{1/2+s}(\Gamma_I)$ *and*

$$\|\mathbf{u}\|_{s,\Omega_F} + \|\mathbf{v}\|_{1+t,\Omega_S} + \|\mu\|_{1/2+s,\Gamma_I} \leq C \|(\mathbf{f}, \mathbf{g})\|_{\mathbf{X}}. \tag{3.12}$$

Proof. The proof of $\mathbf{T}(\mathbf{K}^{\perp_{\mathbf{H}}}) \subseteq \mathbf{K}^{\perp_{\mathbf{W}}}$ is similar to that of [17, Lemma 4.1]. We omit further details. Let $(\mathbf{f},\mathbf{g}) \in \mathbf{K}^{\perp_{\mathbf{W}}}$ and let $(\mathbf{u},\mathbf{v},\mu) \in \mathbf{Y} \times P$ be the solution of problem (3.8). Since $(\mathbf{u},\mathbf{v}) \in \mathbf{K}^{\perp_{\mathbf{W}}}$, there exists $\varphi \in H^1(\Omega_F)$ such that $\mathbf{u} = \nabla\varphi$ and, in addition, div $\mathbf{u} = 0$ in Ω_F and $\mathbf{u}\cdot\boldsymbol{\nu} = \mathbf{v}\cdot\boldsymbol{\nu}$ on Γ_I. Thus, φ is a solution of the compatible Neumann problem

$$\Delta\varphi = 0 \quad \text{in} \quad \Omega_F, \qquad \nabla\varphi\cdot\boldsymbol{\nu} = \mathbf{v}\cdot\boldsymbol{\nu} \quad \text{on} \quad \Gamma_I.$$

As it is well-known (see [32, Corollary 23.5]), $\varphi \in H^{1+s}(\Omega_F)$ with $s > 1/2$. In addition,

$$\|\mathbf{u}\|_{s,\Omega_F} = \|\nabla\varphi\|_{s,\Omega_F} \leq C\sum_{j=1}^{J}\|\mathbf{v}\cdot\boldsymbol{\nu}\|_{1/2,\Gamma_j} \leq C\|(\mathbf{f},\mathbf{g})\|_{\mathbf{X}},$$

where the last inequality follows from (3.10).

Now, since $(\mathbf{f},\mathbf{g}) \in \mathbf{K}^{\perp_{\mathbf{W}}}$, there exists $z \in H^1(\Omega_F)$ such that $\mathbf{f} = \nabla z$ and, in particular, z satisfies $\Delta z =$ div $\mathbf{f} = 0$ in Ω_F and $\nabla z\cdot\boldsymbol{\nu} = \mathbf{g}\cdot\boldsymbol{\nu}$ on Γ_I. Since $\mathbf{g} \in [H^1(\Omega_S)]^3$, z also belongs to $H^{1+s}(\Omega_F)$. Replacing $\mathbf{f}$ and $\mathbf{u}$ by ∇z and $\nabla\varphi$, respectively, in (3.8a) and considering as test function $(\boldsymbol{\phi},\boldsymbol{\psi}) = (\nabla r, \mathbf{0})$ with $r \in H^1(\Omega_F)$ being the solution of $\Delta r = 0$ in Ω_F and $\nabla r\cdot\boldsymbol{\nu} = s$ on Γ_I with $s \in L^2_0(\Gamma_I)$, we obtain

$$\int_{\Omega_F}\rho_F\nabla\varphi\cdot\nabla r + \int_{\Gamma_I}\mu\, s = \int_{\Omega_F}\rho_F\nabla z\cdot\nabla r.$$

Integrating by parts we get $\mu = \rho_F z - \rho_F\varphi \in H^{1/2+s}(\Gamma_I)/\mathbb{R}$ and, in addition,

$$\|\mu\|_{H^{1/2+s}(\Gamma_I)/\mathbb{R}} \leq C\|(\mathbf{f},\mathbf{g})\|_{\mathbf{X}}.$$

On the other hand, its is well known that there exists $C > 0$ such that

$$\|\mu\|_{1/2+s,\Gamma_I} \leq C\left(\|\mu\|_{H^{1/2+s}(\Gamma_I)/\mathbb{R}} + \|\mu\|_{0,\Gamma_I}\right).$$

From the above inequality and (3.10), we obtain that $\mu \in H^{1/2+s}(\Gamma_I)$ and

$$\|\mu\|_{1/2+s,\Gamma_I} \leq C\|(\mathbf{f},\mathbf{g})\|_{\mathbf{X}}.$$

Now, proceeding as in the proof of Theorem 3.2, we obtain that $\mathbf{v}$ is the solution, in the sense of distributions, of the following problem:

$$\begin{aligned} -\,\text{div}\,\boldsymbol{\sigma}(\mathbf{v}) + \rho_S\mathbf{v} &= \rho_S\mathbf{g} \quad \text{in} \quad \Omega_S,\\ \boldsymbol{\sigma}(\mathbf{v})\boldsymbol{\nu} &= -\mu\boldsymbol{\nu} \quad \text{on} \quad \Gamma_I,\\ \boldsymbol{\sigma}(\mathbf{v})\boldsymbol{n} &= \mathbf{0} \quad \text{on} \quad \Gamma_N,\\ \mathbf{v} &= \mathbf{0} \quad \text{on} \quad \Gamma_D. \end{aligned}$$

Then, there exists $t > 0$ such that $\mathbf{v} \in [H^{1+t}(\Omega_S)]^3$ and satisfies

$$\|\mathbf{v}\|_{1+t,\Omega_S} \leq C \left(\|\mathbf{g}\|_{0,\Omega_S} + \|\mu\|_{1/2+s,\Gamma_I} \right) \leq C \|(\mathbf{f},\mathbf{g})\|_{\mathbf{X}},$$

which completes the proof.

□

Theorem 3.6. $\mathbf{T}(\mathbf{K}^{\perp \mathbf{W}}) \subseteq \mathbf{K}^{\perp \mathbf{W}}$ *and the operator* $\mathbf{T}\big|_{\mathbf{K}^{\perp \mathbf{W}}} : \mathbf{K}^{\perp \mathbf{W}} \longrightarrow \mathbf{K}^{\perp \mathbf{W}}$ *is compact.*

Proof. Because of Lemma 3.5, $\mathbf{T}(\mathbf{K}^{\perp \mathbf{W}}) \subseteq \left\{ [H^s(\Omega_F)]^3 \times [H^{1+t}(\Omega_S)]^3 \right\} \cap \mathbf{K}^{\perp \mathbf{W}}$, with s and t positive. On the other hand, $\left\{ [H^s(\Omega_F)]^3 \times [H^{1+t}(\Omega_S)]^3 \right\} \cap \mathbf{W}$ is compactly imbedded in $\mathbf{W}$. Hence, $\mathbf{T}\big|_{\mathbf{K}^{\perp \mathbf{W}}}$ is compact. □

Since the eigenvalues of Problem 3 are the reciprocal of the nonvanishing eigenvalues of $\mathbf{T}|_{\mathbf{W}}$ and the associated eigenfunctions coincide, the above Theorem yields a spectral characterization of Problem 3.

Theorem 3.7. *The spectrum of* $\mathbf{T}|_{\mathbf{W}} : \mathbf{W} \longrightarrow \mathbf{W}$ *consists of the eigenvalue* $\gamma = 1$ *and a sequence of finite multiplicity eigenvalues* $\{\gamma_n\}_{n \in \mathbb{N}} \subseteq (0,1)$ *converging to 0.* $\mathbf{K}$ *is the eigenspace associated to* $\gamma = 1$.

Proof. The spectral characterization is a direct consequence of the fact that $\mathbf{T}|_{\mathbf{K}}$ is the identity and Theorem 3.6. Moreover, it is easy to check that $\gamma_n \in (0, 1)$. □

3.4 Finite element discretization

As it was proved in the previous section, $\mathbf{T}|_{\mathbf{K}}^{\perp \mathbf{W}}$ is compact. However, it is not clear at all how this space could be discretized, since the fluid displacement ought to be gradients with divergence in $L^2(\Omega)$. Because of this, we will deal with the full non-compact operator $\mathbf{T}$ instead.

Let $\{\mathcal{T}_h\}$ be a family of regular triangulation of $\Omega_F \cup \Omega_S$ such that each tetrahedron is completely contained either in Ω_F or in Ω_S compatible with the partition $\Gamma_D \cup \Gamma_N$ of the exterior boundary.

For each component of the displacements in the solid we use the standard piecewise linear finite element space

$$L_h(\Omega_S) := \left\{ v \in H^1(\Omega_S) \,:\, v|_T \in \mathbb{P}_1(T) \quad \forall T \in \mathcal{T}_h, \quad T \subseteq \overline{\Omega}_S \right\},$$

where $\mathbb{P}_1$ is the set of polynomials of degree not greater than 1.

For any $T \in \mathcal{T}_h$ lying in Ω_F, let

$$\mathcal{R}_0(T) := \left\{ \mathbf{u} \in [\mathbb{P}_1(T)]^3 \ : \ \mathbf{u}(x,y,z) = (a+dx, b+dy, c+dz), \ \ a,\, b,\, c,\, d \in \mathbb{R} \right\}.$$

The corresponding global space to approximate the fluid is the well-known Raviart–Thomas space defined as follows:

$$\mathbf{R}_h(\Omega_F) := \left\{ \mathbf{u} \in H(\mathrm{div}; \Omega_F) \ : \ \mathbf{u}|_T \in \mathcal{R}_0(T) \quad \forall\, T \in \mathcal{T}_h, \quad T \subseteq \overline{\Omega}_F \right\}.$$

Given $\delta \in (0,1]$, let $\mathbf{I}_h^{\mathcal{R}} : [H^\delta(\Omega_F)]^3 \cap H(\mathrm{div}; \Omega_F) \longrightarrow \mathbf{R}_h(\Omega_F)$ be the standard Raviart–Thomas interpolant, which for a sufficiently smooth function $\mathbf{u}$ is characterized by the identity:

$$\int_F \mathbf{I}_h^{\mathcal{R}}(\mathbf{u}) \cdot \boldsymbol{\nu}_F = \int_F \mathbf{u} \cdot \boldsymbol{\nu}_F, \tag{3.13}$$

for all faces F of elements $T \in \mathcal{T}_h$, $T \subseteq \overline{\Omega}_F$, with $\boldsymbol{\nu}_F$ being a unit vector normal to the face F.

It is well-known that $\mathbf{I}_h^{\mathcal{R}}$ is a bounded linear operator satisfying the following commuting diagram property (cf. [28]):

$$\mathrm{div}\left(\mathbf{I}_h^{\mathcal{R}}\mathbf{u}\right) = \mathcal{P}_h\left(\mathrm{div}\,\mathbf{u}\right) \qquad \forall\, \mathbf{u} \in [H^\delta(\Omega_F)]^3 \cap H(\mathrm{div}; \Omega_F), \tag{3.14}$$

where $\mathcal{P}_h : L^2(\Omega_F) \longrightarrow \mathcal{Z}_h$ is the $L^2(\Omega_F)$-orthogonal projector onto $\mathcal{Z}_h := \{v \in L^2(\Omega_F) : v|_T \in \mathbb{P}_0(T) \quad \forall\, T \in \mathcal{T}_h\}$. In addition, following the arguments from [47, Theorem 3.16], it can be proved that there exists $C > 0$, independent of h, such that

$$\|\mathbf{u} - \mathbf{I}_h^{\mathcal{R}}\mathbf{u}\|_{0,\Omega_F} \leq C h^\delta \left\{ \|\mathbf{u}\|_{\delta,\Omega_F} + \|\,\mathrm{div}\,\mathbf{u}\|_{0,\Omega_F} \right\} \qquad \forall \mathbf{u} \in [H^\delta(\Omega_F)]^3 \cap H(\mathrm{div}; \Omega_F). \tag{3.15}$$

On the other hand, let

$$\mathbf{X}_h := \left\{ (\mathbf{u}_h, \mathbf{v}_h) \in \mathbf{R}_h(\Omega_F) \times [L_h(\Omega_S)]^3 \ : \ \mathbf{v}_h|_{\Gamma_D} = \mathbf{0} \right\}$$

be the finite element discretization of $\mathbf{X}$.

Finally, the discrete analogue of $\mathbf{Y}$ and P are

$$\begin{aligned} \mathbf{Y}_h &:= \{(\mathbf{u}_h, \mathbf{v}_h) \in \mathbf{X}_h \ : \ \mathrm{div}\ \mathbf{u}_h = 0 \text{ in } \Omega_F\} \quad \text{and} \\ P_h &:= \left\{ \mu_h \in L^2(\Gamma_I) \ : \ \mu_h|_F \in \mathbb{P}_0(F)\ \forall\, F \subseteq \Gamma_I, \ F \text{ face of } T,\, T \in \mathcal{T}_h \right\}, \end{aligned}$$

respectively. Let us remark that the divergence-free constraint in the definition of $\mathbf{Y}_h$ will be imposed below by choosing appropiate basis functions of this space.

Notice that, according to (3.13), for all faces $F \subseteq \Gamma_I$,

$$\mathbf{I}_h^{\mathcal{R}}(\mathbf{u}) \cdot \boldsymbol{\nu}_F = \mathcal{P}_{h,\Gamma_I}(\mathbf{u} \cdot \boldsymbol{\nu}_F), \tag{3.16}$$

where $\mathcal{P}_{h,\Gamma_I} : L^2(\Gamma_I) \to P_h$ is the orthogonal projector, which satisfies (see, for instance, [36])

$$\|v - \mathcal{P}_{h,\Gamma_I} v\|_{0,F} \leq C h_F^{\min\{1/2+\delta,1\}} \|v\|_{1/2+\delta,F}, \qquad \forall\, v \in H^{1/2+\delta}(F). \tag{3.17}$$

Now, we are in position to introduce the following finite element discretization of Problem 3.

Problem 4. Find $\lambda_h \in \mathbb{R}$ and $(\mathbf{u}_h, \mathbf{v}_h, \mu_h) \in \mathbf{Y}_h \times P_h$, $(\mathbf{u}_h, \mathbf{v}_h, \mu_h) \neq (\mathbf{0}, \mathbf{0}, 0)$, such that

$$a^*((\mathbf{u}_h, \mathbf{v}_h), (\boldsymbol{\phi}_h, \boldsymbol{\psi}_h)) + b((\boldsymbol{\phi}_h, \boldsymbol{\psi}_h), \mu_h) = \widehat{\lambda}_h\, d((\mathbf{u}_h, \mathbf{v}_h), (\boldsymbol{\phi}_h, \boldsymbol{\psi}_h)), \tag{3.18a}$$

$$b((\mathbf{u}_h, \mathbf{v}_h), \zeta_h) = 0, \tag{3.18b}$$

for all $(\boldsymbol{\phi}_h, \boldsymbol{\psi}_h) \in \mathbf{Y}_h$ and $\zeta_h \in P_h$.

In what follows we will show that the bilinear forms a^* and b satisfy both of Brezzi's conditions on the finite element spaces $\mathbf{Y}_h$ and P_h. We include its proof since, in this case, we cannot proceed as in that of [17, Lemma 8.2], because some of its arguments hold only in 2D.

Lemma 3.8. *The bilinear forms a^* and b satisfy:*

H1$_h$*: There exists $\widehat{\alpha} > 0$, independent of h, such that*

$$a^*((\mathbf{u}_h, \mathbf{v}_h), (\mathbf{u}_h, \mathbf{v}_h)) \geq \widehat{\alpha} \|(\mathbf{u}_h, \mathbf{v}_h)\|_{\mathbf{Y}}^2 \qquad \forall\, (\mathbf{u}_h, \mathbf{v}_h) \in \mathbf{W}_h,$$

where $\mathbf{W}_h := \{(\mathbf{u}_h, \mathbf{v}_h) \in \mathbf{Y}_h \,:\, b((\mathbf{u}_h, \mathbf{v}_h), \zeta_h) = 0 \quad \forall\, \zeta_h \in P_h\}$.

H2$_h$*: There exists $\widehat{\beta} > 0$, independent of h, such that*

$$\inf_{\zeta_h \in P_h} \left[\sup_{\substack{(\mathbf{u}_h, \mathbf{v}_h) \in \mathbf{Y}_h \\ (\mathbf{u}_h, \mathbf{v}_h) \neq (\mathbf{0}, \mathbf{0})}} \frac{b((\mathbf{u}_h, \mathbf{v}_h), \zeta_h)}{\|(\mathbf{u}_h, \mathbf{v}_h)\|_{\mathbf{Y}} \|\zeta_h\|_{0,\Gamma_I}} \right] \geq \widehat{\beta}.$$

Proof. Since

$$\mathbf{W}_h = \left\{ (\mathbf{u}_h, \mathbf{v}_h) \in \mathbf{Y}_h \;:\; \int_F (\mathbf{u}_h \cdot \boldsymbol{\nu} - \mathbf{v}_h \cdot \boldsymbol{\nu}) = 0 \;\; \forall\, F \subseteq \Gamma_I,\; F \text{ face of } T,\; T \in \mathcal{T}_h \right\},$$

the first argument from the proof of Lemma 3.1 holds true for $(\mathbf{u}_h, \mathbf{v}_h) \in \mathbf{W}_h$, so that

$$a^*((\mathbf{u}_h, \mathbf{v}_h), (\mathbf{u}_h, \mathbf{v}_h)) \geq \widehat{\alpha} \|(\mathbf{u}_h, \mathbf{v}_h)\|^2_{\mathbf{X}}.$$

Hence, $\mathbf{H1}_h$ is a consequence of the above inequality and the fact that $\mathbf{u}_h \cdot \boldsymbol{\nu}|_{\Gamma_I}$ is the $L^2(\Gamma_I)$ projection of $\mathbf{v}_h \cdot \boldsymbol{\nu}|_{\Gamma_I}$ onto P_h and, therefore, $\|\mathbf{u}_h \cdot \boldsymbol{\nu}\|_{0,\Gamma_I} \leq \|\mathbf{v}_h \cdot \boldsymbol{\nu}\|_{0,\Gamma_I} \leq C\|\mathbf{v}_h\|_{1,\Omega_S} \leq C\|(\mathbf{u}_h, \mathbf{v}_h)\|_{\mathbf{X}}$.

The proof of $\mathbf{H2}_h$ follows from an adaptation of that of [17, Lemma 8.2] to 3D. In fact, let $\zeta_h \in P_h \subseteq L^2(\Gamma_I)$. Thanks to (3.3) we know that there exists $(\mathbf{u}, \mathbf{v}) \in \mathbf{Y}$ such that

$$(\mathbf{u} \cdot \boldsymbol{\nu} - \mathbf{v} \cdot \boldsymbol{\nu}) = \zeta_h \ \text{ on } \ \Gamma_I, \qquad \mathbf{v} = \mathbf{0} \ \text{ on } \ \Gamma_D \cup \Gamma_N \qquad \text{and} \qquad \|(\mathbf{u}, \mathbf{v})\|_{\mathbf{Y}} \leq C\|\zeta_h\|_{0,\Gamma_I}. \tag{3.19}$$

Now, let $\mathbf{v}_h \in [L_h(\Omega_S)]^3$ be a Clément's type interpolant of $\mathbf{v}$, vanishing on $\Gamma_D \cup \Gamma_N$ which is defined at the nodes $B \in \Gamma_I$ as follows:

$$\mathbf{v}_h(B) := \frac{1}{|\omega_B|} \int_{\omega_B} \mathbf{v},$$

where ω_B is the union of all the faces on Γ_I sharing B. Notice that [67, Corollary 4.1] and (3.19) imply that

$$\|\mathbf{v}_h\|_{1,\Omega_S} \leq C\|\mathbf{v}\|_{1,\Omega_S} \leq \widetilde{C}\|\zeta_h\|_{0,\Gamma_I}.$$

On the other hand, by construction, $\int_{\Gamma_I} \mathbf{v}_h = \int_{\Gamma_I} \mathbf{v}$ and, hence, using (3.19) again,

$$\int_{\Gamma_I} \mathbf{v}_h \cdot \boldsymbol{\nu} = \int_{\Gamma_I} \mathbf{v} \cdot \boldsymbol{\nu} = \int_{\Gamma_I} \mathbf{u} \cdot \boldsymbol{\nu} - \int_{\Gamma_I} \zeta_h.$$

Since $\operatorname{div} \mathbf{u} = 0$ in Ω_F, then by using Gauss' Theorem, we obtain that $\int_{\Gamma_I} \mathbf{v}_h \cdot \boldsymbol{\nu} = -\int_{\Gamma_I} \zeta_h$. Hence, the following Neumann problem is compatible:

$$\Delta\varphi = 0 \quad \text{in} \quad \Omega_F, \qquad \nabla\varphi \cdot \boldsymbol{\nu} = \mathbf{v}_h \cdot \boldsymbol{\nu} + \zeta_h \quad \text{on} \quad \Gamma_I.$$

In addition, since $\mathbf{v}_h \cdot \boldsymbol{\nu} + \zeta_h \in L^2(\Gamma_I)$, [54, Theorem 3.17] ensures that $\varphi \in H^{3/2}(\Omega_F)$ and, therefore, $\nabla\varphi \in [H^{1/2}(\Omega_F)]^3 \cap H(\operatorname{div}^0; \Omega_F)$, so that we can define its Raviart–Thomas interpolant $\mathbf{u}_h = \mathbf{I}^{\mathcal{R}}_h(\nabla\varphi) \in \mathbf{R}_h(\Omega_F)$. Then, from (3.14) and (3.13) we have that

$$\operatorname{div} \mathbf{u}_h = 0 \quad \text{in} \quad \Omega_F, \qquad \int_F \mathbf{u}_h \cdot \boldsymbol{\nu} = \int_F (\mathbf{v}_h \cdot \boldsymbol{\nu} + \zeta_h) \quad \text{for all } F \subseteq \Gamma_I$$

and $\|\mathbf{u}_h\|_{\operatorname{div},\Omega_F} \leq C\|\nabla\varphi\|_{1/2,\Omega_F} \leq \widetilde{C}\|\mathbf{v}_h \cdot \boldsymbol{\nu} + \zeta_h\|_{0,\Gamma_I} \leq \widehat{C}\|\zeta_h\|_{0,\Gamma_I}$.

Thus, $(\mathbf{u}_h, \mathbf{v}_h) \in \mathbf{Y}_h$ and $\|(\mathbf{u}_h, \mathbf{v}_h)\|_{\mathbf{Y}} = \|(\mathbf{u}_h, \mathbf{v}_h)\|_{\mathbf{X}} + \|\mathbf{u}_h \cdot \boldsymbol{\nu}\|_{0,\Gamma_I} \leq C\|\zeta_h\|_{0,\Gamma_I}$. □

As a consequence of this lemma and the standard theory of mixed methods, we obtain an analogous result to Theorem 3.4 for the discrete problem.

Theorem 3.9. *Given* $(\mathbf{f},\mathbf{g}) \in \mathbf{H}$*, there exists a unique solution* $(\mathbf{u}_h,\mathbf{v}_h,\mu_h) \in \mathbf{Y}_h \times P_h$ *of the following source problem:*

$$a^*((\mathbf{u}_h,\mathbf{v}_h),(\boldsymbol{\phi}_h,\boldsymbol{\psi}_h)) + b((\boldsymbol{\phi}_h,\boldsymbol{\psi}_h),\mu_h) = d((\mathbf{f},\mathbf{g}),(\boldsymbol{\phi}_h,\boldsymbol{\psi}_h)), \tag{3.20a}$$

$$b((\mathbf{u}_h,\mathbf{v}_h),\zeta_h) = 0, \tag{3.20b}$$

for all $(\boldsymbol{\phi}_h,\boldsymbol{\psi}_h) \in \mathbf{Y}_h$ *and* $\zeta_h \in P_h$*. Moreover, there exists* $C > 0$*, independent of* h*, such that*

$$\|(\mathbf{u}_h,\mathbf{v}_h)\|_{\mathbf{Y}} + \|\mu_h\|_{0,\Gamma_I} \leq C\|(\mathbf{f},\mathbf{g})\|_{\mathbf{H}}. \tag{3.21}$$

Proof. See, for instance, [28]. □

As for the continuous problem, we define the corresponding discrete solution operator:

$$\begin{aligned} \mathbf{T}_h : \mathbf{H} &\longrightarrow \mathbf{Y}_h \subseteq \mathbf{H}, \\ (\mathbf{f},\mathbf{g}) &\longmapsto \mathbf{T}_h(\mathbf{f},\mathbf{g}) := (\mathbf{u}_h,\mathbf{v}_h) \end{aligned}$$

with $(\mathbf{u}_h,\mathbf{v}_h) \in \mathbf{Y}_h$ such that there exists $\mu_h \in P_h$ satisfying (3.20).

It is easy to check that $\mathbf{T}_h$ is self-adjoint with respect to a^* and d. Clearly, as a consequence of Theorem 3.9, $\mathbf{T}_h$ is a well-defined bounded linear operator. Moreover, $(\gamma_h,(\mathbf{u}_h,\mathbf{v}_h))$ with $\gamma_h \neq 0$, is an eigenpair of $\mathbf{T}_h$ if and only if there exists $\mu_h \in P_h$ such that $(1/\gamma_h,(\mathbf{u}_h,\mathbf{v}_h,\mu_h))$ is a solution of Problem 4.

Similarly to the continuous case, it can be proved that Problem 4 is equivalent to the following:

Problem 4*. Find $\widehat{\lambda}_h \in \mathbb{R}$ and $(\mathbf{u}_h,\mathbf{v}_h) \in \mathbf{W}_h$, $(\mathbf{u}_h,\mathbf{v}_h) \neq (\mathbf{0},\mathbf{0})$, such that

$$a^*((\mathbf{u}_h,\mathbf{v}_h),(\boldsymbol{\phi}_h,\boldsymbol{\psi}_h)) = \widehat{\lambda}_h\, d((\mathbf{u}_h,\mathbf{v}_h),(\boldsymbol{\phi}_h,\boldsymbol{\psi}_h)) \quad \forall\, (\boldsymbol{\phi}_h,\boldsymbol{\psi}_h) \in \mathbf{W}_h.$$

3.5 Spectral approximation

Analogously to the continuous case, (3.20b) implies that $\mathbf{T}_h(\mathbf{H}) \subseteq \mathbf{W}_h$. In addition, notice that $\mathbf{W}_h \not\subseteq \mathbf{W}$ because, for $(\mathbf{u}_h,\mathbf{v}_h) \in \mathbf{W}_h$, it does not hold $\mathbf{u}_h \cdot \boldsymbol{\nu} = \mathbf{v}_h \cdot \boldsymbol{\nu}$ on Γ_I, so that we are dealing with a non-conforming approximation of the spectral problem. In order to prove that the eigenvalues and eigenfunctions of $\mathbf{T}|_{\mathbf{W}}$ are well-approximated by those of

$\mathbf{T}_h|_{\mathbf{W}_h}$, we will use the theory developed in [34] for noncompact operators and, following the ideas in [17], will adapt this theory to our nonconforming case. In fact, let $\mathrm{sp}(\cdot)$ denote the spectrum of an operator. Since $\mathbf{W}_h \subseteq \mathbf{Y} \subseteq \mathbf{X}$, then $\mathbf{T}_h|_{\mathbf{W}_h}$ can be seen as a conforming discretization of $\mathbf{T}|_{\mathbf{X}} : \mathbf{X} \longrightarrow \mathbf{X}$. It is easy to prove that $\mathrm{sp}(\mathbf{T}|_{\mathbf{X}}) = \mathrm{sp}(\mathbf{T}|_{\mathbf{W}}) \cup \{0\}$ (see, for instance, [15, Lemma 4.1]). Thus, it is enough to prove the following two approximations properties to be able to apply the theory from [34]:

P1. For each eigenfunction $(\mathbf{u}, \mathbf{v})$ of $\mathbf{T}$ associated with an eigenvalue $\gamma \in (0, 1)$, there holds

$$\lim_{h \to 0} \mathrm{dist}\ ((\mathbf{u}, \mathbf{v}), \mathbf{W}_h) = 0,$$

where dist is the distance measured in the norm $\|\cdot\|_{\mathbf{X}}$;

P2. There holds

$$\lim_{h \to 0} \|(\mathbf{T} - \mathbf{T}_h)|_{\mathbf{W}_h}\|_{\mathbf{X}} = 0.$$

Before proving **P1** and **P2**, we will introduce the following result.

Theorem 3.10. *$\gamma_h = 1$ is an eigenvalue of $\mathbf{T}_h$ with eigenspace $\mathbf{K}_h = \mathbf{K} \cap \mathbf{W}_h$.*

Proof. The proof is similar to that in 2D. See, for instance, [15, Theorem 4.2]. □

In what follows, we establish some properties and definitions that will be used in the sequel.

First, we denote by $\boldsymbol{\pi}_h : [H^1(\Omega_S)]^3 \longrightarrow [L_h(\Omega_S)]^3$ the orthogonal projector with respect to the $H^1(\Omega_S)$-norm, which, for any $\epsilon \in (0, 1]$, satisfies

$$\|\mathbf{v} - \boldsymbol{\pi}_h \mathbf{v}\|_{1,\Omega_S} \leq C h^{\epsilon} \|\mathbf{v}\|_{1+\epsilon,\Omega_S} \qquad \forall\, \mathbf{v} \in [H^{1+\epsilon}(\Omega_S)]^3. \tag{3.22}$$

On the other hand, for any $\mathbf{v} \in [H^1(\Omega_S)]^3$ such that $\int_{\Gamma_I} \mathbf{v} \cdot \boldsymbol{\nu} = 0$, we proceed as in [53] and define $\mathcal{E}(\mathbf{v}) \in H(\mathrm{div}^0; \Omega_F)$ as follows:

$\mathcal{E}(\mathbf{v}) := \nabla q$ where q is the solution of the following compatible Neumann problem:

$$\Delta q = 0 \quad \text{in} \quad \Omega_F, \qquad \nabla q \cdot \boldsymbol{\nu} = \mathbf{v} \cdot \boldsymbol{\nu} \quad \text{on} \quad \Gamma_I.$$

Note that for all $\mathbf{v} \in [H^1_{\Gamma_D}(\Omega_S)]^3$, $\mathbf{v} \cdot \boldsymbol{\nu}|_{\Gamma_j} \in H^{1/2}(\Gamma_j)$, $j = 1, \ldots, J$. Therefore, $q \in H^{1+s}(\Omega_F)$ with $s > 1/2$, so that

$$\mathcal{E}(\mathbf{v}) \in [H^s(\Omega_F)]^3 \cap \overset{0}{H}(\mathrm{div}; \Omega_F) \qquad \text{and} \qquad \|\mathcal{E}(\mathbf{v})\|_{s,\Omega_F} \leq C \|\mathbf{v}\|_{1,\Omega_S}. \tag{3.23}$$

Consequently, $\mathbf{I}_h^{\mathcal{R}}\mathcal{E}(\mathbf{v})$ is well defined and the following result holds true.

Lemma 3.11. *There exists a constant $C > 0$, independent of h, such that*

$$\|\mathbf{I}_h^{\mathcal{R}}\mathcal{E}(\mathbf{v})\|_{0,\Omega_F} \leq C\|\mathbf{v}\|_{1,\Omega_S} \qquad \forall\, \mathbf{v} \in [H^1(\Omega_S)]^3.$$

Now, we are in a position to define an appropriate divergence-free approximation of smooth functions in $\mathbf{W}$.

Lemma 3.12. *For $(\mathbf{u},\mathbf{v}) \in \mathbf{W} \cap \left\{[H^s(\Omega_F)]^3 \times [H^{1+t}(\Omega_S)]^3\right\}$ with $s \in (1/2,\, 1]$ and $t \in (0,\, 1]$, let*

$$(\mathbf{u}_h,\mathbf{v}_h) := \left(\mathbf{I}_h^{\mathcal{R}}\mathbf{u} + \left(\mathbf{I}_h^{\mathcal{R}}\mathcal{E}(\boldsymbol{\pi}_h\mathbf{v}-\mathbf{v})\right),\boldsymbol{\pi}_h\mathbf{v}\right).$$

Then, $(\mathbf{u}_h,\mathbf{v}_h) \in \mathbf{W}_h$ and

$$\|(\mathbf{u},\mathbf{v})-(\mathbf{u}_h,\mathbf{v}_h)\|_{\mathbf{Y}} \leq Ch^r\left\{\|\mathbf{u}\|_{s,\Omega_F} + \|\mathbf{v}\|_{1+t,\Omega_S}\right\}, \tag{3.24}$$

where $r := min\,\{s,t\}$.

Proof. Notice that $\mathbf{u}_h$ is divergence-free in Ω_F thanks to (3.14), the fact that $\mathbf{u}$ is divergence-free in Ω_F and the definition of the operator $\mathcal{E}$. In addition, from the definition of $\mathcal{E}$, (3.13) and the fact that $\mathbf{u}\cdot\boldsymbol{\nu} = \mathbf{v}\cdot\boldsymbol{\nu}$ on Γ_I, we easily obtain that

$$\int_F \mathbf{u}_h\cdot\boldsymbol{\nu}_F = \int_F \mathbf{v}_h\cdot\boldsymbol{\nu}_F \qquad \forall\, F \subseteq \Gamma_I.$$

Hence, $(\mathbf{u}_h,\mathbf{v}_h) \in \mathbf{W}_h$. On the other hand, by using triangle inequality, the fact that $\mathbf{u}$ and $\mathcal{E}(\boldsymbol{\pi}_h\mathbf{v}-\mathbf{v})$ are divergence-free and (3.14), we obtain

$$\begin{aligned}\|(\mathbf{u},\mathbf{v})-(\mathbf{u}_h,\mathbf{v}_h)\|_{\mathbf{Y}} \leq{}& \|\mathbf{u}-\mathbf{I}_h^{\mathcal{R}}\mathbf{u}\|_{0,\Omega_F} + \|\mathbf{I}_h^{\mathcal{R}}\mathcal{E}(\boldsymbol{\pi}_h\mathbf{v}-\mathbf{v})\|_{0,\Omega_F} + \|\mathbf{v}-\boldsymbol{\pi}_h\mathbf{v}\|_{1,\Omega_S}\\ &+ \|\left(\mathbf{u}-\mathbf{I}_h^{\mathcal{R}}\mathbf{u}\right)\cdot\boldsymbol{\nu}\|_{0,\Gamma_I} + \|\left(\mathbf{I}_h^{\mathcal{R}}\mathcal{E}(\boldsymbol{\pi}_h\mathbf{v}-\mathbf{v})\right)\cdot\boldsymbol{\nu}\|_{0,\Gamma_I}.\end{aligned} \tag{3.25}$$

From Lemma 3.11 and (3.22), we have that

$$\|\mathbf{I}_h^{\mathcal{R}}\mathcal{E}(\boldsymbol{\pi}_h\mathbf{v}-\mathbf{v})\|_{0,\Omega_F} \leq C\|\mathbf{v}-\boldsymbol{\pi}_h\mathbf{v}\|_{1,\Omega_S} \leq Ch^t\|\mathbf{v}\|_{1+t,\Omega_S}. \tag{3.26}$$

On the other hand, since $\mathbf{u}\cdot\boldsymbol{\nu} = \mathbf{v}\cdot\boldsymbol{\nu}$ on Γ_I, we have that the fourth term of (3.25) can be rewritten as $\|\left(\mathbf{v}-\mathbf{I}_h^{\mathcal{R}}\mathbf{v}\right)\cdot\boldsymbol{\nu}\|_{0,\Gamma_I}$. Hence, from (3.16) and (3.17), we obtain that

$$\|\left(\mathbf{u}-\mathbf{I}_h^{\mathcal{R}}\mathbf{u}\right)\cdot\boldsymbol{\nu}\|_{0,\Gamma_I} \leq Ch^{\min\{1/2+t,1\}}\|\mathbf{v}\|_{1+t,\Omega_S}. \tag{3.27}$$

To estimate the last term in (3.25) we use that $(\mathbf{I}_h^{\mathcal{R}}\mathcal{E}(\boldsymbol{\pi}_h\mathbf{v}-\mathbf{v}))\cdot\boldsymbol{\nu}_F = \mathcal{P}_{h,\Gamma_I}((\mathcal{E}(\boldsymbol{\pi}_h\mathbf{v}-\mathbf{v}))\cdot\boldsymbol{\nu}_F)$, for all $F\subseteq\Gamma_I$. Then, from the fact that this projector is bounded, the definition of $\mathcal{E}$ and (3.22) we write

$$\|\left(\mathbf{I}_h^{\mathcal{R}}\mathcal{E}(\boldsymbol{\pi}_h\mathbf{v}-\mathbf{v})\right)\cdot\boldsymbol{\nu}\|_{0,\Gamma_I} \leq C\sum_{F\subseteq\Gamma_I}\|(\boldsymbol{\pi}_h\mathbf{v}-\mathbf{v})\cdot\boldsymbol{\nu}_F\|_{0,F} \leq Ch^t\|\mathbf{v}\|_{1+t,\Omega_S}. \tag{3.28}$$

Thus, (3.24) follows from (3.25), (3.15), (3.22), (3.26), (3.27) and (3.28). □

Now, we are in a position to prove property **P1**.

Lemma 3.13. *For each eigenfunction $(\mathbf{u},\mathbf{v})$ of $\mathbf{T}$ associated to an eigenvalue $\gamma\in(0,1)$, with $\|(\mathbf{u},\mathbf{v})\|_{\mathbf{X}}=1$, there exists a constant $C>0$, independent of h, such that*

$$\operatorname{dist}((\mathbf{u},\mathbf{v}),\mathbf{W}_h) \leq Ch^r, \tag{3.29}$$

where $r:=\min\{s,t\}$ with s and t as in Lemma 3.5.

Proof. Let $(\mathbf{u},\mathbf{v})\in\mathbf{W}$ with $\|(\mathbf{u},\mathbf{v})\|_{\mathbf{X}}=1$ such that $\mathbf{T}(\mathbf{u},\mathbf{v})=\gamma(\mathbf{u},\mathbf{v})$. Then, there exists $\mu\in P$ such that $(\mathbf{u},\mathbf{v},\mu)$ is an eigenfunction of Problem 3 with eigenvalue $1/\gamma>1$. In particular, from Lemma 3.5, $\mathbf{u}\in[H^s(\Omega_F)]^3$ for some $s>1/2$ and $\mathbf{v}\in[H^{1+t}(\Omega_S)]^3$ for some $t>0$. Hence, from Lemma 3.12 we obtain (3.29). □

On the other hand, the first part of the proof of property **P2** follows very closely that of [17, Theorem 6.3]. We include a sketch of this proof.

Lemma 3.14. *There exists a constant $C>0$, independent of h, such that for all $(\mathbf{f}_h,\mathbf{g}_h)\in\mathbf{W}_h$,*

$$\|(\mathbf{T}-\mathbf{T}_h)(\mathbf{f}_h,\mathbf{g}_h)\|_{\mathbf{X}} \leq Ch^r\|(\mathbf{f}_h,\mathbf{g}_h)\|_{\mathbf{X}},$$

where $r:=\min\{s,t\}$ with s and t as in Lemma 3.5.

Proof. First, note that it is enough to prove the theorem for $(\mathbf{f}_h,\mathbf{g}_h)\in\mathbf{K}_h^{\perp^{\mathbf{W}_h}}$ since $\mathbf{T}$ and $\mathbf{T}_h$ coincide on $\mathbf{K}_h$. So, let $(\mathbf{f}_h,\mathbf{g}_h)\in\mathbf{K}_h^{\perp^{\mathbf{W}_h}}$. Since $(\mathbf{f}_h,\mathbf{g}_h)\in\mathbf{W}_h$, we have that $\displaystyle\int_{\Gamma_I}\mathbf{f}_h\cdot\boldsymbol{\nu}=\int_{\Gamma_I}\mathbf{g}_h\cdot\boldsymbol{\nu}$ and the following Neumann problem is compatible:

$$\Delta\varphi = \operatorname{div}\mathbf{f}_h = 0 \quad \text{in} \quad \Omega_F, \qquad \nabla\varphi\cdot\boldsymbol{\nu}=\mathbf{g}_h\cdot\boldsymbol{\nu} \quad \text{on} \quad \Gamma_I.$$

As it is well-known, φ belongs to $H^{1+s}(\Omega_F)$ with $s>1/2$ and, moreover, satisfies $\|\nabla\varphi\|_{s,\Omega_F}\leq C\|(\mathbf{f}_h,\mathbf{g}_h)\|_{\mathbf{X}}$. Let $\boldsymbol{\chi}:=\mathbf{f}_h-\nabla\varphi$. Then,

$$(\mathbf{f}_h,\mathbf{g}_h) = (\boldsymbol{\chi},\mathbf{0}) + (\nabla\varphi,\mathbf{g}_h)\,, \tag{3.30}$$

$$\mathrm{div}(\boldsymbol{\chi}) = 0 \quad \text{in } \Omega_F \quad \text{and} \quad \int_{\Gamma_I} \boldsymbol{\chi}\cdot\boldsymbol{\nu} = 0. \tag{3.31}$$

Therefore,

$$\|(\mathbf{T}-\mathbf{T}_h)(\mathbf{f}_h,\mathbf{g}_h)\|_{\mathbf{X}} \leq \|(\mathbf{T}-\mathbf{T}_h)(\boldsymbol{\chi},\mathbf{0})\|_{\mathbf{X}} + \|(\mathbf{T}-\mathbf{T}_h)(\nabla\varphi,\mathbf{g}_h)\|_{\mathbf{X}}. \tag{3.32}$$

Since $\mathbf{T}$ and $\mathbf{T}_h$ are bounded uniformly on h, the first term on the right hand side can be controlled as follows:

$$\|(\mathbf{T}-\mathbf{T}_h)(\boldsymbol{\chi},\mathbf{0})\|_{\mathbf{X}} \leq (\|\mathbf{T}\|+\|\mathbf{T}_h\|)\|(\boldsymbol{\chi},\mathbf{0})\|_{\mathbf{X}} \leq C\|\boldsymbol{\chi}\|_{0,\Omega_F}. \tag{3.33}$$

In order to estimate $\|\boldsymbol{\chi}\|_{0,\Omega_F}$, we first notice that $(\mathbf{I}_h^{\mathcal{R}}\nabla\varphi - \mathbf{f}_h) \in \mathbf{R}_h(\Omega_F)$. Hence,

$$\mathrm{div}(\mathbf{I}_h^{\mathcal{R}}\nabla\varphi-\mathbf{f}_h)|_T \in \mathbb{P}_0(T) \quad \forall\, T\subseteq\Omega_F \quad \text{and} \quad (\mathbf{I}_h^{\mathcal{R}}\nabla\varphi-\mathbf{f}_h)|_F\cdot\boldsymbol{\nu} \in \mathbb{P}_0(F) \quad \forall\, F\subseteq\Gamma_I.$$

Then, from the Gauss Theorem, (3.13) and (3.31), we easily obtain that for each $T\subseteq\Omega_F$, $\mathrm{div}(\mathbf{I}_h^{\mathcal{R}}\nabla\varphi-\mathbf{f}_h)|_T = 0$ and for every face $F\subseteq\Gamma_I$, $(\mathbf{I}_h^{\mathcal{R}}\nabla\varphi-\mathbf{f}_h)|_F\cdot\boldsymbol{\nu}=0$.

So, $((\mathbf{I}_h^{\mathcal{R}}\nabla\varphi-\mathbf{f}_h),\mathbf{0}) \in \mathbf{K}\cap\mathbf{W}_h = \mathbf{K}_h$. Since, in addition, $(\mathbf{f},\mathbf{g}) \in \mathbf{K}_h^{\perp^{\mathbf{W}_h}}$, we easily obtain that

$$\begin{aligned}\|\boldsymbol{\chi}\|_{0,\Omega_F}^2 &= \int_{\Omega_F}(\nabla\varphi-\mathbf{f}_h)\cdot(\nabla\varphi-\mathbf{I}_h^{\mathcal{R}}\nabla\varphi) + \int_{\Omega_F}(\nabla\varphi-\mathbf{f}_h)\cdot(\mathbf{I}_h^{\mathcal{R}}\nabla\varphi-\mathbf{f}_h)\\ &= \int_{\Omega_F}(\nabla\varphi-\mathbf{f}_h)\cdot(\nabla\varphi-\mathbf{I}_h^{\mathcal{R}}\nabla\varphi).\end{aligned}$$

Now, by using the previous equality, the approximation property (3.15) and the a priori estimate $\|\nabla\varphi\|_{s,\Omega_F}\leq C\|(\mathbf{f}_h,\mathbf{g}_h)\|_{\mathbf{Y}}$, we obtain

$$\|\boldsymbol{\chi}\|_{0,\Omega_F}^2 \leq \|\boldsymbol{\chi}\|_{0,\Omega_F}\|\nabla\varphi-\mathbf{I}_h^{\mathcal{R}}\nabla\varphi\|_{0,\Omega_F}^2 \leq \|\boldsymbol{\chi}\|_{0,\Omega_F}Ch^s\|\nabla\varphi\|_{0,\Omega_F}^2 \leq Ch^s\|\boldsymbol{\chi}\|_{0,\Omega_F}\|(\mathbf{f}_h,\mathbf{g}_h)\|_{\mathbf{X}}.$$

Hence,

$$\|\boldsymbol{\chi}\|_{0,\Omega_F} \leq Ch^s\|(\mathbf{f}_h,\mathbf{g}_h)\|_{\mathbf{X}}. \tag{3.34}$$

Thus, from (3.33) and (3.34) we obtain

$$\|(\mathbf{T}-\mathbf{T}_h)(\boldsymbol{\chi},\mathbf{0})\|_{\mathbf{X}} \leq Ch^s\|(\mathbf{f}_h,\mathbf{g}_h)\|_{\mathbf{X}}\,. \tag{3.35}$$

On the other hand, let $(\mathbf{u},\mathbf{v}) := \mathbf{T}(\nabla\varphi,\mathbf{g}_h)$ and $(\mathbf{u}_h,\mathbf{v}_h) := \mathbf{T}_h(\nabla\varphi,\mathbf{g}_h)$. Then, there exist μ and μ_h such that $(\mathbf{u},\mathbf{v},\mu)\in\mathbf{Y}\times P$ and $(\mathbf{u}_h,\mathbf{v}_h,\mu_h)\in\mathbf{Y}_h\times P_h$ are the solutions of

the source problems (3.8) and (3.20), respectively, with $\mathbf{f}$ substituted by $\nabla\varphi$. Now, since $\mathbf{Y}_h \subseteq \mathbf{Y}$, (3.20) is a conforming approximation of (3.8). Therefore, since a^* and b satisfy the continuity, discrete ellipticity in the kernel and inf-sup conditions, the standard theory (see, for instance, [28]) yields

$$\|(\mathbf{u},\mathbf{v})-(\mathbf{u}_h,\mathbf{v}_h)\|_{\mathbf{X}} \leq \|(\mathbf{u},\mathbf{v})-(\mathbf{u}_h,\mathbf{v}_h)\|_{\mathbf{Y}} \leq C\left\{\operatorname{dist}((\mathbf{u},\mathbf{v}),\mathbf{W}_h)+\operatorname{dist}(\mu,P_h)\right\}$$

with a constant C independent of h. Hence, from Lemmas 3.5, 3.13 and estimate (3.17), we obtain

$$\|(\mathbf{T}-\mathbf{T}_h)(\nabla\varphi,\mathbf{g}_h)\|_{\mathbf{X}} = \|(\mathbf{u},\mathbf{v})-(\mathbf{u}_h,\mathbf{v}_h)\|_{\mathbf{X}} \leq Ch^{\min\{s,t\}}\|(\mathbf{f}_h,\mathbf{g}_h)\|_{\mathbf{X}},$$

which together with (3.35) allow us to conclude the proof. □

Next theorem, which shows that there are no spurious eigenvalues for h small enough, has been proved in [34].

Theorem 3.15. *Let J be a closed interval such that $J\cap \operatorname{sp}(\mathbf{T})=\emptyset$. There exists a strictly positive constant h_J such that if $h\leq h_J$, then $J\cap\operatorname{sp}(\mathbf{T}_h)=\emptyset$.*

For an open interval $I\subseteq(0,\,1)$, let $\mathbf{E}_I$ be the direct sum of the eigenspaces of $\mathbf{T}$ associated with eigenvalues lying in I. Let us denote by $\mathbf{E}_I^h$ the analogue for $\mathbf{T}_h$. We have the following error estimates to approximate eigenfunctions.

Theorem 3.16. *There exist strictly positive constants C and h_I such that, if $h\leq h_I$, then*

(i) for each $(\mathbf{u}_h,\mathbf{v}_h)\in\mathbf{E}_I^h$ with $\|(\mathbf{u}_h,\mathbf{v}_h)\|_{\mathbf{X}}=1$, $\operatorname{dist}((\mathbf{u}_h,\mathbf{v}_h),\mathbf{E}_I)\leq Ch^r$,

(ii) for each $(\mathbf{u},\mathbf{v})\in\mathbf{E}_I$ with $\|(\mathbf{u},\mathbf{v})\|_{\mathbf{X}}=1$, $\operatorname{dist}((\mathbf{u},\mathbf{v}),\mathbf{E}_I^h)\leq Ch^r$,

where $r:=\min\{s,t\}$ and s and t as in Lemma 3.5.

Proof. From [64, Theorem 2.1], we have that

$$\operatorname{dist}((\mathbf{u}_h,\mathbf{v}_h),\mathbf{E}_I)+\operatorname{dist}((\mathbf{u},\mathbf{v}),\mathbf{E}_I^h)\leq C\delta_h$$

where

$$\delta_h := \sup_{\substack{(\mathbf{u},\mathbf{v})\in\mathbf{E}_I\\ \|(\mathbf{u},\mathbf{v})\|_{\mathbf{X}}=1}}\left(\inf_{(\mathbf{f}_h,\mathbf{g}_h)\in\mathbf{W}_h}\|(\mathbf{u},\mathbf{v})-(\mathbf{f}_h,\mathbf{g}_h)\|_{\mathbf{X}}\right)+\sup_{\substack{(\mathbf{f}_h,\mathbf{g}_h)\in\mathbf{W}_h\\ \|(\mathbf{f}_h,\mathbf{g}_h)\|_{\mathbf{X}}=1}}\|(\mathbf{T}-\mathbf{T}_h)(\mathbf{f}_h,\mathbf{g}_h)\|_{\mathbf{X}}.$$

Hence, the proof follows from Lemmas 3.13 and 3.14. □

Let $I \subseteq (0,\,1)$ be an interval containing a unique eigenvalue γ of $\mathbf{T}$. As a consequence of this theorem, for h sufficiently small, the dimension of the linear space $\mathbf{E}_h^I$ must coincide with that of $\mathbf{E}_I$ (let us say n). This implies the convergence to γ of exactly n eigenvalues of the discrete problem $\gamma_h^{(1)}, \ldots, \gamma_h^{(n)}$. Moreover, the following double-order error estimate holds true.

Theorem 3.17. *There exist strictly positive constants C and h_I such that, if $h \leq h_I$, then*

$$\left|\gamma - \gamma_h^{(i)}\right| \leq Ch^{2r}, \quad i = 1, ..., n,$$

with $r := min\,\{s, t\}$, s and t as in Lemma 3.5, and C depending on γ.

Proof. From [64, Theorem 2.3] and the fact that $\mathbf{T}$ is self-adjoint with respect to a^*, we have that

$$\max_{i=1,\ldots,n} \left|\gamma - \gamma_h^{(i)}\right| \leq C(\delta_h^2 + M_h), \tag{3.36}$$

where δ_h is as in Theorem 3.16 and

$$M_h := \sup_{\substack{(\mathbf{u},\mathbf{v})\in\mathbf{E}_I \\ \|(\mathbf{u},\mathbf{v})\|_{\mathbf{X}}=1}} \sup_{\substack{(\boldsymbol{\phi},\boldsymbol{\psi})\in\mathbf{E}_I \\ \|(\boldsymbol{\phi},\boldsymbol{\psi})\|_{\mathbf{X}}=1}} (a^*(\mathbf{T}(\mathbf{u},\mathbf{v}), \Pi_h(\boldsymbol{\phi},\boldsymbol{\psi})) - d((\mathbf{u},\mathbf{v}), \Pi_h(\boldsymbol{\phi},\boldsymbol{\psi})))$$

with Π_h being the projection onto $\mathbf{W}_h$ with respect to a^*.

We focus on estimating M_h. In order to put our problem in the context of [64], we consider the continuous and discrete Problems 3* and 4*, respectively, in which case we are dealing with a non-conforming scheme. Let $(\mathbf{u}, \mathbf{v}) \in \mathbf{E}_I$, so that $\mathbf{T}(\mathbf{u}, \mathbf{v}) = \gamma(\mathbf{u}, \mathbf{v})$. Let $\widehat{\lambda} = 1/\gamma$. Arguing as in Theorem 3.2, it can be proved that $(\mathbf{u}, \mathbf{v})$ is the solution of the following problem:

$$\begin{aligned}
\nabla p + \rho_F \mathbf{u} &= \widehat{\lambda}\rho_F \mathbf{u} && \text{in} && \Omega_F,\\
\operatorname{div} \mathbf{u} &= 0 && \text{in} && \Omega_F,\\
-\operatorname{div} \boldsymbol{\sigma}(\mathbf{v}) + \rho_S \mathbf{v} &= \widehat{\lambda}\rho_S \mathbf{v} && \text{in} && \Omega_S,\\
\boldsymbol{\sigma}(\mathbf{v})\boldsymbol{\nu} + p\boldsymbol{\nu} &= \mathbf{0} && \text{on} && \Gamma_I,\\
\mathbf{u}\cdot\boldsymbol{\nu} - \mathbf{v}\cdot\boldsymbol{\nu} &= 0 && \text{on} && \Gamma_I,\\
\boldsymbol{\sigma}(\mathbf{v})\boldsymbol{n} &= \mathbf{0} && \text{on} && \Gamma_N,\\
\mathbf{v} &= \mathbf{0} && \text{on} && \Gamma_D.
\end{aligned}$$

Hence, from Lemma 3.5, we observe that $p \in H^{1+s}(\Omega_F)$, with $s > 1/2$.

Let $(\mathbf{u}, \mathbf{v})$, $(\boldsymbol{\phi}, \boldsymbol{\psi}) \in \mathbf{E}_I$ and $(\boldsymbol{\phi}_h, \boldsymbol{\psi}_h) := \Pi_h(\boldsymbol{\phi}, \boldsymbol{\psi})$. Integrating by parts, we obtain that

$$a^*(\mathbf{T}(\mathbf{u}, \mathbf{v}), \Pi_h(\boldsymbol{\phi}, \boldsymbol{\psi})) - d((\mathbf{u}, \mathbf{v}), \Pi_h(\boldsymbol{\phi}, \boldsymbol{\psi})) = \int_{\Gamma_I} p(\boldsymbol{\phi}_h \cdot \boldsymbol{\nu} - \boldsymbol{\psi}_h \cdot \boldsymbol{\nu}).$$

For $(\boldsymbol{\phi}_h, \boldsymbol{\psi}_h) \in \mathbf{W}_h$ we have that $\boldsymbol{\phi}_h \cdot \boldsymbol{\nu} = \mathcal{P}_{h,\Gamma_I}(\boldsymbol{\psi} \cdot \boldsymbol{\nu})$, where, once more, $\mathcal{P}_{h,\Gamma_I}$ is the $L^2(\Gamma_I)$ projection onto P_h. Therefore,

$$\begin{aligned}\left| \int_{\Gamma_I} p(\boldsymbol{\phi}_h \cdot \boldsymbol{\nu} - \boldsymbol{\psi}_h \cdot \boldsymbol{\nu}) \right| &= \left| \int_{\Gamma_I} (p - \mathcal{P}_{h,\Gamma_I}(p)) \, (\mathcal{P}_{h,\Gamma_I}(\boldsymbol{\psi}_h \cdot \boldsymbol{\nu}) - \boldsymbol{\psi}_h \cdot \boldsymbol{\nu}) \right| \\ &\leq \|p - \mathcal{P}_{h,\Gamma_I}(p)\|_{0,\Gamma_I} \|\mathcal{P}_{h,\Gamma_I}(\boldsymbol{\psi}_h \cdot \boldsymbol{\nu}) - \boldsymbol{\psi}_h \cdot \boldsymbol{\nu}\|_{0,\Gamma_I}.\end{aligned}$$

Since, $p|_{\Gamma_I} \in H^{1/2+s}(\Gamma_I)$ with $s > 1/2$, we have that $\|p - \mathcal{P}_{h,\Gamma_I} p\|_{0,\Gamma_I} \leq Ch\|p\|_{1,\Gamma_I} \leq Ch\|(\mathbf{u}, \mathbf{v})\|_{\mathbf{X}}$. For the other term, we proceed as in the proof of [64, Theorem 3.1] to derive that $\|\mathcal{P}_{h,\Gamma_I}(\boldsymbol{\psi}_h \cdot \boldsymbol{\nu}) - \boldsymbol{\psi}_h \cdot \boldsymbol{\nu}\| \leq Ch^r$. Therefore, $M_h \leq Ch^{1+r}\|(\mathbf{u}, \mathbf{v})\|_{\mathbf{X}}$ which allows us to conclude the proof. □

Remark 3.1. *Notice that* $\mathbf{T}_h$ *can also be seen as a conforming discretization of* $\mathbf{T}|_{\mathbf{Y}} : \mathbf{Y} \longrightarrow \mathbf{Y}$ *which would allow us to do an alternative analysis. However, in such a case, only a suboptimal order of convergence can be proved in Theorems 3.16 and 3.17.*

3.6 Numerical experiments

In this section, we report numerical results for a couple of tests obtained with a MATLAB code based on [12, 58]. For the incompressible fluid, we have used two approaches to construct basis for the divergence-free lowest-order Raviart–Thomas finite element space. Let $\mathcal{T}_h^F$ be a mesh of Ω_F. The first approach, that we call [A], has been proposed in [8, Sec. 3.1]. For a topologically trivial domain Ω_F, this method consists of the following steps:

1. consider the graph with nodes the vertices of $\mathcal{T}_h^F$ and arcs the edges of $\mathcal{T}_h^F$;
2. construct a spanning tree of the graph;
3. consider the classical basis of the lowest-order Nédélec finite element space;
4. the proposed divergence-free basis is formed by the curl of the basis functions associated to those arcs that are not in the spanning tree.

For topologically non trivial domains, an alternative approach was proposed in [8, Sec. 3.1].

The second approach, that we call [B], has been proposed in [8, Sec. 3.2]. It consists of obtaining a basis of the divergence-free lowest-order Raviart–Thomas elements, written as appropriate linear combinations of the classical Raviart–Thomas basis functions. The coefficients of each linear combination are determined by using a spanning tree of the *dual graph* (a graph where the arcs are the faces of $\mathcal{T}_h^F$ and the nodes are the tetrahedra of $\mathcal{T}_h^F$, plus one extra node for the exterior of the fluid domain). See [8, Sec. 3.2] for details and [7] for an efficient algorithm.

3.6.1 Cubic vessel

For our first test, we have considered a cubic vessel completely filled with a fluid and clamped by its bottom. We use the geometrical setting shown in Fig. 3.2.

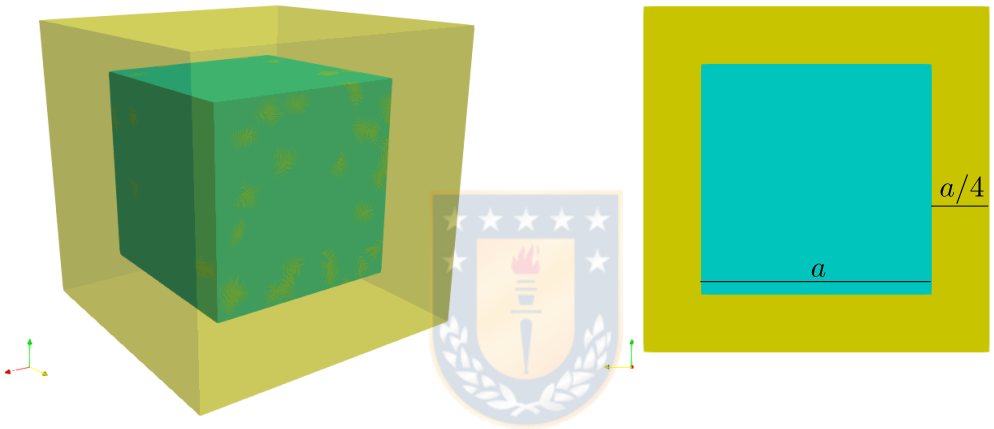

(a) Cubic vessel. (b) Vertical section of the cubic vessel: $a = 1\,\mathrm{m}$.

Figure 3.2: Topologically trivial fluid domain (figure produced by the author).

Physical parameters of steel have been used for the solid: density $\rho_S = 7700\,\mathrm{kg/m^3}$, Young's modulus $= 1.44 \times 10^{11}\,\mathrm{Pa}$, Poisson's ratio $= 0.35$. For the fluid, we have used 'perfectly incompressible' water; i.e., an incompressible liquid with the same density as that of water: $\rho_F = 1000\,\mathrm{kg/m^3}$.

In order to validate our code, we have resorted to the results from [17, Sec. 7] which show that the vibration frequencies for an incompressible fluid are limits of the corresponding ones for a compressible fluid as the acoustic speed going to infinity. Therefore, we have also solved the problem for a compressible fluid with increasing values of the acoustic speed. In

particular, we have taken successive multiples of the acoustic speed of water: $c = 1430\,\mathrm{m/s}$. Table 3.1 shows the vibration frequencies obtained in a same mesh with $88,262$ elements for several values of the sound speed in the fluid and for the incompressible case. Let us remark that, for the latter, we have solved the problem applying the two strategies described above to construct the lowest-order divergence-free Raviart–Thomas basis.

Mode	$10^0 \times c$	$10^1 \times c$	$10^2 \times c$	$10^3 \times c$	[A]	[B]
ω_1	1560.443	1563.435	1563.461	1563.462	1563.462	1563.462
ω_2	1560.624	1563.616	1563.642	1563.642	1563.642	1563.642
ω_3	2495.252	2495.312	2495.313	2495.313	2495.313	2495.313
ω_4	3454.110	3578.650	3581.309	3581.337	3581.338	3581.338
ω_5	4152.016	4416.885	4417.155	4417.158	4417.158	4417.158

Table 3.1: Lowest vibration frequencies for a compressible fluid with different values of acoustic speed, and for an incompressible fluid in a mesh $\mathcal{T}_h$ with $88,262$ elements (table produced by the author).

It can be seen from Table 3.1 that both strategies lead to identical results (as the theory in [8] predicts). It can also be seen that the vibration frequencies computed with the compressible fluid clearly converge to those of the incompressible one as the acoustic speed goes to infinity. This agrees with the theory from [17, 16] and allows us to validate our code. Figures 3.3 and 3.4 show two vibration modes of the coupled system. These modes qualitatively agree with those reported in [21] (see Figures 6 and 8 from this reference).

In order to appreciate the convergence of our proposed scheme, we have solved the same problem on several meshes with different degrees of refinement. We report in Table 3.2 the five smallest computed vibration frequencies, which allows us to appreciate the convergence of all of them.

N	$53,447$	$111,433$	$150,741$	$217,260$	$256,006$	$298,547$
ω_1	1573.05	1559.70	1555.81	1551.52	1549.40	1548.22
ω_2	1573.60	1560.25	1555.98	1551.64	1549.53	1548.26
ω_3	2506.28	2490.63	2485.86	2480.40	2478.02	2476.59
ω_4	3614.97	3567.39	3551.04	3534.02	3525.98	3521.20
ω_5	4501.34	4381.43	4341.64	4300.28	4280.97	4269.29

Table 3.2: Convergence of the smallest vibration frequencies for different meshes $\mathcal{T}_h$ with N elements (table produced by the author).

We appreciate from Table 3.2 the convergence of each vibration frequency.

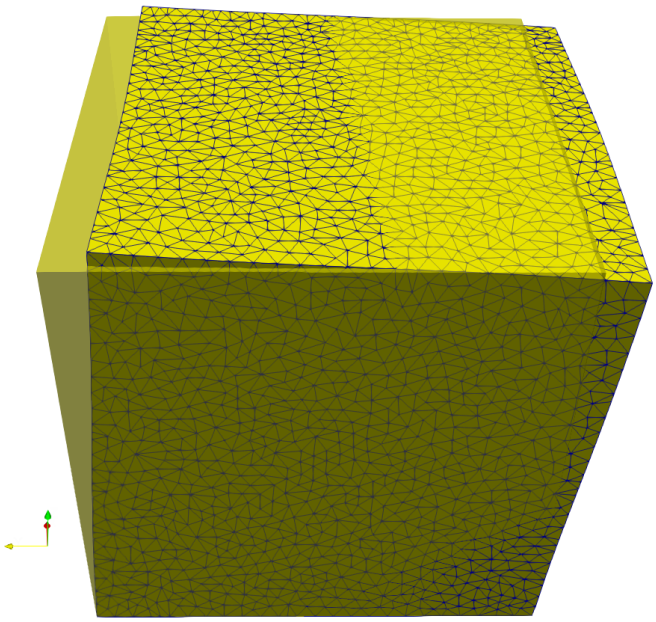

(a) Deformed structure.

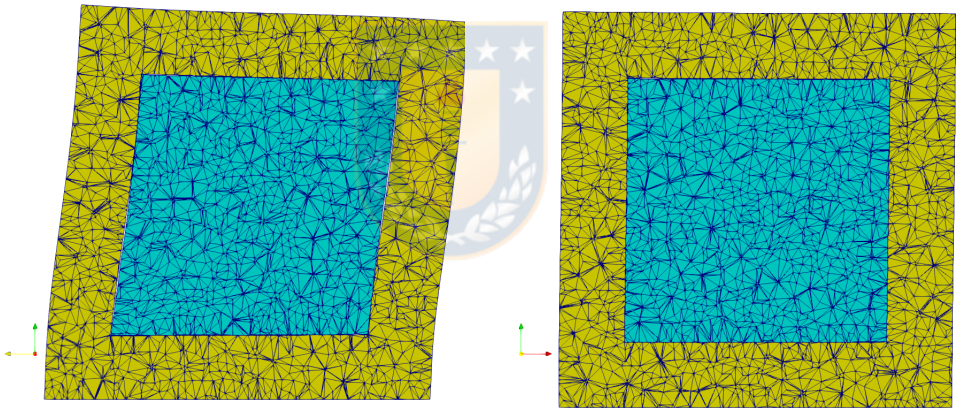

(b) Section x constant, at the middle of the cube.

(c) Section y constant, at the middle of the cube.

Figure 3.3: Mode ω_1: deformed structure (figure produced by the author).

3.6.2 Hollow ring

In order to test our code with a topologically non trivial fluid domain, we have considered a hollow ring filled with a fluid. We have used a hollow circular rod of square section with

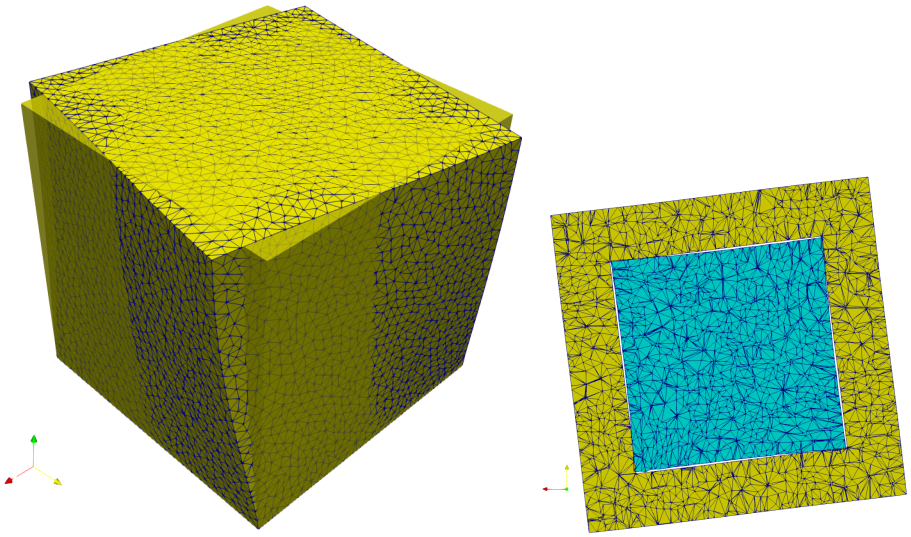

(a) Deformed structure. (b) Section z constant, at the middle of the cube.

Figure 3.4: Mode ω_3: deformed structure (figure produced by the author).

the radius of the centroid line taken as $R = 0.5\,\text{m}$. We have used the geometrical setting shown in Fig. 3.5 and the same physical parameters as in Section 3.6.1.

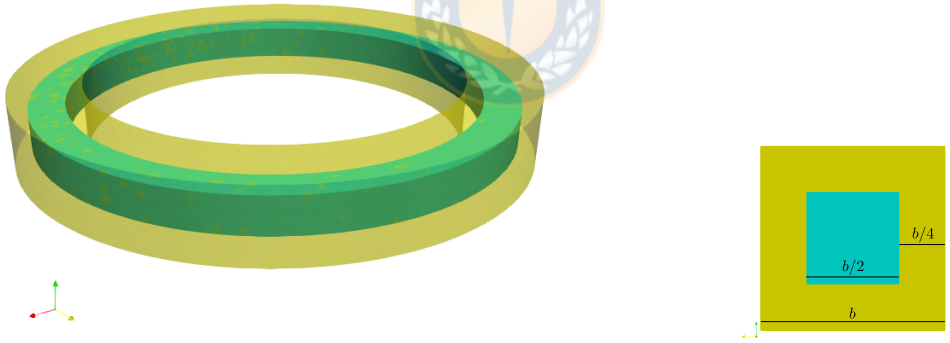

(a) Hollow ring filled with a fluid. (b) Vertical section of the hollow ring: $b = 0.05\pi\,\text{m}$.

Figure 3.5: Topologically non trivial fluid domain (figure produced by the author).

First, as in the previous test, we have validated the proposed methodology by solving the

same problem for a compressible fluid with sound speed going to infinity. We do not report here the computed values since their behavior is similar to that shown in Table 3.1 for the cubic vessel. Secondly, we have solved the problem on several meshes with different degrees of refinement. We report in Table 3.3 the ten smallest computed vibration frequencies.

N	$213,743$	$244,777$	$274,079$	$349,383$
ω_1	1973.83	1968.98	1966.54	1962.18
ω_2	1974.43	1969.20	1966.92	1962.49
ω_3	2145.59	2142.21	2140.40	2136.37
ω_4	2145.93	2142.53	2141.23	2136.66
ω_5	5190.65	5177.57	5171.43	5160.60
ω_6	5190.97	5178.32	5172.28	5161.13
ω_7	5534.93	5524.93	5520.34	5507.62
ω_8	5536.67	5526.38	5521.29	5507.76
ω_9	6122.00	6111.01	6104.86	6090.66
ω_{10}	7899.31	7880.38	7869.53	7844.82

Table 3.3: Convergence of the smallest vibration frequencies for different meshes $\mathcal{T}_h$ with N elements (table produced by the author).

We appreciate from Table 3.3 the convergence behavior for each vibration frequency. Finally, we show in Figure 3.6 the deformed structures corresponding to three of the vibration modes: ω_2, ω_3 and ω_9. Let us remark that they look similar to those of a solid ring reported in Figures 15, 16 and 17 from [46].

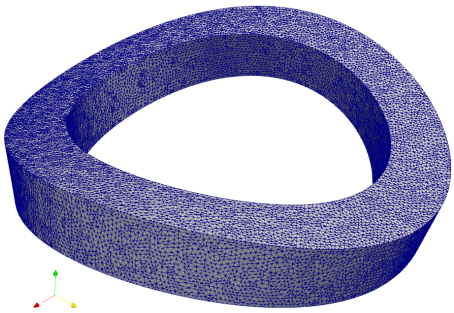

(a) Mode ω_2.

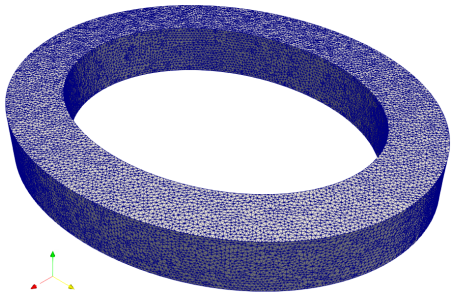

(b) Mode ω_3.

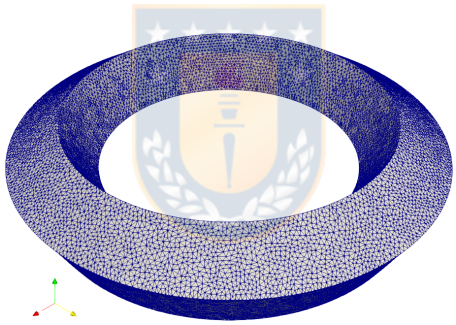

(c) Mode ω_9.

Figure 3.6: Deformed structure for the vibration modes corresponding to ω_2, ω_3 and ω_9 (figure produced by the author).

Conclusions and future works

Conclusions

In this thesis we developed two approaches to construct high order divergence-free Raviart–Thomas basis functions in an efficient way. To be precise, we extended to arbitrary high polynomial degree the two approaches presented in [8] for a three-dimensional domain with arbitrary topology. Finally we solved a fluid-structure interaction spectral problem in the three-dimensional case showing that both approaches work fine even for arbitrary topology of the domain. In addition, we illustrated the performance of these methods with some numerical test developed with MATLAB.

The main conclusions of this work are:

1. In Chapter 1 we have introduced and analyzed an efficient method for the computation of the moments of a function in the space of Raviart–Thomas finite elements of degree $r+1$ with assigned divergence. The proposed algorithm is based on basic results from graph theory. It turns to be so performant that it can be used to construct a basis of the space RT_h^0 of divergence-free Raviart–Thomas elements of any degree.

   Concerning the construction of a basis of divergence-free Raviart–Thomas finite elements of degree $r+1$, for $r=1$ and $r=2$, the numerical tests show that the efficiency of the algorithm is analogous in the two cases and that the behavior depends on the dimension of the finite elements space but not on the polynomial degree of the approximation. Moreover, it is robust with respect to the topology of the domain. When using a breadth-first spanning tree on big enough meshes, the computational time is of order $\left(d_{RT_h^0}\right)^{1.2}$, where $d_{RT_h^0}$ is the dimension of RT_h^0.

2. In Chapter 2 we have proved that, for a particular choice of degrees of freedom, the matrix associated to the gradient operator is the transposed of the all-nodes incidence matrix of a directed, connected and without self-loop graph. This fact,

that was well-known when $r = 0$, allow us to extend to high order finite elements the construction technique of a basis of the space of divergence-free finite elements of degree one analyzed in [66] and [8]. This method uses the cardinal (namely, canonical or dual) basis for the choosen degrees of freedom, whose elements, for $r > 0$, are not explicitly known. However, on each tetrahedron of the mesh, the elements of the canonical basis are related with the elements of a more natural basis by mean of a generalized Vandermonde matrix that is independent of the tetrahedra up to its orientation, using in this way the generalized Vandermonde matrix as a change of basis matrix.

3. Finally in Chapter 3 we propose a finite element method to solve the vibration problem of a coupled system which consists of an elastic structure in contact with an incompressible fluid. With this aim, we extend to the 3D case, the analysis in [17, 16], where the divergence-free displacements are written as curls of a stream function.

   The extension to 3D is not trivial at all, since the kernel of the curl operator is much more complicated in 3D than in 2D. In particular, we follow the approach from [8, 7] to construct appropriate basis for the space of the divergence-free fields. The proposed strategy holds for topologically non-trivial domains, too.

   We prove spectral convergence with optimal-order error estimates and report results for some numerical tests.

Future work

The methodologies we presented in this thesis have given rise to several ongoing and future projects. We briefly describe some of them below.

1. To analize the mass matrix associated to the introduced divergence-free basis (both approaches), i.e., size, sparsity and conditioning of the referred matrices and to understand its behavior as the order r increase. To propose and test suitable preconditioners for those matrix.

2. To extend the methodology presented in this thesis to incorporate boundary conditions to the divergence-free basis. With those basis, to solve other problems, eventually with different boundary conditions as, for example, Darcy problem, problems involving the Curl-Div system, etc. Also, in the fluid-structure vibration problem considered in Chapter 3, to avoid using the Lagrange multiplier that help us to impose the interface condition.

3. The divergence-free bases constructed in this thesis are based on the first family of Nédélec finite elements of degree $r+1$. Since many people prefer the second family of Nédélec finite elements of degree $r+1$, (not trimmed polynomial for the basis functions), we propose to analize how to extend the construction techniques to those spaces.

4. The fluid dynamic community is also very much interested in imposing strongly the divergence-free constraint to approximate the velocity field of incompressible fluids, but as a subspace of the space $[H^1(\Omega)]^3$. For this reason we propose to study new methodologies to construct divergence-free basis to approximate those spaces.

Conclusiones y trabajos futuros

Conclusiones

En esta tesis desarrollamos dos enfoques para construir funciones base del espacio de elementos finitos de Raviart–Thomas con divergencia nula de alto orden de un modo eficiente. Para ser precisos, extendimos al orden polinomial arbitrariamente alto dos enfoques presentados en [8] para un dominio tridimensional con topología arbitraria. Finalmente resolvimos un problema espectral de interacción fluido-estructura en el caso tridimensional mostrando que ambos enfoques funcionan bien incluso para dominios con topología arbitraria. Además, evidenciamos el buen desempeño de estos métodos con algunos experimentos numéricos desarrollados con MATLAB.

Las principales conclusiones de este trabajo son:

1. En el Capítulo 1 hemos presentado y analizado un método eficiente para el cálculo de los momentos de una función en el espacio de los elementos finitos de Raviart–Thomas de grado $r+1$ con divergencia asignada. El algoritmo propuesto está basado en resultados básicos de la tería de grafos. Y permite construir una base del espacio RT_h^0, de los elementos finitos de Raviart–Thomas con divergencia nula de cualquier grado.

   Los experimentos numérico en los casos $r = 1$ y $r = 2$, muestran que la eficiencia del algoritmo es análoga en los dos casos y que el comportamiento depende de la dimensión del espacio de los elementos finitos pero no del grado polinomial de la aproximación. Además, es robusto con respecto a la topología del dominio. Cuando se usa un árbol generador del tipo breadth-first en mallas suficientemente grandes, el tiempo de cálculo es del orden $\left(d_{RT_h^0}\right)^{1.2}$, donde $d_{RT_h^0}$ es la dimensión de RT_h^0.

2. En el Capítulo 2 hemos probado que, para una elección particular de grados de libertad, la matriz asociada al operador gradiente es la transpuesta de la matriz de

incidencia de todos los nodos de un grafo orientado, conexo y sin auto-bucles. Este hecho, que ya era bien conocido cuando $r = 0$, nos permite extender a los elementos finitos de alto orden la técnica de construcción de una base del espacio de los elementos finitos a divergencia nula de grado uno analizado en [66] y [8]. Este método utiliza la base cardinal (dual) para los grados de libertad seleccionados. Esta base cardinal no se conoce explícitamente pero en cada tetraedro de la malla la base cardinal esta relacionada con una base conocida mediante una matriz de Vandermonde generalizada. Esta matriz de Vandermonde es independiente del tetrahedro (salvo la orientacion del tetraedro).

3. Finalmente en el Capítulo 3 proponemos un método de elementos finitos para resolver el problema de vibración de un sistema acoplado que consiste de una estructura elástica en contacto con un fluido incompresible. Con este objetivo, extendemos al caso 3D, el análisis en [17, 16], donde los desplazamientos con divergencia nula son escritos como rotacionales de una función de corriente.

   La extensión a 3D no es trivial, dado que el núcleo del operador rotacional es más complicado en 3D con respecto al caso 2D. En particular, seguimos el enfoque de [8, 7] para construir bases apropiadas para el espacio de los campos con divergencia nula. La estrategia propuesta es válida también para dominios topológicamente no triviales.

   Demostramos convergencia espectral con estimaciones de error óptimas y reportamos los resultados de algunos experimentos numéricos.

Trabajos futuros

Las metodologías que presentamos en esta tesis han dado origen a varios trabajos en curso y futuros. Describimos brevemente algunos de ellos.

1. Analizar la matriz de masa asociada a las bases con divergencia nula presentadas con ambos enfoques, i.e., tamaño, condicionamiento y qué tan ralas son las matrices referidas y además entender su comportamiento según se incrementa r. Proponer y evaluar precondicionadores adecuados para estas matrices.

2. Extender la metodología presentada en esta tesis para incorporar condiciones de contorno a las bases con divergencia nula. Con estas bases, resolver otros problemas, eventualmente con diferentes condiciones de contorno, como por ejemplo, el problema

de Darcy, problemas que involucren el sistema curl-div, etc. En el problema de vibraciones fluido-estructura considerado en el Capítulo 3, reconsiderar el modo de imponer la condición de continuidad de traza normal, para evitar el uso de los multiplicadores de Lagrange al imponer la condición en la interfaz.

3. Las bases con divergencia nula construidas en esta tesis están basadas en la primera familia de los elementos finitos de Nédélec de grado $r+1$. Dado que varias personas prefieren la segunda familia de elementos finitos de Nédélec de grado $r+1$, (polinomios completos para las funciones bases), proponemos analizar cómo extender las técnicas de construcción a estos espacios.

4. La comunidad de dinámica de fluidos también está muy interesada en imponer de manera fuerte la condición de divergencia nula para aproximar el campo de velocidades de un fluido incompresible, pero como subespacio del espacio $[H^1(\Omega)]^3$. Por este motivo proponemos estudiar nuevas metodologías para construir bases con divergencia nula para aproximar estos espacios.

References

[1] M. Ainsworth, G. Andriamaro, and O. Davydov, *Bernstein-Bézier finite elements of arbitrary order and optimal assembly procedures*, SIAM J. Sci. Comput., 33 (2011), pp. 3087–3109.

[2] M. Ainsworth and G. Fu, *Bernstein–Bézier bases for tetrahedral finite elements*, Comput. Methods Appl. Mech. Engrg., 340 (2018), pp. 178–201.

[3] R. Albanese and G. Rubinacci, *Magnetostatic field computations in terms of two-component vector potentials*, Int. J. Numer. Meth. Engnrg., 29 (1990), pp. 515–532.

[4] ——, *Finite element methods for the solution of 3D eddy current problems*, Adv. Imag. Electron. Phys., 102 (1998), pp. 1–86.

[5] A. Alonso Rodríguez, E. Bertolazzi, R. Ghiloni, and A. Valli, *Construction of a finite element basis of the first de Rham cohomology group and numerical solution of 3D magnetostatic problems*, SIAM J. Numer. Anal., 51 (2013), pp. 2380–2402.

[6] A. Alonso Rodríguez, E. Bertolazzi, and A. Valli, *Simple finite element schemes for the solution of the curl-div system.* arXiv:1512.08532v1, 2015.

[7] A. Alonso Rodríguez, J. Camaño, E. De Los Santos, and F. Rapetti, *A graph approach for the construction of high order divergence-free Raviart-Thomas finite elements*, Calcolo, 55 (2018), pp. Art. 42, 28.

[8] A. Alonso Rodríguez, J. Camaño, R. Ghiloni, and A. Valli, *Graphs, spanning trees and divergence-free finite elements in domains of general topology*, IMA J. Numer. Anal., 37 (2017), pp. 1986–2003.

[9] A. Alonso Rodríguez and A. Valli, *Finite element potentials*, Appl. Numer. Math., 95 (2015), pp. 2–14.

[10] P. Alotto and I. Perugia, *Mixed finite element methods and tree-cotree implicit condensation*, Calcolo, 36 (1999), pp. 233–248.

[11] ——, *Tree-cotree implicit condensation in magnetostatics*, IEEE Transactions on Magnetics, 36 (2000), pp. 1523–1526.

[12] I. Anjam and J. Valdman, *Fast MATLAB assembly of FEM matrices in 2D and 3D: edge elements*, Appl. Math. Comput., 267 (2015), pp. 252–263.

[13] D. N. Arnold, R. S. Falk, and R. Winther, *Finite element exterior calculus, homological techniques, and applications*, Acta Numer., 15 (2006), pp. 1–155.

[14] M. A. Barrientos, G. N. Gatica, R. Rodríguez, and M. E. Torrejón, *Analysis of a coupled BEM/FEM eigensolver for the hydroelastic vibrations problem*, M2AN Math. Model. Numer. Anal., 38 (2004), pp. 653–672.

[15] A. Bermúdez, R. Durán, M. A. Muschietti, R. Rodríguez, and J. Solomin, *Finite element vibration analysis of fluid-solid systems without spurious modes*, SIAM J. Numer. Anal., 32 (1995), pp. 1280–1295.

[16] A. Bermúdez, R. Durán, and R. Rodríguez, *Finite element solution of incompressible fluid-structure vibration problems*, Internat. J. Numer. Methods Engrg., 40 (1997), pp. 1435–1448.

[17] ——, *Finite element analysis of compressible and incompressible fluid-solid systems*, Math. Comp., 67 (1998), pp. 111–136.

[18] A. Bermúdez, R. G. Durán, R. Rodríguez, and J. Solomin, *Finite element analysis of a quadratic eigenvalue problem arising in dissipative acoustics*, SIAM J. Numer. Anal., 38 (2000), pp. 267–291.

[19] A. Bermúdez, P. Gamallo, L. Hervella-Nieto, and R. Rodríguez, *Finite element analysis of pressure formulation of the elastoacoustic problem*, Numer. Math., 95 (2003), pp. 29–51.

[20] A. Bermúdez, P. Gamallo, L. Hervella-Nieto, R. Rodríguez, and D. Santamarina, *Fluid-structure acoustic interaction.*, in Computational Acoustics of Noise Propagation in Fluids - Finite and Boundary Element Methods., S. Marburg and B. Nolte, eds., Springer, Berlin, Heidelberg, 2008, ch. 9, pp. 253–286.

[21] A. Bermúdez, L. Hervella-Nieto, and R. Rodríguez, *Finite element computation of three-dimensional elastoacoustic vibrations*, Journal of Sound Vibration, 219 (1999), pp. 279–306.

[22] A. Bermúdez, R. Rodríguez, and D. Santamarina, *A finite element solution of an added mass formulation for coupled fluid-solid vibrations*, Numer. Math., 87 (2000), pp. 201–227.

[23] J. Bevis, F. Hall, and I. Katz, *Integer generalized inverses of incidence matrices*, Linear Algebra Appl., 39 (1981), pp. 247–258.

[24] D. Boffi, F. Brezzi, and M. Fortin, *Mixed finite element methods and applications*, vol. 44 of Springer Series in Computational Mathematics, Springer, Heidelberg, 2013.

[25] M. Bonazzoli and F. Rapetti, *High-order finite elements in numerical electromagnetism: degrees of freedom and generators in duality*, Numer. Algorithms, 74 (2017), pp. 111–136.

[26] A. Bossavit, *Computational Electromagnetism*, Academic Press Inc., San Diego, 1998.

[27] J. Boujot, *Mathematical formulation of fluid-structure interaction problems*, RAIRO Modél. Math. Anal. Numér., 21 (1987), pp. 239–260.

[28] F. Brezzi and M. Fortin, *Mixed and hybrid finite element methods*, vol. 15 of Springer Series in Computational Mathematics, Springer-Verlag, New York, 1991.

[29] W. Cai, J. Wu, and J. Xin, *Divergence-free $\mathcal{H}(\mathrm{div})$-conforming hierarchical bases for magnetohydrodynamics (MHD)*, Commun. Math. Stat., 1 (2013), pp. 19–35.

[30] Z. Cai, R. R. Parashkevov, T. F. Russell, J. D. Wilson, and X. Ye, *Domain decomposition for a mixed finite element method in three dimensions*, SIAM J. Numer. Anal., 41 (2003), pp. 181–194.

[31] J. Cantarella, D. DeTurck, and H. Gluck, *Vector calculus and the topology of domains in 3-space*, Amer. Math. Monthly, 109 (2002), pp. 409–442.

[32] M. Dauge, *Elliptic boundary value problems on corner domains*, vol. 1341 of Lecture Notes in Mathematics, Springer-Verlag, Berlin, 1988. Smoothness and asymptotics of solutions.

[33] J. Descloux, N. Nassif, and J. Rappaz, *On spectral approximation. I. The problem of convergence*, RAIRO Anal. Numér., 12 (1978), pp. 97–112, iii.

[34] ——, *On spectral approximation. II. Error estimates for the Galerkin method*, RAIRO Anal. Numér., 12 (1978), pp. 113–119, iii.

[35] F. Dubois, *Discrete vector potential representation of a divergence-free vector field in three-dimensional domains: numerical analysis of a model problem*, SIAM J. Numer. Anal., 27 (1990), pp. 1103–1141.

[36] A. Ern and J.-L. Guermond, *Theory and practice of finite elements*, vol. 159 of Applied Mathematical Sciences, Springer-Verlag, New York, 2004.

[37] V. Girault and P.-A. Raviart, *Finite element methods for Navier-Stokes equations*, vol. 5 of Springer Series in Computational Mathematics, Springer-Verlag, Berlin, 1986. Theory and algorithms.

[38] D. F. Griffiths, *An approximately divergence-free* 9*-node velocity element (with variations) for incompressible flows*, Internat. J. Numer. Methods Fluids, 1 (1981), pp. 323–346.

[39] P. W. Gross and P. R. Kotiuga, *Electromagnetic theory and computation: a topological approach*, vol. 48 of Mathematical Sciences Research Institute Publications, Cambridge University Press, Cambridge, 2004.

[40] K. Gustafson and R. Hartman, *Graph theory and fluid dynamics*, SIAM J. Algebraic Discrete Methods, 6 (1985), pp. 643–656.

[41] K. Gustafson and R. a. Hartman, *Divergence-free bases for finite element schemes in hydrodynamics*, SIAM J. Numer. Anal., 20 (1983), pp. 697–721.

[42] C. A. Hall and X. Ye, *Construction of null bases for the divergence operator associated with incompressible Navier-Stokes equations*, Linear Algebra Appl., 171 (1992), pp. 9–52.

[43] M. A. Hamdi, Y. Ousset, and G. Verchery, *A displacement method for the analysis of vibrations of coupled fluid-structure systems*, International Journal for Numerical Methods in Engineering, 13 (1978), pp. 139–150.

[44] S. Hang, *Tetgen, a delaunay-based quality tetrahedral mesh generator*, ACM Trans. on Mathematical Software, 41 (2015), pp. Art. 11, 36.

[45] F. Hecht, *Construction d'une base de fonctions* P_1 *non conforme à divergence nulle dans* $\mathbf{R}^3$, RAIRO Anal. Numér., 15 (1981), pp. 119–150.

[46] E. Hernández, E. Otárola, R. Rodríguez, and F. Sanhueza, *Approximation of the vibration modes of a Timoshenko curved rod of arbitrary geometry*, IMA J. Numer. Anal., 29 (2009), pp. 180–207.

[47] R. Hiptmair, *Finite elements in computational electromagnetism*, Acta Numer., 11 (2002), pp. 237–339.

[48] R. Hiptmair and J. Ostrowski, *Generators of $H_1(\Gamma_h, \mathbb{Z})$ for triangulated surfaces: construction and classification*, SIAM J. Comput., 31 (2002), pp. 1405–1423.

[49] L. Kettunen, K. Forsman, and A. Bossavit, *Formulation of the eddy current problem in multiply connected regions in terms of h*, Internat. J. Numer. Methods Engrg., 41 (1998), pp. 935–954.

[50] S. Le Borne, *Preconditioned nullspace method for the two-dimensional Oseen problem*, SIAM J. Sci. Comput., 31 (2009), pp. 2494–2509.

[51] S. Le Borne and D. Cook, II, *Construction of a discrete divergence-free basis through orthogonal factorization in $\mathcal{H}$-arithmetic*, Computing, 81 (2007), pp. 215–238.

[52] J. B. Manges and Z. J. Cendes, *Tree-cotree decompositions for first-order complete tangential vector finite elements*, Int. J. Numer. Methods Eng, 40 (1997), pp. 1667–1685.

[53] S. Meddahi, D. Mora, and R. Rodríguez, *Finite element analysis for a pressure-stress formulation of a fluid-structure interaction spectral problem*, Comput. Math. Appl., 68 (2014), pp. 1733–1750.

[54] P. Monk, *Finite element methods for Maxwell's equations*, Numerical Mathematics and Scientific Computation, Oxford University Press, New York, 2003.

[55] H. J.-P. Morand and R. Ohayon, *Fluid structure interaction*, John Wiley, 1995.

[56] J.-C. Nédélec, *Mixed finite elements in $\mathbf{R}^3$*, Numer. Math., 35 (1980), pp. 315–341.

[57] A. Quarteroni and A. Valli, *Numerical approximation of partial differential equations*, vol. 23 of Springer Series in Computational Mathematics, Springer-Verlag, Berlin, 1994.

[58] T. Rahman and J. Valdman, *Fast MATLAB assembly of FEM matrices in 2D and 3D: nodal elements*, Appl. Math. Comput., 219 (2013), pp. 7151–7158.

[59] F. Rapetti, *High order edge elements on simplicial meshes*, M2AN Math. Model. Numer. Anal., 41 (2007), pp. 1001–1020.

[60] F. Rapetti and A. Bossavit, *Whitney forms of higher degree*, SIAM J. Numer. Anal., 47 (2009), pp. 2369–2386.

[61] F. Rapetti, F. Dubois, and A. Bossavit, *Discrete vector potentials for nonsimply connected three-dimensional domains*, SIAM J. Numer. Anal., 41 (2003), pp. 1505–1527.

[62] P.-A. Raviart and J.-M. Thomas, *A mixed finite element method for 2nd order elliptic problems*, in Mathematical aspects of finite element methods (Proc. Conf., Consiglio Naz. delle Ricerche Rome, 1975), vol. 606 of Lecture Notes in Mathematics, 1977, pp. 292–315.

[63] Z. Ren and A. Razek, *Boundary edge elements and spanning tree technique in three-dimensional electromagnetic field computation*, Internat. J. Numer. Methods Engrg., 36 (1993), pp. 2877–2893.

[64] R. Rodríguez and J. E. Solomin, *The order of convergence of eigenfrequencies in finite element approximations of fluid-structure interaction problems*, Math. Comp., 65 (1996), pp. 1463–1475.

[65] R. Scheichl, *Iterative solution of saddle point problems using divergence-free finite elements with applications to groundwater flow*, ProQuest LLC, Ann Arbor, MI, 2000. Thesis (Ph.D.)–University of Bath (United Kingdom).

[66] R. Scheichl, *Decoupling three-dimensional mixed problems using divergence-free finite elements*, SIAM J. Sci. Comput., 23 (2002), pp. 1752–1776.

[67] L. R. Scott and S. Zhang, *Finite element interpolation of nonsmooth functions satisfying boundary conditions*, Math. Comp., 54 (1990), pp. 483–493.

[68] K. Thulasiraman and M. Swamy, *Graphs: theory and algorithms*, A Wiley-Interscience Publication, John Wiley & Sons, Inc., New York, 1992.

[69] J. Wang, Y. Wang, and X. Ye, *A robust numerical method for Stokes equations based on divergence-free $H(\mathrm{div})$ finite element methods*, SIAM J. Sci. Comput., 31 (2009), pp. 2784–2802.

[70] J. Webb and B. Forghani, *A single scalar potential method for 3D magnetostatics using edge elements*, IEEE Transactions on Magnetics, 25 (1989), pp. 4126–4128.